Title
Molecular Determinants of Stimulus-Specificity in Macrophage Reprogramming

Author
Cheng, Quen

Publication Date
2020

Peer reviewed|Thesis/dissertation

UNIVERSITY OF CALIFORNIA

Los Angeles

Molecular Determinants of Stimulus-Specificity in Macrophage Reprogramming

A dissertation submitted in partial satisfaction of the requirements for the degree

Doctor of Philosophy in Molecular Biology

by

Quen Joshua Cheng

2020

ABSTRACT OF THE DISSERTATION

Molecular Determinants of Stimulus-Specificity in Macrophage Reprogramming

by

Quen Joshua Cheng

Doctor of Philosophy in Molecular Biology

University of California, Los Angeles, 2020

Professor Alexander Hoffmann, Chair

The clinical outcome of infectious diseases is largely dictated by the response of the immune system to the pathogen. Immune responses are context-specific and significantly affected by factors such as tissue microenvironment, age, chronic diseases, cytokines, or previous infections. Contextual variables alter immune function by reprogramming cells of the innate immune system such as macrophages, altering their signaling networks and epigenetic states. Importantly, this reprogramming is stimulus-specific, and both the scope and underlying mechanisms of this specificity are areas of great interest.

In Chapter Two, we investigate the differential effects of Type I and II interferon (IFN) cytokines on human macrophage reprogramming by employing a sequential conditioning-stimulation approach. Whereas prior studies have examined direct effects of IFNs, we found that IFNs produced indirect effects that could only be appreciated upon subsequent stimulation with a pathogen-associated molecule and transcriptomic analysis across multiple time points. We

identified 713 genes that were unaffected by IFN alone, yet after IFN conditioning had an altered gene expression response to a subsequent stimulus. Surprisingly, we also found that the IFNs were not uniformly pro- or anti-inflammatory as previously described. Instead, the effects of Type I and II IFN were gene-specific and stimulus-specific. IFN conditioning affected both signaling networks and the epigenetic state, providing mechanistic explanations for our findings.

In Chapter Three we further explore the ability of stimuli to alter the epigenome of macrophages. We found that although many stimuli activate the transcription factor (TF) NFκB, only some were capable of altering the enhancer landscape through the formation of *de novo* enhancers. We showed that the capacity of NFκB to produce *de novo* enhancers was correlated with the temporal dynamics of NFκB activity, which are stimulus-specific. In particular, we found that whether NFκB is oscillatory or non-oscillatory was the primary determinant of its capacity to reprogram the epigenome. Thus, we propose a novel mechanism based on temporal dynamics to explain why TFs like NFκB reprogram macrophage epigenomes in a stimulus-specific manner. Future work will investigate the functional and disease consequences of the *de novo* enhancers that arise specifically from non-oscillatory NFκB-inducing stimuli.

The dissertation of Quen Joshua Cheng is approved.

Scott Filler

Melody Li

Stephen Smale

Otto Yang

Alexander Hoffmann, Committee Chair

University of California, Los Angeles

2020

Table of Contents

Abstract..... ii
Dissertation Committee..... iv
Table of Contents..... v
List of Figures..... vi
Acknowledgements..... xiii
Preface..... x
Vita..... xi
Chapter One: Introduction..... 1
The Clinical Perspective..... 2
The Molecular Perspective..... 7
Summary..... 14
Bibliography..... 16
Chapter Two: Sequential conditioning-stimulation reveals distinct gene- and stimulus-specific effects of Type I and II IFN on human macrophage functions..... 22
Summary..... 23
Introduction..... 24
Results..... 26
Discussion..... 43
Supplemental Figures..... 48
Materials and Methods..... 53
Bibliography..... 58
Chapter Three: NFκB dynamics determine the stimulus-specificity of epigenomic reprogramming in macrophages..... 63
Summary..... 64
Body Text..... 65
Extended Data Figures..... 76
Methods..... 82
Bibliography..... 92
Chapter Four: Conclusion..... 97
Bibliography..... 102

List of Figures

Figure 1.1: Variable outcomes of infectious diseases..... 4
Figure 1.2: Immune sentinel cells produce stimulus-appropriate responses. 8
Figure 1.3: Macrophage reprogramming..... 10

Figure 2.1: Stimulus-responsive gene expression in human macrophages..... 28
Figure 2.2: Type I and II IFN have gene-specific and stimulus-specific effects on gene expression..... 30
Figure 2.3: IFN conditioning potentiates or diminishes the stimulus-responsiveness of genes not induced by IFN alone..... 33
Figure 2.4: Effects of IFNβ vs IFNγ conditioning on inflammatory and anti-inflammatory cytokines..... 36
Figure 2.5: IFN conditioning alters innate immune signaling networks..... 38
Figure 2.6: IFN conditioning affects chromatin landscape..... 41
Figure 2.S1: IFN effects on basal gene expression..... 48
Figure 2.S2: PCA plots..... 49
Figure 2.S3: Nine category analysis..... 50
Figure 2.S4: Indirect IFN effects..... 51
Figure 2.S5: Effect on chemokines..... 52

Figure 3.1: NFκB-driven *de novo* enhancers are stimulus-specific and correlate to dynamic features of NFκB activity..... 66
Figure 3.2: Mathematical model predicts epigenetic response to distinct dynamic features of NFκB..... 68
Figure 3.3: IκBα knockout abolishes NFκB oscillations, increasing chromatin accessibility and *de novo* enhancer formation..... 70
Figure 3.4: NFκB dynamics-dependent enhancers are associated with dynamics-dependent gene expression..... 73
Extended data, Figure 3.1: Genome browser tracks..... 76
Extended data, Figure 3.2: Correlation of NFκB dynamics to ChIP-seq data..... 76
Extended data, Figure 3.3: Supplemental model simulations..... 77
Extended data, Figure 3.4: Parameter sensitivity analysis..... 78

Extended data, Figure 3.5: NFκB dynamics in TNF-stimulated IκB$\alpha^{-/-}$ vs WT BMDMs..... 78
Extended data, Figure 3.6: Supplemental ATAC-seq data..... 79
Extended data, Figure 3.7: *Nfkbia*$^{\kappa B/\kappa B}$ mutant as a complementary model of non-oscillatory NFκB..... 80
Extended data, Figure 3.8: Gene-centric approach to investigate the function of dynamics-dependent enhancers..... 81

Acknowledgements

Chapter Two is adapted from a published work for which the authors retain copyright: *Sequential conditioning-stimulation reveals distinct gene- and stimulus-specific effects of Type I and II IFN on human macrophage functions.* Q Cheng, F Behzadi, S Sen, S Ohta, R Spreafico, R Teles, R Modlin, A Hoffmann. Scientific Reports, 2019 Mar 27. DOI: 10.1038/s41598-019-40503-y. QC, SS, SO, and RS performed the experiments. QC, FB, RS, RT, and AH analyzed the data. RT obtained the biological samples. AH and RM conceived of the project. QC and AH wrote the manuscript. All authors reviewed the final manuscript. We also thank Diane Lefaudeux and Zhang (Frank) Cheng for valuable bioinformatics advice, and Adewunmi Adelaja, Simon Mitchell, and Kim Ngo for helpful discussions. Sequencing was performed at the UCLA Broad Stem Cell Center Sequencing Core. This work was supported by NIH grants P50AR063020, R01AI127864, and T32AI089398 and the Specialized Training for Advanced Research (STAR) program of the UCLA Department of Medicine.

Chapter Three is a work in submission and also available on bioRxiv: *NFκB dynamics determine the stimulus-specificity of epigenomic reprogramming in macrophages.* QJ Cheng, S Ohta, KS Sheu, R Spreafico, A Adelaja, B Taylor, A Hoffmann. 2020. bioRxiv DOI: 10.1101/2020.02.18.954602. QC, SO, AA, and BT performed the experiments. QC, SO, KS, RS, and AA analyzed the data. KS and BT developed the mathematical model. QC and AH wrote the manuscript with input from KS. All authors reviewed the manuscript. AH coordinated and funded the work. We also thank Diane Lefaudeux and Kensei Kishimoto for bioinformatics advice, and Siavash Kurdistani, Michael Carey, Eason Lin and Ying Tang for their insights and critical reading of the manuscript. Sequencing was performed at the UCLA Broad Stem Cell Center Sequencing Core. This work was supported by NIH grants R01-AI127864, R01-

GM117134, F31AI138450, T32GM008042, and T32-AI089398, as well as the Specialty Training and Advanced Research (STAR) program of the UCLA Department of Medicine.

I am indebted to a long list of professional mentors, beginning with Jill Fuss at LBNL who gave me all the building blocks for scientific success, followed by Kirk Knowlton and Sylvia Evans at UCSD who inspired me, believed in me, and gave me confidence to say "yes" to this career. Risa Hoffman, Judith Currier, Otto Yang, Jennifer Fulcher, and Scott Filler have been pillars of support within the UCLA and Harbor-UCLA Divisions of Infectious Diseases as I've navigated the uncertainties of an early career in academic medicine. The UCLA STAR program under the leadership of Alan Fogelman, Linda Demer, and Mitchell Wong has been vital in providing both a structured training program as well as a culture that values physician-scientists. Finally, I could not have imagined a better fit in a Ph.D. mentor than Alexander Hoffmann, who has not only taught me and shaped my scientific perspective but has enthusiastically and generously supported my dreams for the kind of physician-scientist I want to be.

Preface

As an internal medicine and infectious diseases physician, I am repeatedly challenged by the question, "What determines the outcome of an infection?" In many instances, with many of my patients' illnesses, biomedical science has been unable to provide a satisfactory answer. I have been especially perplexed and intrigued by cases where the immune response actually causes subsequent disease. Our lack of mechanistic understanding was evident during residency as I took care of patients who became paraplegic due to transverse myelitis after a viral syndrome, suffered debilitating stroke after a shingles episode, or died of necrotizing MRSA pneumonia after influenza infection. My desire to understand these rare but devastating post-infectious complications, with the hopes of developing prognostic and therapeutic tools to identify patients at risk and prevent these complications, has been the underlying motivation for my research career and the reason I pursued a Ph.D. in molecular biology.

Thus, this dissertation is written from the perspective of a physician-scientist exploring the complex molecular interplay between host immune system and pathogen. Chapter One starts from a high-level clinical perspective, broadly reviewing the factors that may contribute to the outcomes of human infectious diseases. I then narrow the focus to the reprogramming of innate immune cells, which is the focus of my dissertation work in Chapters Two and Three. Chapter Four re-expands the scope as I discuss the clinically-motivated questions I hope to pursue in the years to come.

Vita

EDUCATION

2005 B.A., University of California, Berkeley
2012 M.D., University of California, San Diego

POST-DOCTORAL TRAINING

2012-2014 Residency in Internal Medicine, UCLA Medical Center
2014-2018 Fellowship in Infectious Diseases, UCLA Medical Center

LICENSURE AND BOARD CERTIFICATION

2018 American Board of Internal Medicine, Infectious Disease Certification
2015 American Board of Internal Medicine Certification
2013 Medical Board of California Physician and Surgeon License

PROFESSIONAL EXPERIENCE

2018-current Clinical Instructor, Department of Medicine, Division of Infectious Diseases, UCLA
2015-2020 Specialized Training in Advanced Research (STAR) Fellowship, UCLA
2014-2018 Infectious Diseases Fellow Physician, UCLA Medical Center
2012-2014 Internal Medicine Resident Physician, UCLA Medical Center
2009-2011 NIH Research Fellow, UC San Diego School of Medicine
2005-2008 Research Associate, Lawrence Berkeley National Laboratory
2002 Laboratory Assistant, UCSF Cancer Center

TRAINEES

2018-current Kensei Kishimoto, Undergraduate Researcher
2017-2018 Faraz Behzadi, Undergraduate Researcher
2016-2018 Justin I. Buchanan, Undergraduate Researcher

HONORS AND AWARDS

Nov 2019 Invited speaker, NIH/NIAID Symposium on Innate Immune Memory
Oct 2018 UCLA Department of Medicine Research Symposium Poster Competition, 3rd place
Sep 2018 Research Innovator Award, Department of Medicine, UCLA
2015-current Fellowship for Specialized Training in Advanced Research (STAR), UCLA
May 2015 Outstanding Fellow Teaching Award, UCLA
July 2013 Commendation of Excellence in Medical Student Teaching, UCLA
Dec 2012 Commendation of Excellence in Medical Student Teaching, UCLA
Dec 2012 Commendation of Excellence in Patient Communication, UCLA
June 2012 Thomas E. Carew Prize for Cardiovascular Research
June 2012 Samuel B. Hamburger Memorial Thesis Award for Outstanding Research Project
Jan 2010 Award for Best Use of Literature, NIH Trainees' Poster Session
April 2009 Awardee, NIH Short-Term Research Training Grant

PUBLICATIONS/BIBLIOGRAPHY

Peer-Reviewed Research Papers

1. XPD helicase structures and activities: insights into the cancer and aging phenotypes from XPD mutations. L Fan, JO Fuss, **QJ Cheng**, AS Arvai, M Hammel, VA Roberts, PK Cooper, JA Tainer. *Cell* 2008, 133:789.

2. Characterization of a Y-Family DNA Polymerase eta from the Eukaryotic Thermophile Alvinella pompejana. S Kashiwagi, I Kuraoka, Y Fujiwara, K Hitomi, **QJ Cheng**, JO Fuss, DS Shin, C

Masutani, JA Tainer, F Hanaoka, S Iwai. *J. Nucleic Acids* 2010, 701472.

3. Who provides primary care? An assessment of HIV patient and provider practices and preferences. **QJ Cheng,** EM Engelage, TR Grogan, JS Currier, RM Hoffman. *J AIDS Clin Res.* 2014 Nov; 5(11).

4. Probing chromatin landscape reveals roles of endocardial TBX20 in septation. CJ Boogerd, I Aneas, N Sakabe, RJ Dirschinger, **QJ Cheng**, B Zhou, J Chen, MA Nobrega, SM Evans. *J Clin Invest.* 2016 Jun 27.

5. Duodenoscope-related outbreak of a carbapenem-resistant *Klebsiella pneumoniae* identified using advanced molecular diagnostics. RM Humphries, S Yang, S Kim, VR Muthusamy, D Russell, A Trout, T Zaroda, **QJ Cheng,** G Aldrovandi, DZ Uslan, P Hemarajata, Z Rubin. *Clin Infect Dis.* 2017 Aug 8.

6. Sequential conditioning-stimulation reveals distinct gene- and stimulus-specific effects of Type I and II IFN on human macrophage functions. **Q Cheng,** F Behzadi, S Sen, S Ohta, R Spreafico, R Teles, R Modlin, A Hoffmann. *Scientific Reports,* 2019 Mar 27.

7. Type I and type II interferon modulate NFκB signaling via distinct mechanisms. EL Mercado, S Mitchell, J Ho, K Fortmann, A Adelaja, **QJ Cheng,** G Ghosh, A Hoffmann. *Frontiers in Immunology,* 2019 Jun 25. PMC6604663.

8. NFκB dynamics determine the stimulus-specificity of epigenomic reprogramming in macrophages. QJ Cheng, S Ohta, KS Sheu, R Spreafico, A Adelaja, B Taylor, A Hoffmann. 2020. *bioRxiv* DOI: 10.1101/2020.02.18.954602.

Abstracts

1. The Endocardial Role of Tbx20 in Heart Development. **QJ Cheng**, R Dirschinger, SM Evans. NIH Training Grant Poster Session at UCSD, 2010

2. Thyrotoxicosis Complicated by Hypercalcemia and Demand-Mediated Cardiac Ischemia. **QJ Cheng**, A Rodgers, M Kistler. Society of General Internal Medicine Regional Conference, 2013

3. Priming with type I or II interferon differentially alters human macrophage responses in a gene-specific and stimulus-specific manner. **QJ Cheng**, F Behzadi, S Sen, S Ohta, R Spreafico, R Teles, R Modlin, A Hoffmann. Keystone Symposium on Myeloid Cells, April 2018.

4. The oscillatory behavior of NFκB ensures maintenance of epigenetic state. **Q Cheng**, S Ohta, R Spreafico, K Sheu, A Hoffmann. UCLA Dept of Medicine Research Symposium, October 2018

5. Interferon type-specific control of ISGF3 dynamics. CL Wilder, **QJ Cheng**, S Mitchell, A Meyer, A Hoffmann. Keystone Symposium on Transcription and RNA Regulation in Immunity, February 2019

6. Type I interferon induces temporally distinct activities of two STAT1-containing transcription factor complexes. K Kishimoto, **Q Cheng**, C Wilder, J Buchanan, A Hoffmann. American Physician-Scientist Association Annual Meeting, April 2019

7. Stimulus-specific *de novo* enhancer formation through epigenetic decoding of NFκB signaling dynamics. **QJ Cheng**, S Ohta, KM Sheu, R Spreafico, A Adelaja, A Hoffmann. International Conference on Systems Biology of Human Disease, May 2019

CHAPTER ONE:

Introduction

The Clinical Perspective

It is abundantly clear from medical literature and clinical experience that the same infection in different patients can produce different outcomes. For example, in a typical influenza season in the United States, an estimated 8.3% of the population are symptomatically infected, corresponding to approximately 27 million cases per year[1,2]. Most recover without complication, but 1-2% become sick enough to require hospitalization, with the most severe cases resulting in respiratory failure and death[3]. Additionally, influenza inflicts a large proportion of its damage by predisposing the host to a secondary bacterial infection. Bacterial pneumonia accounts for the majority of fatal influenza cases, ranging from 12,000-61,000 deaths annually since 2010[3]. What determines the outcome of infection – who recovers without complication, who gets secondary pneumonia, and who dies of respiratory failure (Fig. 1.1A) – is highly complex.

From a microbiology perspective, one explanation for the heterogeneity of outcomes is that different strains of a pathogen may be variably virulent. This is true, for instance, of certain *Klebsiella pneumoniae* strains carrying *Rmp* genes that confer a hyperviscous, mucoid phenotype that is associated with invasive infections[4]. Additionally, the size of the initial inoculum of pathogen into host also plays a role in disease severity[5]. Inoculum effects are well-characterized in animal models of infection[6] and very likely applicable to human disease.

Host genetic factors are also an important variable. For example, mutations in IFN-γ receptor results in increased susceptibility to mycobacterial infections[7], while patients lacking functional TLR3 or IRF7 proteins are highly susceptible to influenza[8,9]. These single-gene immunodeficiencies represent only a small fraction of genetic predispositions to infection. Multigenic traits, as well as polymorphisms in non-coding regions of the genome[10], likely

determine the course of disease in many cases. Thus, both host and pathogen genetics are important factors.

However, genetics alone are insufficient to explain the diversity of outcomes of infectious diseases. When in-bred, genetically identical mice are infected with a controlled inoculum of a pathogen, variable results are still observed in individual animals within an experiment. Clinical data indicates that non-genetic factors such as age[11], nutritional status[12], diabetes[13], and chronic liver[14] and kidney[15] disease are all associated with worse outcomes in human infectious diseases. Toxins and drugs, including therapies that intentionally inhibit immune function, also have an effect. Broadly speaking, environmental factors or "context" affect the outcome of infection by modulating the immune system (Fig. 1.1B). How contextual variables reprogram immune function is the subject of this dissertation.

Importantly, infections themselves represent another type of "context" that reprograms the immune system, altering subsequent immune function. In particular, infections reprogram cells of the innate immune system such as macrophages, dendritic cells, and monocytes. This has been variably referred to as "innate immune memory,"[16] "trained immunity,"[17] or "innate immune adaptation."[18] This reprogramming can be driven by pathogen-associated molecular patterns (PAMPs) directly, or cytokines produced by the immune system in response to an infection. Innate immune memory is distinct from the memory that is formed by T- and B-cells of the adaptive immune system. Adaptive memory is highly specific for a single antigen and protects the host from future infections with the same pathogen. In contrast, innate immune memory is characterized by a broad shift in the state of an immune cell, which is not antigen-specific but alters the response to diverse heterologous stimuli.

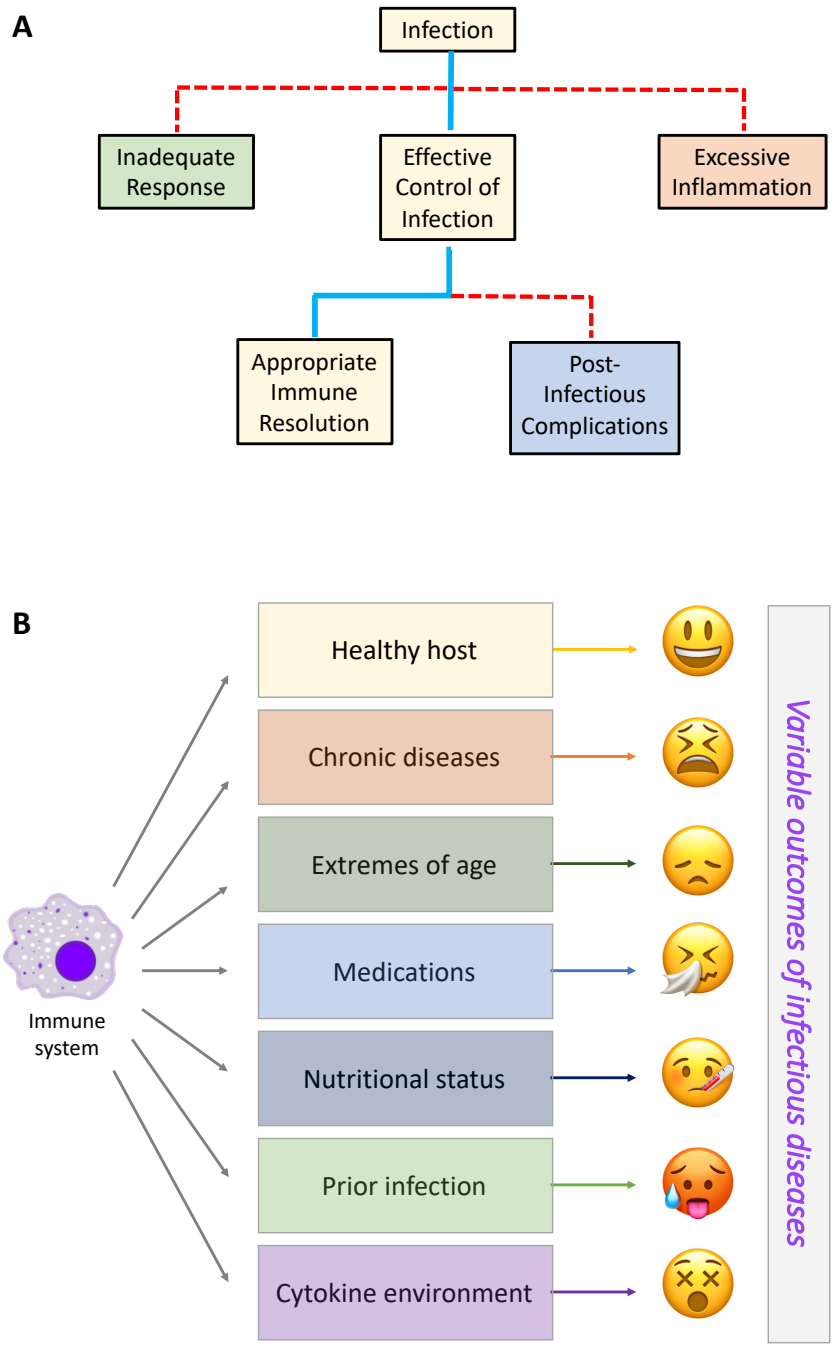

Figure 1.1: Variable outcomes of infectious diseases. A) Schematic of possible outcomes. Solid blue path indicates effective host response. Dashed red lines lead to disease. B) The immune function is context-dependent. Different contexts produce variable outcomes of infectious diseases.

Innate immune memory was initially described in plants that lack adaptive immunity[19], and it occurs in all vertebrate animals[16]. One can speculate, therefore, that the ability of innate immune cells to be reprogrammed by infection has been conserved as a protective mechanism for the host. Indeed, observational data from Malawi indicates that the anti-tuberculosis BCG vaccine, which has been a model stimulus used to induce innate immune memory experimentally[20,21], confers a prolonged, non-specific protection against neonatal sepsis due to salmonella[22]. In this example, exposure to BCG enhances innate immune responses against bacterial infections in a protective manner. A second example of an evolutionarily protective mechanism proposes the converse: prolonged exposure to lipopolysaccharide (LPS), a component of gram-negative bacterial cell walls, induces a state of immune "tolerance," potentially mitigating the damage caused by excessive inflammation[23]. Intuitively, it seems likely that innate immune memory exists in plants and humans alike for the benefit of the host. Thus, there has been substantial interest in leveraging innate immune memory for therapeutic purposes. Enhancing the host's natural tendencies toward immune innate immune memory is a strategy that is being considered to treat excessive inflammation in sepsis[24], as an immunomodulatory strategy to treat cancer[25], or as an adjuvant for vaccines[26].

However, in some instances, innate immune memory may have detrimental effects. It is increasingly evident that even mild infections increase the risk for myocardial infarction[27], stroke[28], solid organ transplant rejection[29], and autoimmune diseases[30]. The mechanisms of these post-infectious complications are multi-factorial, but dysregulated function of innate immune cells plays a central role by driving excessive inflammation. Indeed, lung transplant patients that develop allograft rejection after a respiratory viral infection display increased levels of the monocyte-recruiting chemokines CXCL9 and CXCL10[31,32]. And adoptive transfer of

macrophages treated with low dose LPS *in vitro* promotes greater aortic plaque formation in a mouse model of atherosclerosis[33]. These post-infectious complications involving dysregulated inflammation indicate that the effects of innate immune memory can be either protective or detrimental.

Given the variable effects of innate immune memory – which can either heighten or diminish inflammation and carries potential to either prevent or cause disease – a deeper understanding of the underlying mechanisms will be essential for harnessing its therapeutic potential. A critical knowledge gap is our understanding of the mechanisms underlying stimulus-specificity of innate immune memory. For instance, mice previously exposed to influenza are more susceptible to secondary pneumococcal infection[34], while mice previously exposed to adenovirus are protected from secondary pneumococcal infection[35]. Exposure to different pathogens – in these examples two viruses that cause similar respiratory diseases – can produce divergent memory effects. Whether a given stimulus will promote inflammation as in the adenovirus example or dampen inflammation as in the influenza example is unclear. Additionally, broadly categorizing phenotypes as "pro-inflammatory" or "anti-inflammatory" is also insufficiently descriptive, as innate immunity is more than just a simple on/off inflammation switch. Thus, a more detailed understanding of the molecular mechanisms of innate immune memory, i.e. macrophage reprogramming, is needed. Particular attention should be drawn to the determinants of stimulus-specificity and a characterization of the downstream effects beyond simply "pro-" or "anti-inflammatory."

The Molecular Perspective

Innate immune memory arises from the reprogramming of sentinel cells of the immune system: monocytes, macrophages, and dendritic cells. A critical function of these immune sentinel cells is to survey the environment and coordinate downstream immune responses. They are equipped with a diverse set of receptors, both cell membrane-associated and intra-cellular, that recognize a broad range of ligands including PAMPs, cytokines, and tissue damage-associated molecular patterns (DAMPs) such as oxidized LDL or soluble histones[36]. In response to a given stimulus, immune sentinel cells can activate a wide variety of downstream immune responses that must be appropriate to the stimulus (Fig. 1.2A). For instance, in response to a bacterial infection, neutrophils are recruited to phagocytose and kill the invading bacteria[37]. In response to an intracellular viral infection, cytotoxic T-cells are activated to eradicate infected cells and prevent spread of disease[38]. In response to tissue damage, fibroblasts are recruited to participate in wound healing[39]. These discrete effector functions are tied to specific gene expression programs (Fig. 1.2B). For example, the expression of chemokines such as CXCL1, CXCL2, and CXCL3 recruit neutrophils[40]. The expression of MHC class II and immunoproteasome genes promotes activation of cytotoxic T-cells[41,42]. The expression of matrix metalloproteinases such as MMP10 are critical for wound healing and tissue regeneration[43,44]. These effector functions are all coordinated by immune sentinel cells, and the choice of effector function depends not only on stimulus identity but also the context in which the immune sentinel cell is seeing the stimulus. That is, immune sentinel cells can be reprogrammed by their context – whether that be disease states, drugs, cytokines, or prior infections – and this context together with stimulus identity determines the response to a given stimulus.

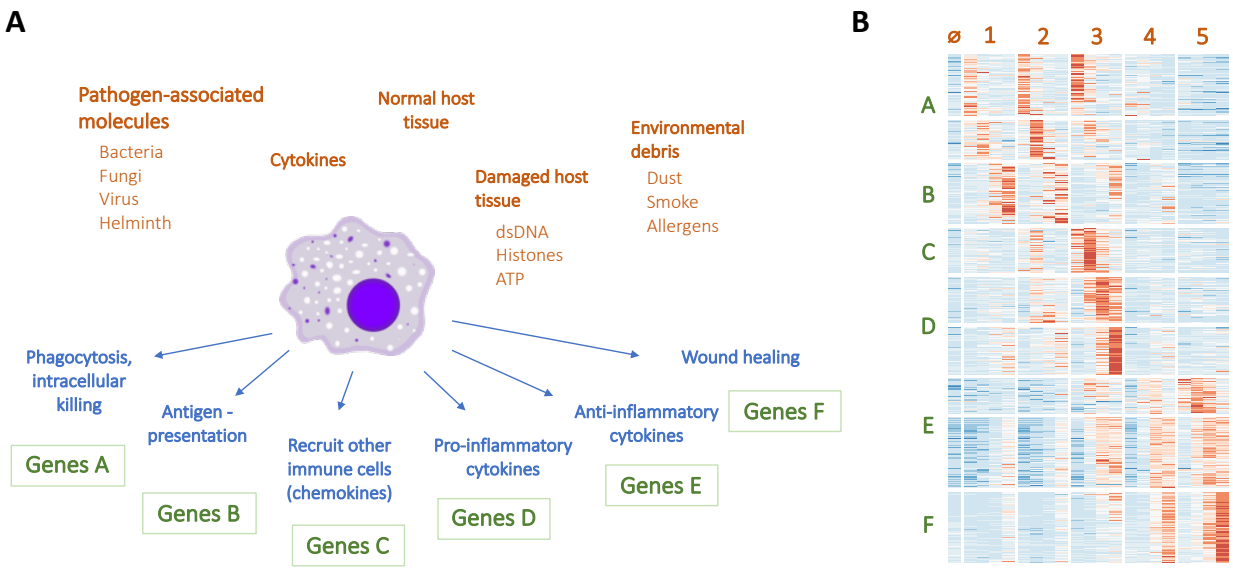

Figure 1.2: Immune sentinel cells produce stimulus-appropriate responses. A) Immune sentinel cells detect a diverse array of signals and activate stimulus-appropriate responses. Each of these downstream responses requires the induction of a distinct set of genes. B) Schematic of stimulus-responsive gene expression profile of an immune sentinel cell in response to five stimuli (columns), with clusters of genes (rows) corresponding to the downstream immune responses in Panel A.

For over two decades, macrophages, which adopt different phenotypes in different contexts, have been a model cell type in the study of cellular reprogramming and plasticity. Resident macrophages of different tissues are highly diverse, with glial cells in the brain serving a distinct function from Kuppfer cells in the liver or osteoclasts in the bone[36]. These tissue microenvironments dramatically alter macrophage responses to stimuli. For instance, bone marrow-derived macrophages (BMDMs) produce a robust inflammatory gene expression profile when stimulated by LPS, but macrophages isolated from the intestinal epithelium produce undetectable levels of inflammatory chemokines such as MIP-2[45]. Macrophages cultured *in vitro* can also be distinctly reprogrammed into either a pro-inflammatory phenotype by the cytokine IFN-γ, or a tissue-repair phenotype by the cytokine IL-4[46]. These macrophage phenotypes have been referred to as "classically" and "alternatively" activated macrophages, or "M1" and "M2"

macrophages, respectively (Fig. 1.3A). This experimental system of IFN-γ- or IL-4-mediated macrophage "polarization" has provided substantial insight into the mechanisms of macrophage reprogramming.

When a macrophage receptor binds its cognate ligand, a signal transduction cascade involving a network of proteins – scaffolding adapters, ubiquitin ligases, kinases, and phosphatases – is activated[47]. These signaling networks activate stimulus-dependent transcription factors (SDTFs) such as NFκB, STATs, IRFs, and AP1, which bind to enhancer and promoter elements in the genome. This results in the transcription of genes that are required for macrophage effector functions. The molecular interactions that convert a ligand-receptor interaction to stimulus-stimulus gene expression are highly tunable and provide the framework for context-dependent macrophage reprogramming.

Reprogramming occurs primarily at two levels within this framework (Fig. 1.3B). The first is through an alteration of the signaling network. When treated with IFN-γ, macrophages upregulate receptors such as TLR2 and TLR4[48], transcription factors such as IRF-1[49], and negative regulators such as SOCS3[50]. The net result of these signaling network changes is that IFN-γ-primed cells are poised to respond with greater inflammatory gene expression when encountering a PAMP such as LPS; that is, the macrophage is now a pro-inflammatory "M1"-polarized macrophage. Conversely, when treated with IL-4, macrophages upregulate mannose-binding receptor[51], enhancing its ability to phagocytose fungi and mannosylated cell debris and repair injured tissue. Thus, the IL-4-driven changes in receptor abundance promote an "M2"-polarized phenotype.

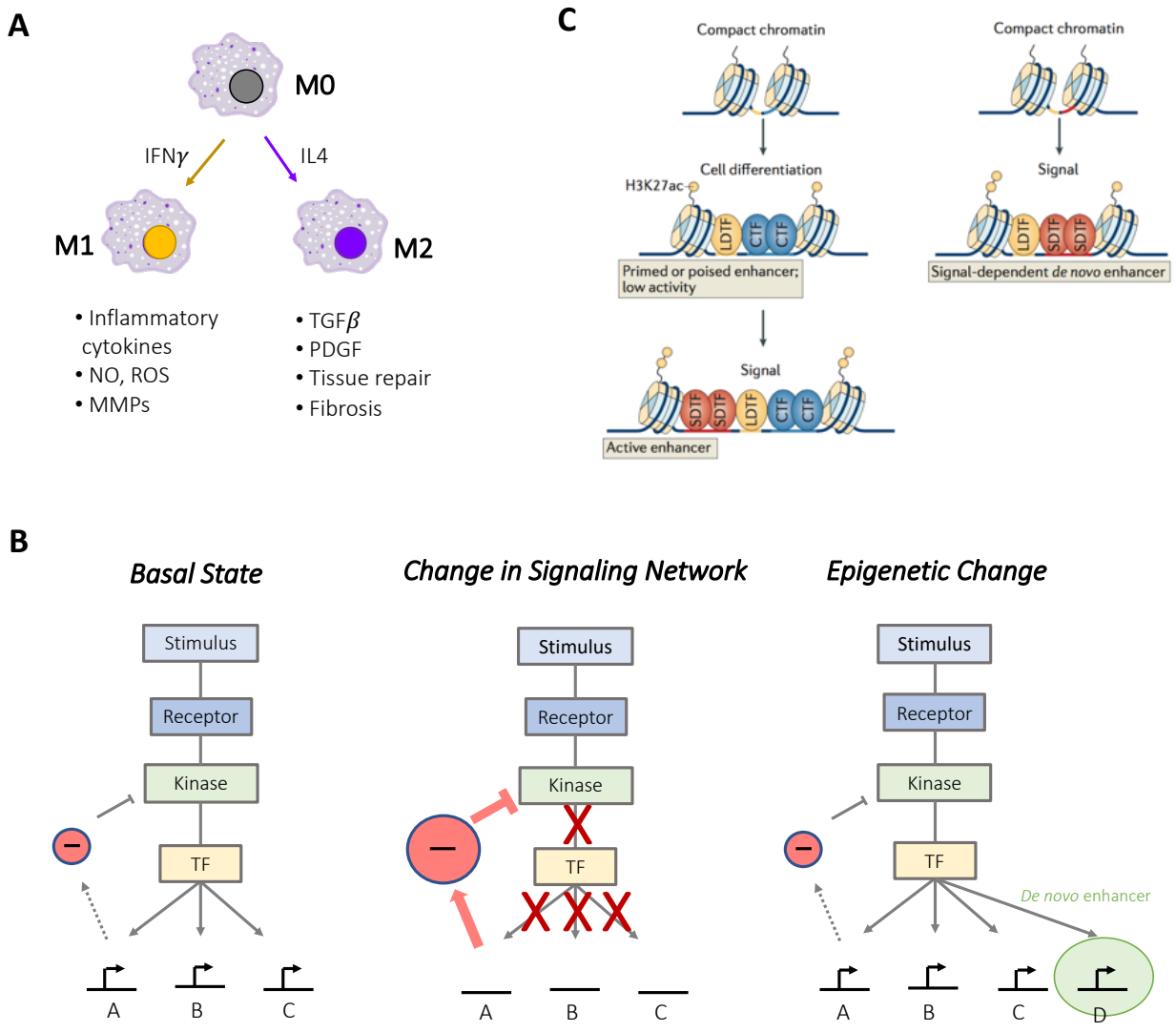

Figure 1.3: Macrophage reprogramming. A) Schematic of "M1" *vs.* "M2" polarization of macrophages by IFN-γ and IL-4 cytokines. B) Schematic of a macrophage signal transduction cascade leading to stimulus-responsive gene expression. Basal state conceptualizes a "naïve" or "M0" macrophage where the produce of Gene A negatively regulates the signaling network. Contextual variables can reprogram the either the signaling network, illustrated by an increased abundance of Gene A product resulting in suppression of gene expression (middle); or reprogram the epigenome, illustrated by Gene D which is a newly available target gene due to the formation of a *de novo* enhancer. TF = transcription factor. C) Schematic of macrophage enhancers adapted from Heinz et al., *Nature Reviews Mol Cell Bio* 2015. Left panel illustrates poised enhancers that are constitutively bound by LDTFs and exploited by SDTFs upon simulation. Right panel illustrates latent enhancers that require SDTF to become an active, *de novo* enhancer. LDTF = lineage-determining transcription factor, SDTF = stimulus-dependent transcription factor, CTF = collaborating transcription factor.

The second molecular mechanism that underlies macrophage reprogramming is epigenetic. The epigenome of a cell is composed of chromatin structure, patterns of histone modification, chemical DNA modifications like methylation, and the stable presence of lineage-determining transcription factors (LDTFs) that bind specific sequences of DNA[52]. These factors work together to define the enhancer repertoire of a cell, which is specific to a given lineage or type of cell. Macrophage enhancers, for instance, are defined by the LDTFs PU.1, IRF8, and C/EBP[53]. A subset of LDTF-bound enhancers drive constitutive expression of cell type-specific genes. At other LDTF-bound sites, enhancers are poised to respond to environmental cues that activate SDTFs, which bind cognate DNA sequences that are typically colocalized with LDTF binding sites[54]. Thus, the enhancer repertoire dictates not only the genes that are constitutively expressed but also the set of genes that respond to a given stimulus in a given cell type.

Until recently, it was thought that the enhancer repertoire of a differentiated cell is fixed by the presence of these LDTFs. In recent years, however, it has become evident that in response to acute stimuli such as LPS, *de novo* enhancers can be formed[54–56]. These *de novo* enhancers correspond to the activity of SDTFs such as NFκB, which are surprisingly capable of interacting with densely compacted regions of the genome not bound by LDTFs. Binding of SDTFs at these latent enhancers is associated with nucleosome repositioning and the deposition of positive-acting histone marks such as H3K27-acetylation and H3K4-methylation[55,56] (Fig. 1.3C). Polarization of macrophages with IFN-γ or IL-4 results in substantial changes in the enhancer landscape, with gains and losses of enhancer sites due to the activity of SDTFs STAT1 or IRF6, respectively[55]. Histone modifying enzymes such as the JMJD3 demethylase contribute by rewriting the adjacent histone code[57]. Intriguingly, these epigenetic changes are durable, as macrophages reprogrammed by IFN-γ are unable to adopt an M2 phenotype when subsequently

treated with IL-4[58]. This suggests that the potential for context-dependent reprogramming is limited and that macrophages reprogrammed by a given context-defining stimulus will continue to function in that reprogrammed state even in the presence of other stimuli.

The reprogramming of signaling networks and enhancer repertoire results in a change in macrophage phenotype. M1 and M2 macrophages differ significantly in their metabolic profile, with classically-activated macrophages utilizing a higher rate of anaerobic glycolysis, while alternatively-activated macrophages favor oxidative phosphorylation[59]. The transcriptome of M1 and M2 macrophages also differs significantly[60], as do patterns of chemokine and chemokine receptor expression[61]. Importantly, although M1 and M2 polarization states have been a useful paradigm to study the mechanisms and consequences of macrophage reprogramming, in reality macrophage phenotypes are far more diverse. M1 and M2 states only represent two discrete possibilities in a spectrum of macrophage phenotypes, and tremendous stimulus-specificity exists in the way different ligands reprogram macrophages[62].

Given the importance of their function as sentinel cells, it is not surprising that macrophage responses are stimulus-specific. Yet relatively few studies have investigated the mechanisms of specificity. One explanation for the paucity of data may be the assumption that specificity is inherently explained by the wide array of macrophage receptors that distinguish specific cytokines and PAMPs. While this notion seems intuitive, a close examination of the signaling networks downstream of these receptors reveals that they converge on only a few kinases and transcription factors (TFs)[63]. NFκB, for instance, is activated by a vast array of PAMPs and cytokines including all toll-like receptors, cytosolic nucleic acid sensors, and the cytokine receptors IL1R, TNFR, just to name a few. Indeed, the diversity of PAMP or cytokine receptors far outnumbers the set of TFs that operate at the terminal end of innate immune

signaling cascades. Thus, the diversity of macrophage receptors would not be predicted to generate the observed degree of specificity in stimulus-responsive gene expression[64].

One mechanism that increases the degree of stimulus-specificity is the combinatorial regulation of genes by different TFs. For example, Gene X may require TF-A and TF-B together, while Gene Y is activated by TF-A or TF-B, and Gene Z is activated by TF-A but not TF-B. Different stimuli acting through their cognate receptors may activate different combinations of TFs, with varying degrees of activation strength. This combinatorial mechanism of gene regulation has been demonstrated experimentally at key immune response genes such as *Ccl5*[65] and *Ifnb*[66]. However, a systems-level analysis of combinatorial strategies reveals that this mechanism alone does not explain all of the stimulus-specificity observed in macrophage gene expression responses[67].

An additional mechanism may be the stimulus-specific dynamics of TF activity. In response to different stimuli, TFs such as NFκB may enter the nucleus with distinct speeds, amplitudes, and durations, and may oscillate between the nucleus and cytoplasm[68]. Under this model, the temporal activation profile of a TF may determine how a given gene is expressed. For instance, longer durations of NFκB activity allow for maximal accumulation of mRNAs with long half-lives such as *Ccl2*[69]. Thus, TF dynamics, which are stimulus-specific, may account for additional stimulus-specificity of macrophage gene expression, and temporal dynamics may work together with combinations of different TFs to produce stimulus-specific responses.

One limitation thus far is that the work on stimulus-specific macrophage responses has largely focused on the regulation of immediate-response genes. Less attention has been paid to the long-term effects of different stimuli on macrophage reprogramming. Yet, as discussed above, reprogrammed macrophages give rise to innate immune memory and are drivers of both

appropriate and aberrant immune responses that result in health or disease. Thus, developing a molecular understanding of the stimulus-specificity of macrophage reprogramming will be critical for our ability to leverage innate immune memory to improve human health.

Summary

Context-dependent function of the innate immune system, termed "innate immune memory," arises from the reprogramming of immune sentinel cells like macrophages at the signaling network and epigenomic levels. Both the molecular and physiologic phenotypes are diverse and stimulus-specific, and although mechanisms have been proposed to explain the diversity of phenotypes, more work is needed to address the molecular determinants of stimulus-specificity. This dissertation aims to further our understanding of these molecular determinants.

Chapter Two is a thorough comparative analysis of the effects of reprogramming human macrophages with two types of interferon (IFN) cytokines. We compare not only the direct effects of Type I vs Type II IFN on macrophages, but also explore their genome-wide effects on subsequent response to a panel of secondary stimuli. We find, contrary to a widely accepted model, that Type I and Type II IFNs are not broadly anti- or pro-inflammatory, but that their effects are gene-specific and stimulus-specific. This nuanced specificity arises from alterations to innate immune signaling networks and reprogramming of the epigenome.

Chapter Three asks a fundamental mechanistic question: "What determines the capacity of a given stimulus to form *de novo* enhancers and reprogram the epigenome of a macrophage?" We find that temporal dynamics of NFκB activity, particularly whether it is oscillatory or non-oscillatory, determine its capacity to produce *de novo* enhancers in response to some stimuli but

not others. We propose a novel mechanism based on temporal dynamics to explain why SDTFs like NFκB reprogram macrophage epigenomes in a stimulus-specific manner.

Chapter Four expands upon these results to explore their implications for human health and disease. We discuss key unanswered questions and propose directions for further research.

Bibliography

1. Rolfes MA, Foppa IM, Garg S, Flannery B, Brammer L, Singleton JA, Burns E, Jernigan D, Olsen SJ, Bresee J, Reed C. Annual estimates of the burden of seasonal influenza in the United States: A tool for strengthening influenza surveillance and preparedness. Influenza Other Respir Viruses. 2018;12(1):132–137. PMCID: PMC5818346

2. Tokars JI, Olsen SJ, Reed C. Seasonal Incidence of Symptomatic Influenza in the United States. Clin Infect Dis. 2018 02;66(10):1511–1518. PMCID: PMC5934309

3. Disease Burden of Influenza. Center for Disease Control [Internet]. Available from: https://www.cdc.gov/flu/about/burden/index.html

4. Shon AS, Bajwa RPS, Russo TA. Hypervirulent (hypermucoviscous) Klebsiella pneumoniae: a new and dangerous breed. Virulence. 2013 Feb 15;4(2):107–118. PMCID: PMC3654609

5. Waddington CS, Darton TC, Jones C, Haworth K, Peters A, John T, Thompson BAV, Kerridge SA, Kingsley RA, Zhou L, Holt KE, Yu L-M, Lockhart S, Farrar JJ, Sztein MB, Dougan G, Angus B, Levine MM, Pollard AJ. An outpatient, ambulant-design, controlled human infection model using escalating doses of Salmonella Typhi challenge delivered in sodium bicarbonate solution. Clin Infect Dis. 2014 May;58(9):1230–1240. PMCID: PMC3982839

6. Asabe S, Wieland SF, Chattopadhyay PK, Roederer M, Engle RE, Purcell RH, Chisari FV. The Size of the Viral Inoculum Contributes to the Outcome of Hepatitis B Virus Infection. Journal of Virology. 2009 Oct 1;83(19):9652–9662.

7. Jouanguy E, Lamhamedi-Cherradi S, Lammas D, Dorman SE, Fondanèche MC, Dupuis S, Döffinger R, Altare F, Girdlestone J, Emile JF, Ducoulombier H, Edgar D, Clarke J, Oxelius VA, Brai M, Novelli V, Heyne K, Fischer A, Holland SM, Kumararatne DS, Schreiber RD, Casanova JL. A human IFNGR1 small deletion hotspot associated with dominant susceptibility to mycobacterial infection. Nat Genet. 1999 Apr;21(4):370–378. PMID: 10192386

8. Lim HK, Huang SXL, Chen J, Kerner G, Gilliaux O, Bastard P, Dobbs K, Hernandez N, Goudin N, Hasek ML, García Reino EJ, Lafaille FG, Lorenzo L, Luthra P, Kochetkov T, Bigio B, Boucherit S, Rozenberg F, Vedrinne C, Keller MD, Itan Y, García-Sastre A, Celard M, Orange JS, Ciancanelli MJ, Meyts I, Zhang Q, Abel L, Notarangelo LD, Snoeck H-W, Casanova J-L, Zhang S-Y. Severe influenza pneumonitis in children with inherited TLR3 deficiency. J Exp Med. 2019 Sep 2;216(9):2038–2056. PMCID: PMC6719423

9. Ciancanelli MJ, Huang SXL, Luthra P, Garner H, Itan Y, Volpi S, Lafaille FG, Trouillet C, Schmolke M, Albrecht RA, Israelsson E, Lim HK, Casadio M, Hermesh T, Lorenzo L, Leung LW, Pedergnana V, Boisson B, Okada S, Picard C, Ringuier B, Troussier F, Chaussabel D, Abel L, Pellier I, Notarangelo LD, García-Sastre A, Basler CF, Geissmann F, Zhang S-Y, Snoeck H-W, Casanova J-L. Infectious disease. Life-threatening influenza

and impaired interferon amplification in human IRF7 deficiency. Science. 2015 Apr 24;348(6233):448–453. PMCID: PMC4431581

10. Ramsuran V, Ewy R, Nguyen H, Kulkarni S. Variation in the Untranslated Genome and Susceptibility to Infections. Front Immunol. 2018;9:2046. PMCID: PMC6137953

11. Simon AK, Hollander GA, McMichael A. Evolution of the immune system in humans from infancy to old age. Proc R Soc B. 2015 Dec 22;282(1821):20143085.

12. Katona P, Katona-Apte J. The Interaction between Nutrition and Infection. CLIN INFECT DIS. 2008 May 15;46(10):1582–1588.

13. Geerlings SE, Hoepelman AIM. Immune dysfunction in patients with diabetes mellitus (DM). FEMS Immunology & Medical Microbiology. 1999 Dec;26(3–4):259–265.

14. Irvine KM, Ratnasekera I, Powell EE, Hume DA. Causes and Consequences of Innate Immune Dysfunction in Cirrhosis. Front Immunol. 2019 Feb 25;10:293.

15. Kato S, Chmielewski M, Honda H, Pecoits-Filho R, Matsuo S, Yuzawa Y, Tranaeus A, Stenvinkel P, Lindholm B. Aspects of Immune Dysfunction in End-stage Renal Disease. CJASN. 2008 Sep;3(5):1526–1533.

16. Netea MG, Schlitzer A, Placek K, Joosten LAB, Schultze JL. Innate and Adaptive Immune Memory: an Evolutionary Continuum in the Host's Response to Pathogens. Cell Host Microbe. 2019 09;25(1):13–26. PMID: 30629914

17. Mulder WJM, Ochando J, Joosten LAB, Fayad ZA, Netea MG. Therapeutic targeting of trained immunity. Nature Reviews Drug Discovery. 2019 Apr 9;1.

18. Natoli G, Ostuni R. Adaptation and memory in immune responses. Nat Immunol. 2019 Jul;20(7):783–792. PMID: 31213714

19. Kuc J. Induced Immunity to Plant Disease. BioScience. 1982 Dec;32(11):854–860.

20. Kleinnijenhuis J, Quintin J, Preijers F, Joosten LAB, Ifrim DC, Saeed S, Jacobs C, van Loenhout J, de Jong D, Stunnenberg HG, Xavier RJ, van der Meer JWM, van Crevel R, Netea MG. Bacille Calmette-Guerin induces NOD2-dependent nonspecific protection from reinfection via epigenetic reprogramming of monocytes. Proc Natl Acad Sci USA. 2012 Oct 23;109(43):17537–17542. PMCID: PMC3491454

21. Kleinnijenhuis J, Quintin J, Preijers F, Benn CS, Joosten LAB, Jacobs C, van Loenhout J, Xavier RJ, Aaby P, van der Meer JWM, van Crevel R, Netea MG. Long-Lasting Effects of BCG Vaccination on Both Heterologous Th1/Th17 Responses and Innate Trained Immunity. Journal of Innate Immunity. 2014;6(2):152–158.

22. Jason J, Archibald LK, Nwanyanwu OC, Kazembe PN, Chatt JA, Norton E, Dobbie H, Jarvis WR. Clinical and immune impact of Mycobacterium bovis BCG vaccination scarring. Infect Immun. 2002 Nov;70(11):6188–6195. PMCID: PMC130324

23. Cavaillon J-M, Adib-Conquy M. Bench-to-bedside review: endotoxin tolerance as a model of leukocyte reprogramming in sepsis. Crit Care. 2006;10(5):233. PMCID: PMC1751079

24. Leijte GP, Kiers D, van der Heijden W, Jansen A, Gerretsen J, Boerrigter V, Netea MG, Kox M, Pickkers P. Treatment With Acetylsalicylic Acid Reverses Endotoxin Tolerance in Humans In Vivo: A Randomized Placebo-Controlled Study. Crit Care Med. 2019 Apr;47(4):508–516. PMCID: PMC6426341

25. Netea MG, Joosten LAB, van der Meer JWM. Hypothesis: stimulation of trained immunity as adjunctive immunotherapy in cancer. J Leukoc Biol. 2017;102(6):1323–1332. PMID: 29018149

26. Sánchez-Ramón S, Conejero L, Netea MG, Sancho D, Palomares Ó, Subiza JL. Trained Immunity-Based Vaccines: A New Paradigm for the Development of Broad-Spectrum Anti-infectious Formulations. Front Immunol. 2018;9:2936. PMCID: PMC6304371

27. Jeffrey C. Kwong, Kevin L. Schwartz, Michael A. Campitelli, Hannah Chung, Natasha S. Crowcroft, Timothy Karnauchow, Kevin Katz, Dennis T. Ko, Allison J. McGeer, Dayre McNally, David C. Richardson, Laura C. Rosella, Andrew Simor, Marek Smieja, George Zahariadis, Jonathan B. Gubbay. Acute Myocardial Infarction after Laboratory-Confirmed Influenza Infection. New England Journal of Medicine. 2018;378(4):345–353.

28. Grau AJ, Urbanek C, Palm F. Common infections and the risk of stroke. Nat Rev Neurol. 2010 Dec;6(12):681–694. PMID: 21060340

29. Allyn PR, Duffy EL, Humphries RM, Injean P, Weigt SS, Saggar R, Shino MY, Lynch JP, Ardehali A, Kubak B, Tseng C-H, Belperio JA, Ross DJ, Gregson AL. Graft Loss and CLAD-Onset Is Hastened by Viral Pneumonia After Lung Transplantation. Transplantation. 2016 Nov;100(11):2424–2431. PMCID: PMC5077663

30. Ercolini AM, Miller SD. The role of infections in autoimmune disease. Clin Exp Immunol. 2009 Jan;155(1):1–15. PMCID: PMC2665673

31. Belperio JA, Keane MP, Burdick MD, Lynch JP, Zisman DA, Xue YY, Li K, Ardehali A, Ross DJ, Strieter RM. Role of CXCL9/CXCR3 chemokine biology during pathogenesis of acute lung allograft rejection. J Immunol. 2003 Nov 1;171(9):4844–4852. PMID: 14568964

32. Weigt SS, Derhovanessian A, Liao E, Hu S, Gregson AL, Kubak BM, Saggar R, Saggar R, Plachevskiy V, Fishbein MC, Lynch JP, Ardehali A, Ross DJ, Wang H-J, Elashoff RM, Belperio JA. CXCR3 chemokine ligands during respiratory viral infections predict lung allograft dysfunction. Am J Transplant. 2012 Feb;12(2):477–484. PMCID: PMC3833088

33. Geng S, Chen K, Yuan R, Peng L, Maitra U, Diao N, Chen C, Zhang Y, Hu Y, Qi C-F, Pierce S, Ling W, Xiong H, Li L. The persistence of low-grade inflammatory monocytes contributes to aggravated atherosclerosis. Nature Communications. 2016 Nov 8;7:13436. PMCID: PMC5105176

34. Shahangian A, Chow EK, Tian X, Kang JR, Ghaffari A, Liu SY, Belperio JA, Cheng G, Deng JC. Type I IFNs mediate development of postinfluenza bacterial pneumonia in mice. J Clin Invest. 2009 Jul;119(7):1910–20. PMCID: PMC2701856

35. Yao Y, Jeyanathan M, Haddadi S, Barra NG, Vaseghi-Shanjani M, Damjanovic D, Lai R, Afkhami S, Chen Y, Dvorkin-Gheva A, Robbins CS, Schertzer JD, Xing Z. Induction of Autonomous Memory Alveolar Macrophages Requires T Cell Help and Is Critical to Trained Immunity. Cell. 2018 Nov 29;175(6):1634-1650.e17. PMID: 30433869

36. Murray PJ, Wynn TA. Protective and pathogenic functions of macrophage subsets. Nat Rev Immunol. 2011 Oct 14;11(11):723–37. PMCID: PMC3422549

37. Kolaczkowska E, Kubes P. Neutrophil recruitment and function in health and inflammation. Nat Rev Immunol. 2013 Mar;13(3):159–175.

38. Zhang N, Bevan MJ. CD8(+) T cells: foot soldiers of the immune system. Immunity. 2011 Aug 26;35(2):161–168. PMCID: PMC3303224

39. Bainbridge P. Wound healing and the role of fibroblasts. J Wound Care. 2013 Aug;22(8):407–408, 410–412. PMID: 23924840

40. McDonald B, Kubes P. Chemokines: Sirens of Neutrophil Recruitment—but Is It Just One Song? Immunity. 2010 Aug;33(2):148–149.

41. King DP, Jones PP. Induction of Ia and H-2 antigens on a macrophage cell line by immune interferon. J Immunol. 1983 Jul;131(1):315–318. PMID: 6408177

42. Ferrington DA, Gregerson DS. Immunoproteasomes: structure, function, and antigen presentation. Prog Mol Biol Transl Sci. 2012;109:75–112. PMCID: PMC4405001

43. Minutti CM, Knipper JA, Allen JE, Zaiss DMW. Tissue-specific contribution of macrophages to wound healing. Seminars in Cell & Developmental Biology. 2017 Jan;61:3–11.

44. Rohani MG, McMahan RS, Razumova MV, Hertz AL, Cieslewicz M, Pun SH, Regnier M, Wang Y, Birkland TP, Parks WC. MMP-10 Regulates Collagenolytic Activity of Alternatively Activated Resident Macrophages. Journal of Investigative Dermatology. 2015 Oct;135(10):2377–2384.

45. Lotz M, Gütle D, Walther S, Ménard S, Bogdan C, Hornef MW. Postnatal acquisition of endotoxin tolerance in intestinal epithelial cells. The Journal of Experimental Medicine. 2006 Apr 17;203(4):973–984.

46. Mills CD, Kincaid K, Alt JM, Heilman MJ, Hill AM. M-1/M-2 Macrophages and the Th1/Th2 Paradigm. J Immunol. 2000 Jun 15;164(12):6166–6173.

47. Newton K, Dixit VM. Signaling in innate immunity and inflammation. Cold Spring Harb Perspect Biol. 2012 Mar 1;4(3). PMCID: PMC3282411

48. Muzio M, Bosisio D, Polentarutti N, D'amico G, Stoppacciaro A, Mancinelli R, van't Veer C, Penton-Rol G, Ruco LP, Allavena P, Mantovani A. Differential Expression and Regulation of Toll-Like Receptors (TLR) in Human Leukocytes: Selective Expression of TLR3 in Dendritic Cells. J Immunol. 2000 Jun 1;164(11):5998–6004.

49. Liu J, Guan X, Ma X. Interferon Regulatory Factor 1 Is an Essential and Direct Transcriptional Activator for Interferon γ-induced RANTES/CCl5 Expression in Macrophages. J Biol Chem. 2005 Jul 1;280(26):24347–24355.

50. Gatto L, Berlato C, Poli V, Tininini S, Kinjyo I, Yoshimura A, Cassatella MA, Bazzoni F. Analysis of SOCS-3 Promoter Responses to Interferon γ. J Biol Chem. 2004 Apr 2;279(14):13746–13754.

51. Stein M, Keshav S, Harris N, Gordon S. Interleukin 4 potently enhances murine macrophage mannose receptor activity: a marker of alternative immunologic macrophage activation. The Journal of Experimental Medicine. 1992 Jul 1;176(1):287–292.

52. Allis CD, Jenuwein T. The molecular hallmarks of epigenetic control. Nat Rev Genet. 2016 Aug;17(8):487–500.

53. Glass CK, Natoli G. Molecular control of activation and priming in macrophages. Nature Immunology. 2015;17:26–33.

54. Heinz S, Romanoski CE, Benner C, Glass CK. The selection and function of cell type-specific enhancers. Nat Rev Mol Cell Biol. 2015 Mar;16(3):144–154. PMCID: PMC4517609

55. Ostuni R, Piccolo V, Barozzi I, Polletti S, Termanini A, Bonifacio S, Curina A, Prosperini E, Ghisletti S, Natoli G. Latent enhancers activated by stimulation in differentiated cells. Cell. 2013 Jan 17;152(1–2):157–71. PMID: 23332752

56. Kaikkonen MU, Spann NJ, Heinz S, Romanoski CE, Allison KA, Stender JD, Chun HB, Tough DF, Prinjha RK, Benner C, Glass CK. Remodeling of the enhancer landscape during macrophage activation is coupled to enhancer transcription. Mol Cell. 2013 Aug 8;51(3):310–325. PMCID: PMC3779836

57. Satoh T, Takeuchi O, Vandenbon A, Yasuda K, Tanaka Y, Kumagai Y, Miyake T, Matsushita K, Okazaki T, Saitoh T, Honma K, Matsuyama T, Yui K, Tsujimura T, Standley DM, Nakanishi K, Nakai K, Akira S. The Jmjd3-Irf4 axis regulates M2 macrophage polarization and host responses against helminth infection. Nat Immunol. 2010 Oct;11(10):936–944. PMID: 20729857

58. Piccolo V, Curina A, Genua M, Ghisletti S, Simonatto M, Sabo A, Amati B, Ostuni R, Natoli G. Opposing macrophage polarization programs show extensive epigenomic and transcriptional cross-talk. Nat Immunol. 2017 Mar 13;

59. Kelly B, O'Neill LA. Metabolic reprogramming in macrophages and dendritic cells in innate immunity. Cell Res. 2015 Jul;25(7):771–784.

60. Xue J, Schmidt S V, Sander J, Draffehn A, Krebs W, Quester I, De Nardo D, Gohel T D, Emde M, Schmidleithner L, Ganesan H, Nino-Castro A, Mallmann M R, Labzin L, Theis H, Kraut M, Beyer M, Latz E, Freeman T C, Ulas T, Schultze J L. Transcriptome-Based Network Analysis Reveals a Spectrum Model of Human Macrophage Activation. Immunity. 2014 Feb 20;40(2):274–88. PMCID: PMC3991396

61. Mantovani A, Sica A, Sozzani S, Allavena P, Vecchi A, Locati M. The chemokine system in diverse forms of macrophage activation and polarization. Trends in Immunology. 2004 Dec;25(12):677–686.

62. Murray PJ, Allen JE, Biswas SK, Fisher EA, Gilroy DW, Goerdt S, Gordon S, Hamilton JA, Ivashkiv LB, Lawrence T, Locati M, Mantovani A, Martinez FO, Mege JL, Mosser DM, Natoli G, Saeij JP, Schultze JL, Shirey KA, Sica A, Suttles J, Udalova I, van Ginderachter JA, Vogel SN, Wynn TA. Macrophage activation and polarization: nomenclature and experimental guidelines. Immunity. 2014 Jul 17;41(1):14–20. PMCID: PMC4123412

63. Kawai T, Akira S. Signaling to NF-κB by Toll-like receptors. Trends in Molecular Medicine. 2007 Nov;13(11):460–469.

64. Sheu KM, Luecke S, Hoffmann A. Stimulus-specificity in the responses of immune sentinel cells. Current Opinion in Systems Biology. 2019 Dec;18:53–61.

65. Tong A-J, Liu X, Thomas BJ, Lissner MM, Baker MR, Senagolage MD, Allred AL, Barish GD, Smale ST. A Stringent Systems Approach Uncovers Gene-Specific Mechanisms Regulating Inflammation. Cell. 2016 Mar 24;165(1):165–179. PMCID: PMC4808443

66. Yie J, Senger K, Thanos D. Mechanism by which the IFN-beta enhanceosome activates transcription. Proceedings of the National Academy of Sciences. 1999 Nov 9;96(23):13108–13113.

67. Cheng CS, Behar MS, Suryawanshi GW, Feldman KE, Spreafico R, Hoffmann A. Iterative Modeling Reveals Evidence of Sequential Transcriptional Control Mechanisms. Cell Syst. 2017 Mar 22;4(3):330-343 e5. PMCID: PMC5434763

68. Taylor B, Adelaja A, Liu Y, Luecke S, Hoffmann A. Macrophages classify immune threats using at least six codewords of the temporal NFkB code. BioRxiv. 2020;

69. Sen S, Cheng Z, Sheu KM, Chen YH, Hoffmann A. Gene Regulatory Strategies that Decode the Duration of NFκB Dynamics Contribute to LPS- versus TNF-Specific Gene Expression. Cell Systems. 2020 Feb;10(2):169-182.e5.

CHAPTER TWO:

Sequential conditioning-stimulation reveals distinct gene- and stimulus-specific effects of Type I and II IFN on human macrophage functions

Summary

Macrophages orchestrate immune responses by sensing and responding to pathogen-associated molecules. These responses are modulated by prior conditioning with cytokines such as interferons (IFNs). Type I and II IFN have opposing functions in many biological scenarios, yet macrophages directly stimulated with Type I or II IFN activate highly overlapping gene expression programs. We hypothesized that a sequential conditioning-stimulation approach would reveal with greater specificity the differential effects of Type I and II IFN on human macrophages. By first conditioning with IFN then stimulating with toll-like receptor ligands and cytokines, followed by genome-wide RNA-seq analysis, we identified 713 genes whose expression was unaffected by IFN alone but showed potentiated or diminished responses to a stimulus after conditioning. For example, responses to the cytokine TNF were restricted by Type II IFN conditioning but potentiated by Type I IFN conditioning. We observed that the effects of IFN were not uniformly pro- or anti-inflammatory, but highly gene-specific and stimulus-specific. By assessing expression levels of key signal transducers and characterizing chromatin accessibility by ATAC-seq, we identify the likely molecular mechanisms underlying Type I and Type II-specific effects, distinguishing between modulation of cytoplasmic signaling networks and the nuclear epigenome that synergistically regulate macrophage immune responses.

Introduction

Macrophages play multiple crucial roles in initiating and coordinating healthy immune responses, and their dysregulation is associated with pathologic processes ranging from atherosclerosis to the cytokine storm seen in sepsis. One of the key functions of macrophages is to sense signals from the environment, such as pathogen associated molecular patterns (PAMPs) and cytokines, and translate these environmental inputs into a coordinated response involving the expression of hundreds of genes[1,2]. The specific nature of this response depends not only on the type of signal but also on the tissue microenvironment and prior cytokine exposures. Stimulus-responsive gene expression programs in macrophages are thus context-dependent. The same environmental signal that elicits an inflammatory response in one context might be immunologically silent in another.

One of the best-defined examples of this context-dependence is the "M1/M2" paradigm of macrophage polarization[1,2]. Macrophages conditioned with interferon (IFN)-γ and lipopolysaccharide (LPS) have been termed "classically activated" M1 macrophages and are skewed towards a pro-inflammatory phenotype that favors killing of intracellular pathogens. In contrast, macrophages conditioned with cytokines such as interleukin (IL)-4 have been termed "alternative" M2 macrophages whose functions are predominantly immunomodulatory and are important for tissue repair. First described in the late 1990s, these M1/M2 polarization states are now viewed as extremes of a wide spectrum of macrophage phenotypes that are defined by their exposure to diverse cytokine microenvironments[3,4]. In this model, cytokines "condition" macrophages, and the conditioning regimen can either "prime" or "tolerize" cells, respectively potentiating or diminishing their response to a subsequent stimulus.

Alterations in the epigenome are the primary mechanism of this phenomenon[5]. For instance, exposure to either IFNγ or IL-4 leads to a gain of enhancers and increases in chromatin accessibility as measured by ChIP- and FAIRE-seq[6,7]. Furthermore, prior IL-4 exposure inhibits the gain of IFNγ-mediated enhancers, illustrating that cross-repressive mechanisms exist amongst the various cytokines to which macrophages are exposed[8]. In addition to epigenetic changes, cytokine conditioning can affect signaling and transcription factor activity as an additional mechanism of priming or tolerance[8-10]. Altogether, there has been a paradigm shift towards understanding macrophage biology within this framework of conditioning and subsequent response to stimulation.

The IFNs have long been appreciated as fundamentally important cytokines in the mammalian immune system whose functions go beyond antiviral host defense[11]. IFNγ, as described above, has a well-appreciated role for activating macrophages and is required for immunity to intracellular pathogens such as tuberculosis and listeria[12,13]. Similarly, the Type I IFNs also play a substantial role in regulating myeloid cell function[14,15]. One of their roles in macrophages is thought to be the induction of an anti-inflammatory state that is in contrast to the pro-inflammatory role of Type II IFN[16,17]. However, others have also shown that Type I IFNs can promote inflammation, induce apoptosis, enhance antigen-presentation, and participate in signaling cross-talk with other cytokines like tumor necrosis factor (TNF)[18-21].

In some human disease states, Type I and II IFNs do indeed have contrasting effects. In *Mycobacterium leprae* infection, patients with lepromatous type, a progressive form of leprosy, possess an IFNβ signature in their skin lesions, while patients with the self-limiting tuberculoid form of leprosy have an IFNγ signature at the site of infection[22]. Similarly, IFNβ inhibits while IFNγ enhances the control of *M. tuberculosis* infection[23]. A variety of mechanisms have been

proposed for the opposing roles of Type I and II IFN, such as IFNβ leading to down-regulation of IL-12 and antimicrobial peptides through IL-10, or IFNβ suppression of IFNγ receptor expression[22,24,25].

Despite these contrasting physiological effects of Type I and II IFN *in vivo*, gene expression studies have found that Type I and Type II IFN have highly overlapping effects on the macrophage transcriptome[26,27]. These results appear insufficient to explain the biological differences, and they challenge the dichotomy that IFNγ is pro-inflammatory while IFNβ is anti-inflammatory. Notably, however, these studies have assessed only the direct gene-expression consequences of IFN and have not addressed the physiologically relevant paradigm of macrophage conditioning followed by stimulation. Additionally, the majority of studies on macrophage conditioning have been done using murine macrophages, and data are lacking from human cells which are likely to be different[28,29].

We therefore sought to define with high resolution the effects of Type I and II IFN on human macrophages using sequential conditioning and stimulation. We hypothesized that additional differences would be revealed by unbiased, genome-wide transcriptomic analyses of macrophages conditioned with IFNβ or IFNγ and subsequently stimulated with various PAMPs and cytokines. Our findings reveal complex and nuanced differences between Type I and II IFNs that are gene-specific and stimulus-specific.

Results

Gene expression programs in human macrophages are stimulus-specific

To characterize the gene expression response of primary human macrophages we isolated CD14+ monocytes from the peripheral blood of three healthy adult donors. These were then

cultured in media containing M-CSF for seven days to differentiate the monocytes to macrophages (Fig 2.1a). On day 7, we stimulated the macrophages with the Toll-like receptor (TLR) ligands Pam3CSK (which activates TLR2), Lipid A (TLR4), and poly(I:C) (TLR3), and the cytokines TNFα and IFNβ in a time course over ten hours, and performed RNA-seq. There was a high degree of reproducibility between the one female (Donor 2) and two male donors, with correlation coefficients between replicates ranging from 0.940 to 0.984.

We observed that the gene expression programs were highly stimulus-specific. Principal component analysis (PCA) revealed divergent gene expression patterns for the five stimuli (Fig 2.1b), and using K-means clustering we identified nine distinct gene expression clusters based on stimulus-specificity (Fig 2.1c). As one would predict from the established models of innate immune signaling networks, TNFα and Pam3CSK displayed similar patterns in the PCA and heatmap with only subtle differences, for instance in Clusters 5 and 6 where Pam3CSK induced more robust gene expression than TNFα. Consistent with the known induction of Type I IFNs by TLR3 signaling, poly(I:C) and IFNβ also induced similar responses, with the exception of a few genes in Clusters 1 and 3, presumably due to poly(I:C)'s activation of NFκB through TRIF. Lipid A was at the center of the PCA plot and induced virtually all the genes in the heatmap as one would predict, given that TLR4 signaling is known to activate multiple transcription factors through MyD88-dependent and independent pathways.

To further our understanding of the regulatory control of stimulus-specific gene expression programs, we performed an analysis of transcription factor binding motifs in promoters of induced genes (Fig 2.1d). Confirming our prior understanding of the signaling networks downstream of PAMPs and cytokines, NFκB motifs were enriched in Clusters 1, 2, 4, 5, and 8, and ISRE motifs were enriched in Clusters 7, 8, and 9. Having validated the stimulus-

specificity of gene expression programs in our macrophage system, we next used these transcriptomic phenotypes to understand the effects of Type I vs Type II IFN conditioning on the stimulus-responsiveness of human macrophages.

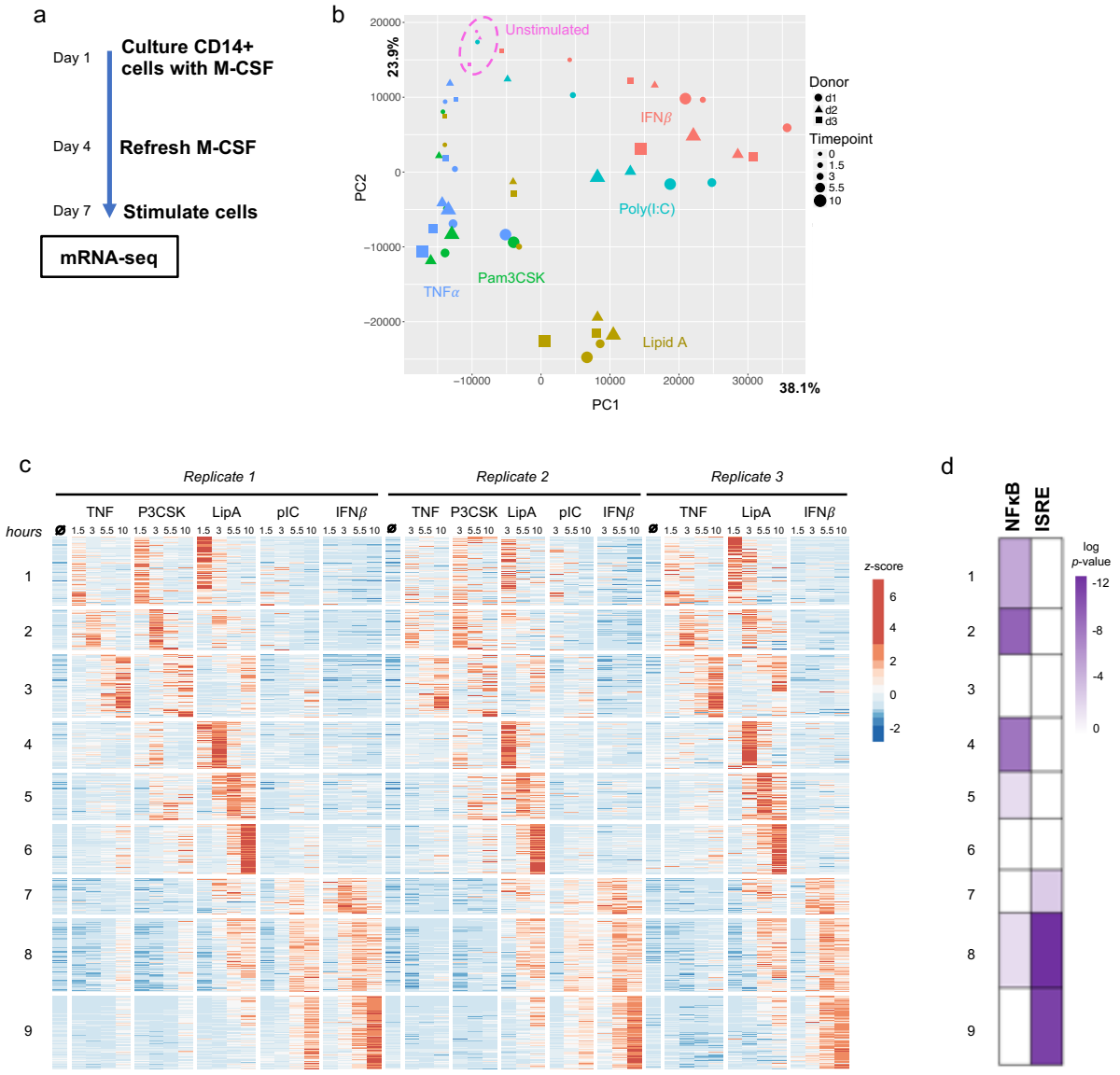

Figure 2.1: Stimulus-responsive gene expression in human macrophages. (a) Experimental design. (b) Principal component analysis of expressed genes in naïve macrophages under with five stimulation conditions. (c) Heat map of 1421 genes induced at least four-fold by any stimulus (FDR<0.05). (d) Transcription factor motif analysis for enrichment of NFκB and ISRE sequences within promoters of clustered genes.

Conditioning with Type I or II IFN differentially alters macrophage gene expression responses to stimuli

On day 4 of the M-CSF differentiation process, IFNβ or IFNγ was added and left in the medium through day 7 to condition the macrophages (Fig 2.2a). IFN-treated and untreated ("naïve") macrophages were then stimulated with the same five stimuli on day 7 in a 10-hour time course, and RNA-seq was performed on all samples. Altogether, RNA-seq libraries from 152 samples encompassing three biological replicates, three conditioning regimens, five stimuli, and five time points were analyzed.

Our first observation was that IFNβ and IFNγ had substantial and distinct effects on the basal transcriptomic state of macrophages, with a correlation coefficient of only 0.110 (Fig 2.S1a) at the zero-hour time point prior to the second stimulation. We found that IFNγ had a larger effect on basal gene expression than IFNβ, in agreement with the fact that our widely accepted protocol of using M-CSF for monocyte-to-macrophage differentiation produces macrophages whose basal transcriptome is dependent on tonic Type I IFN signaling[30]. These effects could be visualized by the distance between unstimulated samples in PCA plots of naïve, IFNβ-, and IFNγ-conditioned macrophages (Fig 2.2b, Fig 2.S2). Despite the overall discordance, we identified a subset of genes that were concordantly down-regulated. Ontology analysis (Fig 2.S1b) of these genes revealed roles in cell cycle, mitosis, and chromosome organization, suggesting that both IFNs inhibit macrophages from proliferating.

Although there were gene expression differences between Type I and II IFN at the basal state, we hypothesized that many effects of IFN conditioning would only be observed upon second simulation. To address this hypothesis, we developed an analytical workflow to address the complexity of the datasets. We first averaged counts across replicates, collapsed the four time

points into a maximum fold-induction for each stimulation condition, and then classified gene expression responses into three categories based on a gene's expression in the IFN-conditioned stimulation relative to the naïve stimulation using a four-fold threshold to define increase, decrease, or unchanged. We then performed K-means clustering based on this discrete

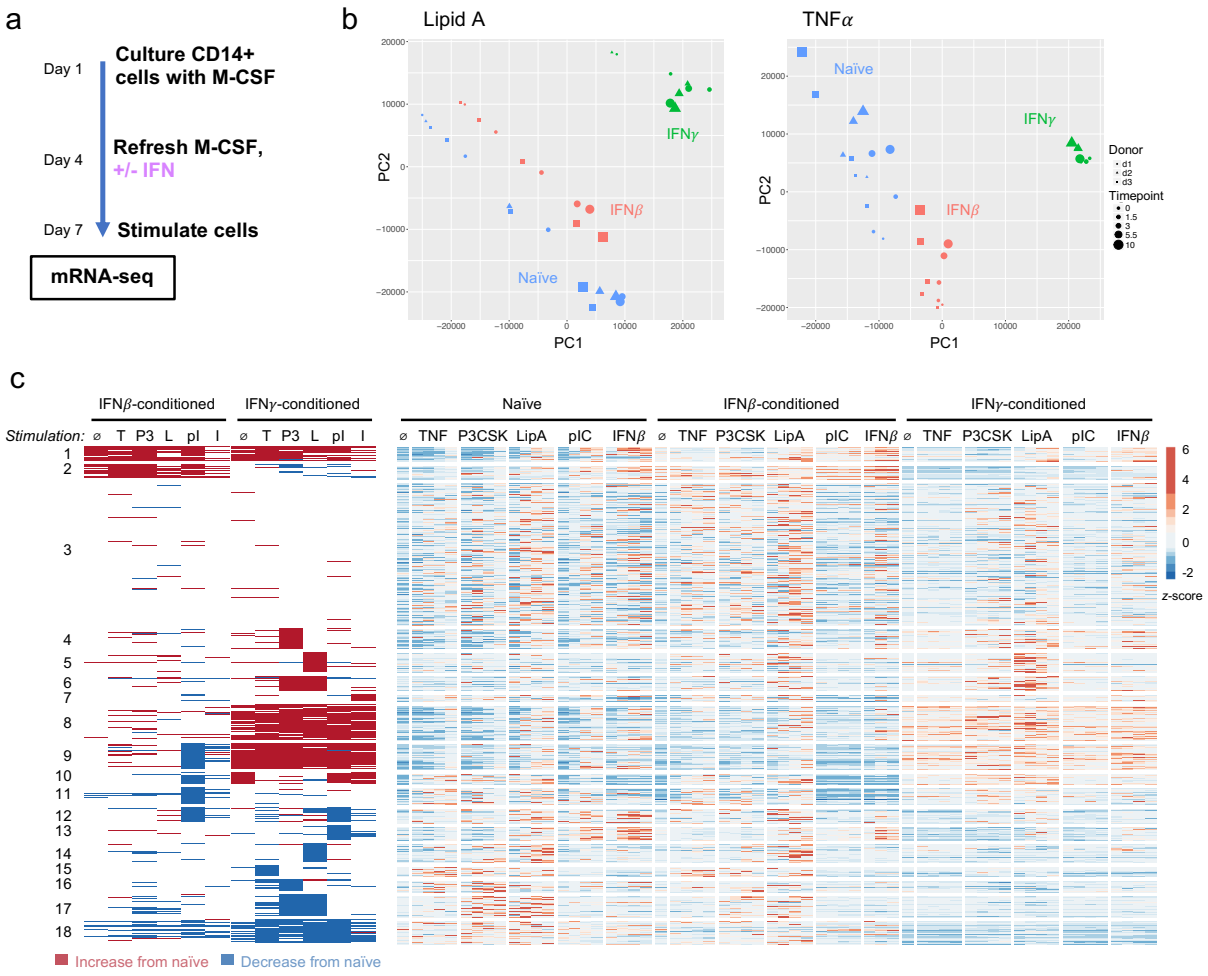

Figure 2.2: Type I and II IFN have gene-specific and stimulus-specific effects on gene expression. (a) Experimental design. IFNβ (200 U/ml) or IFNγ (10 ng/ml) were added on Day 4 of macrophage differentiation, 64 hours prior to stimulation. (b) Representative PCA plots for two of the five stimuli illustrating the differential effect of IFNβ vs IFNγ on stimulus-responsive gene expression. (c) Master heat map of all conditions. On the right, biological replicates are averaged, and z-scores for 1754 genes are represented. "ø" denotes unstimulated sample, and each stimulus contains four time points: 1.5, 3, 5.5, and 10 hours. On the left, the same data are represented as fold-change of IFN-conditioned relative to naïve. Red denotes genes where IFN conditioning results in a maximum induction that is 4-fold greater than naïve, blue denotes genes where IFN conditioning results in 4-fold decrease, and white denotes genes where IFN conditioning does not affect expression. Genes are grouped into 18 clusters by the effect of conditioning on stimulus-responsive gene expression.

classification system and identified 18 clusters that demonstrated the distinct effects of IFN conditioning on gene expression responses to each stimulus (Fig 2.2c, left). 1754 genes were included in the analysis: the 1421 genes that were inducible in naïve macrophages plus an additional 333 genes that met criteria for induction only when conditioned with an IFN.

We found that many genes fit our hypothesis of differential IFN effects that were observable only upon second stimulation. For instance, IFNγ and IFNβ had similar effects on the genes in Cluster 6 at the basal state ("⌀" column), yet IFNγ conditioning potentiated these genes' response to Pam3CSK and Lipid A whereas IFNβ conditioning had no effect. In another example, IFNβ conditioning of the genes in Cluster 10 had no effect on the basal expression but diminished their response to poly(I:C), whereas IFNγ conditioning increased both basal expression responses to poly(I:C).

To visualize these data without imposed thresholds, we plotted z-scores in a heatmap with the same clusters, also including individual time point information (Fig 2.2c, right). We found that the relationships we observed in the thresholded analysis on the left were preserved when visualized as z-scores on the right, though in some instances the thresholded analysis exaggerated the true quantitative effect. Overall, this analysis demonstrated that the differential effects of Type I and II IFN are both gene-specific and stimulus-specific. That is, for a given gene, IFNβ and IFNγ could have opposing effects on its response to one PAMP, but similar effects on its response to another PAMP.

IFN conditioning potentiates or diminishes the stimulus-responsiveness of genes not induced by IFN alone

We next focused on the genes whose expression was unchanged by IFN alone yet exhibited a potentiated or diminished response to second stimulation when conditioned with IFN. To further explore this group of genes we categorized all treatment conditions into nine categories: first by the effect of IFN treatment alone, i.e. “basal” gene expression, then by their conditioned response to stimulation compared to naïve (Fig 2.S3a, S3b). For this analysis, we used a two-fold threshold to more stringently identify genes that had “no change” in the basal state. We then used a four-fold threshold to categorize the stimulus-responsiveness of the conditioned macrophages as “unaffected,” “potentiated,” or “diminished” compared to naïve.

For each of the 1,754 inducible genes, ten cases were analyzed: two conditioning regimens and five stimulation conditions. At the basal state, we found that 65.4% of cases fell within a range of two-fold change and were considered “no change” by IFN treatment alone (Fig 2.3a). Of these cases that were unchanged, we found that 12.4% were nonetheless potentiated or diminished in their response to a second stimulation, with 8.9% of cases showing a diminished response, and 3.5% showing a potentiated response. Altogether 713 genes had responses to one or more stimuli that were potentiated or diminished by IFN conditioning.

We performed Ingenuity pathway analysis on these genes and found that canonical pathways related to immune functions were significantly overrepresented (Fig 2.S3c). For many of these pathways, IFNβ and IFNγ conditioning had a similar effect, frequently diminishing gene expression responses. For instance, IL-10 signaling and granulocyte adhesion and diapedesis were overrepresented in the genes diminished by conditioning with either IFN. On the other hand, some pathways were potentiated by IFNγ but diminished by IFNβ conditioning, such as dendritic cell maturation. This pathway analysis provided a general sense that many relevant

immunological pathways were affected by IFN conditioning, but did not identify any unifying functional themes.

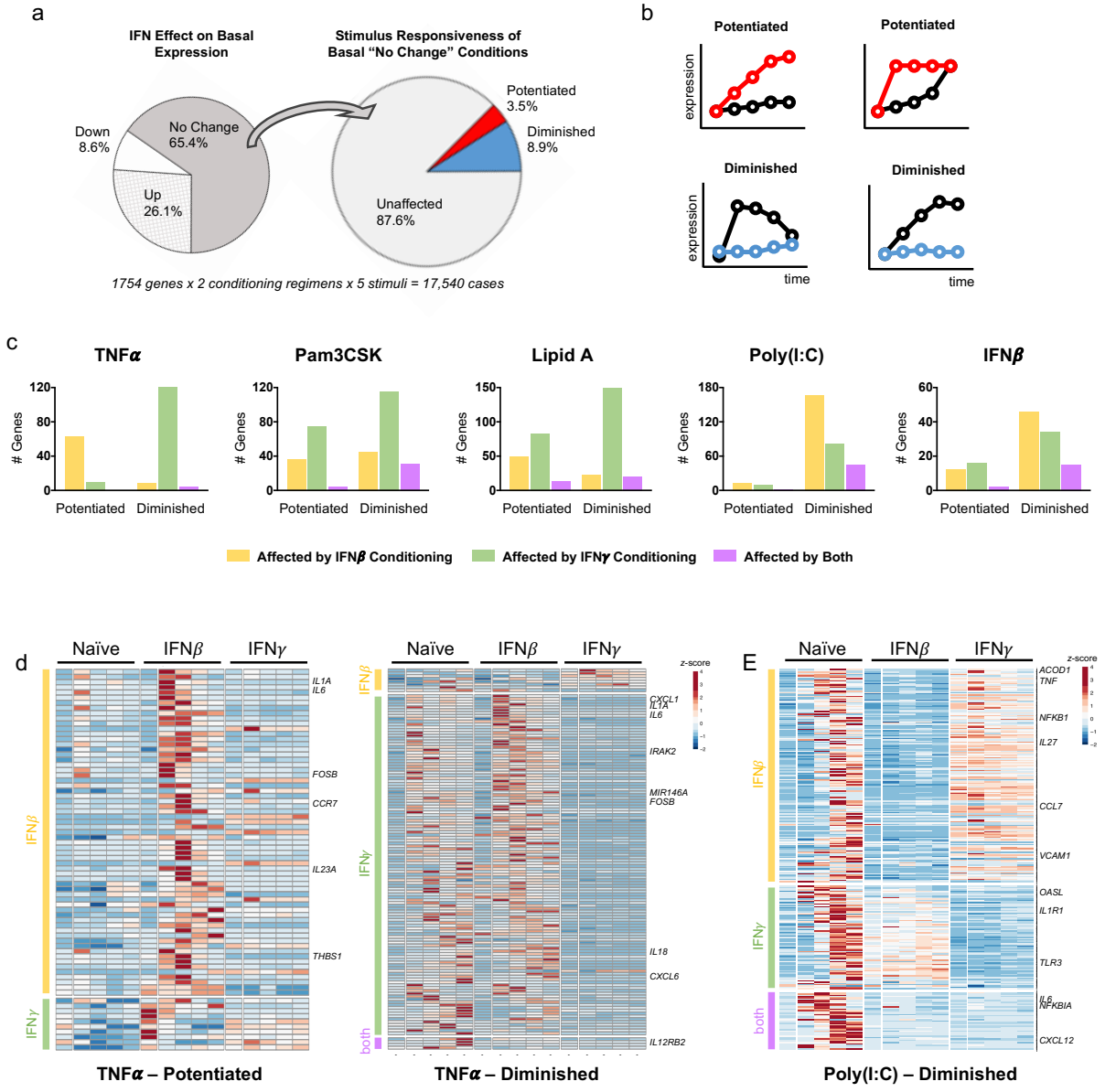

Figure 2.3: IFN conditioning potentiates or diminishes the stimulus-responsiveness of genes not induced by IFN alone. (a) Left: effect of either IFN prior to second stimulation (two-fold threshold). Right: of the genes not changed by IFN alone, the distribution of genes with potentiated or diminished response to a stimulus. (b) Cartoons illustrating the categories in right-hand pie chart of Fig 3A. Black = naïve, Color = conditioned. (c) Number of genes in each category, separated by stimulus. (d) TNFα-inducible genes that are unaffected by IFN alone but have a potentiated (left) or diminished (right) response after IFN conditioning, clustered by whether the criteria are met in IFNβ conditioning, IFNγ conditioning, or both. (e) Genes that are unaffected by IFN alone but have a diminished response to poly(I:C).

To obtain a more detailed understanding of the "no change / potentiated" and "no change / diminished" gene responses, we organized our analysis in a stimulus-centric manner (Fig 2.3c, S4). We found that macrophage responses to TNF were dramatically different in Type I vs Type II IFN conditioning. IFNγ potentiated only 10 genes but diminished 120 genes, while IFNβ potentiated 63 genes and diminished only 8 genes. This included many genes with well-defined roles in immune responses. For instance, IFNβ potentiated *IL1A*, *IL6*, and *CCR7*, while IFNγ diminished the TNF response of *IL1A*, *IL6*, *IL18*, and *CXCL1* (Fig 2.3d, full gene list in Supplemental Table 2). There were also very few genes that were potentiated or diminished by both IFNs. These results suggest that, for genes not directly induced by IFN, Type I and II IFNs have opposing and non-overlapping effects on macrophage responses to TNF.

Pam3CSK and Lipid A responses were also significantly affected by IFN conditioning (Fig 2.3c). In contrast to the TNF responses, one could not make a generalized statement about the direction of the effects of IFNβ or IFNγ on Pam3CSK and Lipid A responses. Instead, both IFNs are able to potentiate and diminish gene expression responses. A key observation, therefore, is that the effects of IFN conditioning on TLR2 and TLR4 responses are gene-specific. For instance, IFNγ had opposing effects on two chemokines that are reported to both recruit neutrophils [31]: in response to Pam3CSK, *CXCL3* was potentiated and *CXCL6* was diminished by IFNγ conditioning (Supplemental Table 2).

IFN conditioning had a striking effect on poly(I:C) and IFNβ responses (Fig 2.3c, 3e). Here, the vast majority of effects were of diminished gene expression response, demonstrating that both IFNs, classically produced in the context of viral infection, can tolerize macrophages and diminish their subsequent response to the viral dsRNA-mimetic poly(I:C) and additional antiviral cytokines. Importantly, however, only a minority of these genes were affected by both

IFNβ and IFNγ. In fact, many genes whose poly(I:C)-responsiveness was diminished by IFNβ were directly upregulated by IFNγ treatment (Fig 2.3e), suggesting that IFNγ directly induces a subset of the poly(I:C) gene expression program that is inhibited by IFNβ conditioning. The reverse is also true – many poly(I:C)-responsive genes that are also induced by IFNβ are inhibited by IFNγ conditioning.

IFN conditioning differentially alters cytokine and chemokine expression in a stimulus-specific manner

Many of the genes we identified in the analysis of "no change / potentiated" and "no change / diminished" groups were cytokines and chemokines. One widely accepted model of Type I and II IFN contends that IFNγ is pro-inflammatory while IFNβ is anti-inflammatory[16,17]. We therefore assessed the effect of IFN conditioning on transcript levels of the well-established inflammatory cytokines IL1β, IL6, and TNF and the anti-inflammatory cytokine IL10 in response to TLR stimulation (Fig 2.4). We found that some conditions were consistent with the proposed model, such as *IL6* and *TNF* in responses to Pam3CSK, where IFNγ primed macrophages for potentiated gene expression. We also saw that IFNγ conditioning dramatically suppressed *IL10* induction, while IFNβ preserved the expression of this anti-inflammatory cytokine. However, there were also conditions where the gene expression pattern did not conform to the proposed model. For instance, conditioning with either IFN completely abrogated the expression of *IL1B* and *IL6* in response to poly(I:C). Both IFNs also had parallel effects on potentiating *IL6* responses to Lipid A. These stimulus-specific effects of IFNβ and IFNγ challenge the idea that IFNγ is strictly pro-inflammatory and IFNβ anti-inflammatory.

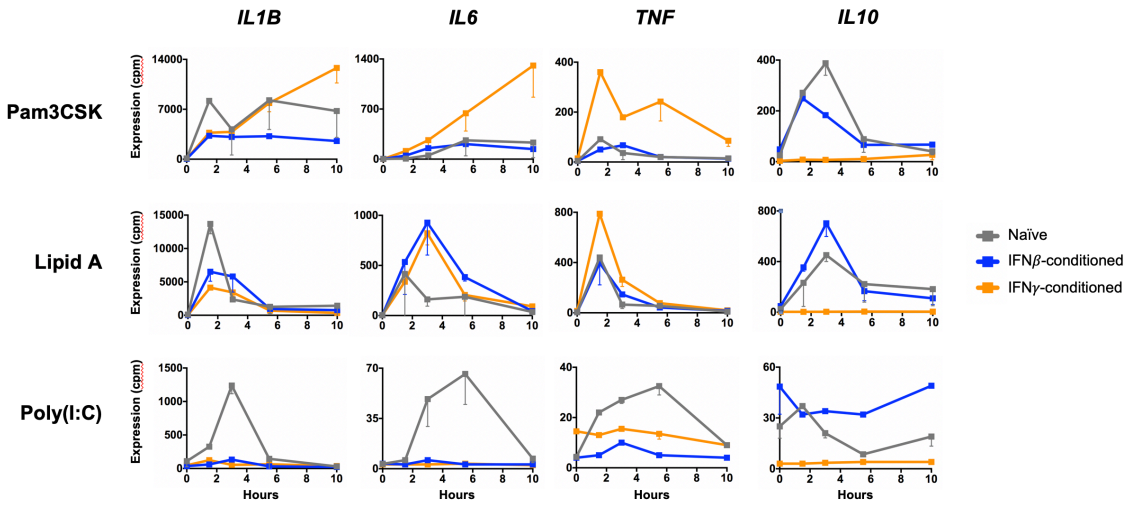

Figure 2.4: Effects of IFNβ vs IFNγ conditioning on inflammatory and anti-inflammatory cytokines.

Our genome-wide analysis also suggested that exposure to Type I or II IFN modulated subsequent chemokine production. We grouped chemokines by the primary cell type recruited[31] and assessed the effect of IFN conditioning on gene expression after TLR stimulation (Fig 2.S5). Even in naïve macrophages, without IFN conditioning, we observed stimulus-specific patterns of chemokine expression. TLR3 stimulation, for instance, induced more expression of lymphocyte and monocyte-recruiting chemokines than neutrophil-recruiting chemokines. Exposure to either IFN had relatively little effect on the basal expression of chemokines prior to second stimulus. However, in response to TLR2 or TLR4 stimulation, conditioning with IFNγ tended to enhance lymphocyte-recruiting chemokines and diminish chemokines involved in recruitment of monocytes and neutrophils. The majority of chemokines, however, had specific effects depending on the type of IFN and the type of PAMP. For instance, expression of *CXCL8* was potentiated by IFNγ but slightly diminished by IFNβ for TLR2 and TLR3 stimulation and unaffected by either IFN for TLR4 stimulation, again illustrating that the effects of IFN conditioning are gene-specific and stimulus-specific.

IFN conditioning differentially affects signaling networks

Having established that IFN conditioning has stimulus-specific effects on a genome-wide level as well as on relevant single genes, we next explored potential mechanisms for these phenomena. We considered that IFN conditioning may affect the strength of stimulus-responsive signaling networks and the chromatin environment of target genes, which together may result in stimulus- and gene-specific potentiation or reduction in gene activation.

To examine whether conditioning with IFN might affect PAMP and cytokine-responsive signaling networks, we assessed the impact of IFNβ and IFNγ conditioning on the basal expression of genes that encode the transcriptional networks downstream of TNFR, TLR2, TLR4, TLR3, and IFNAR (Fig 2.5a). We found a number of substantial changes in expression of both positive and negative regulators. For instance, *TLR3* expression was increased 5.1-fold and *IRF7* was increased 11.9-fold by IFNβ conditioning. The changes in TLR3 and IRF7 would predict increased responses to poly(I:C) when conditioned with IFNβ, but expression of *USP18*, a key negative regulator of IFNAR[32] was also dramatically increased, perhaps mitigating the poly(I:C) response.

The effect of IFNγ conditioning on IRF and ISGF3 signaling was particularly striking. IFNγ conditioning resulted in an 18.7-fold increase in *STAT1*, a 3.4-fold increase in *STAT2*, and a 1.4-fold increase in *IRF9*. These three proteins form the ISGF3 transcription factor downstream of IFNAR signaling, so one might anticipate that IFNγ potentiates IFNβ signaling. However, we also observed a 28.6-fold increase of SOCS1 and a 7.8-fold increase of SOCS3. These suppressors of cytokine signaling inhibit IFNAR signaling by blocking and dephosphorylating JAKs[33].

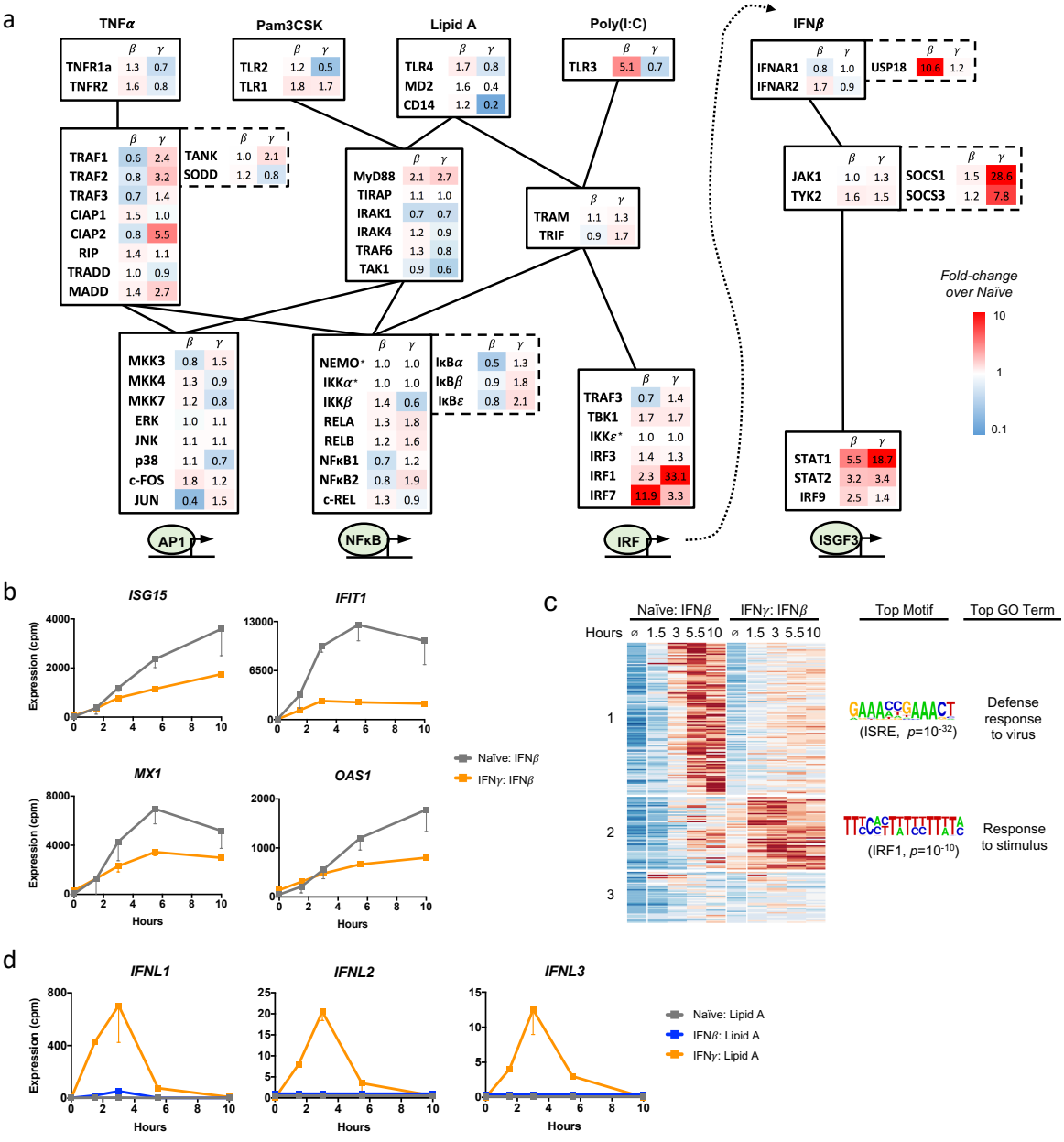

Figure 2.5: IFN conditioning alters innate immune signaling networks. (a) The effects of IFN conditioning on genes that participate in innate immune signaling are shown as fold-change over naïve expression. Genes are arranged in their known signaling networks, and negative regulators appear in dashed boxes. Asterisks (*) denotes genes with zero counts in all samples. (b) Conditioning with IFNγ diminishes responsiveness to IFNβ stimulation for four well-established IFNβ inducible genes, consistent with IFNγ upregulation of SOCS1 and SOCS3. (c) 205 IFNβ-inducible genes (>10-fold induction in naïve macrophages) are plotted in a heatmap and clustered by effect of IFNγ conditioning. Top results of transcription factor motif and gene ontology analyses are shown for the clusters affected by IFNγ conditioning. (d) Conditioning with IFNγ potentiates induction of IFNλ genes in response to Lipid A, consistent with IFNγ upregulation of IRF1.

Given the potentially conflicting activities of STAT and SOCS upregulation as well as the findings in Fig 2.3e, we explored at a more granular level whether IFNγ diminishes or potentiates IFNβ-responsive genes. We found that expression of the well-established IFNβ stimulated genes *ISG15*, *IFIT1*, *MX1*, and *OAS1* were potently diminished by IFNγ conditioning (Fig 2.5b). To address this question in an unbiased manner, we defined IFNβ responsive genes as any gene that was induced 10-fold or higher by IFNβ in naïve macrophages. We then performed K-means clustering of these 205 genes (Fig 2.5c) and found that 113 of them behaved similarly, with relatively unchanged basal expression but diminished responsiveness to IFNβ when conditioned with IFNγ (Cluster 1). However, we also identified a second cluster of genes in which IFNγ conditioning had the opposite effect of increasing expression both at basal and in response to IFNβ and a third cluster in which IFNγ had no effect.

To further understand the differences between the genes in these three clusters, we performed transcription factor motif and gene ontology (GO) analysis. The top GO term for the genes in Cluster 1 was "Defense response to virus," and the top transcription factor binding motif was for ISRE, the canonical binding motif for ISGF3. This suggested that the genes diminished by IFNγ conditioning were classical, antiviral IFNβ stimulated genes under the control of ISGF3, including *ISG15, IFIT1, MX1*, and *OAS1*, whose activity may be diminished by the induction of SOCS proteins. In contrast, the top GO term for Cluster 2 was a generic "response to stimulus," and the top transcription factor motif was for IRF1. These results suggested that the genes potentiated or unchanged by IFNγ conditioning are functionally different from those in Cluster 1 and that they are co-regulated by different transcription factors. The presence of IRF1 binding motifs in the promoters of Cluster 2 is particularly interesting given that *IRF1* expression

was upregulated 33-fold by IFNγ conditioning. This supports the possibility of crosstalk between IFNAR signaling and IRF1 that synergistically activates a subset of IFNβ stimulated genes.

IRF1 is also known to play a key role in the regulation of Type III IFN (IFNλ) expression[34,35]. Indeed, we observed that IFNγ conditioning dramatically up-regulated the IFNλ genes *IFNL1*, *IFNL2*, and *IFNL3* in response to Lipid A (Fig 2.5d). In the naïve condition these Type III IFN genes are not induced at all by any stimulus. Interestingly, IFNγ's ability to potentiate IFNλ expression, which was reproducible between biological replicates, was specific only to Lipid A. Pam3CSK, poly(I:C), TNF, and IFNβ stimulation did not induce IFNλ expression in any condition. This suggests a complex regulation of IFNλ expression involving IRF1 but possibly also requiring other factors that are only activated upon TLR4 stimulation.

IFN conditioning differentially affects chromatin landscape

Whereas changes in signaling networks are likely to result in stimulus-specificity, changes in the epigenome, with gains and losses of accessible enhancers, may be a mechanism for the gene-specific effects of cytokine conditioning. We therefore sought to define the effects of IFNβ and IFNγ on the chromatin landscape by measuring DNA accessibility. On Day 7, prior to secondary stimulation, we performed ATAC-seq on naïve, IFNβ-conditioned, and IFNγ-conditioned macrophages in biological replicate. We found that conditioning with either IFN resulted in differential ATAC-seq signals corresponding to gains and losses of transposase-accessible sites. IFNγ conditioning resulted in 4.5-times more differential peaks than IFNβ (9562 versus 2085), and 705 of these peaks were overlapping.

To assess the biological relevance of these ATAC-seq peaks, we surveyed their genomic distribution relative to transcription start sites (TSSs). We found that both IFNβ and IFNγ peaks

were distributed near TSSs for annotated genes (Fig 2.6a), with 95% of both IFNβ and IFNγ peaks falling within 100 kilobases (kb) of a TSS. Additionally, 19% of IFNβ peaks and 12% of IFNγ peaks were found in potential promoter regions, within 1 kb of a TSS. The proximity of ATAC-seq peaks to gene TSSs suggested that these gains and losses in chromatin accessibility

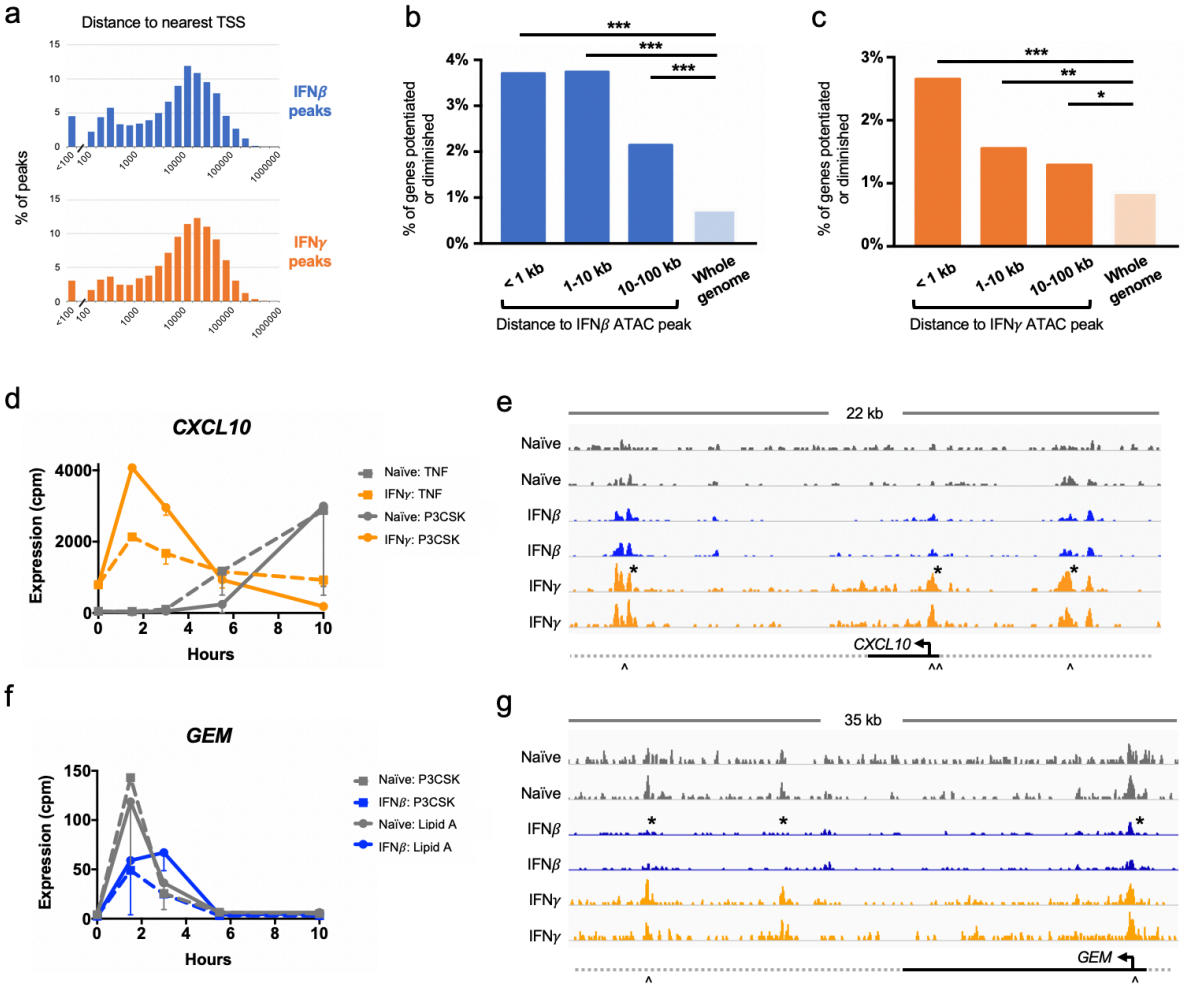

Figure 2.6: IFN conditioning affects chromatin landscape. (a) Distribution of the distance from differential ATAC-seq peaks to the nearest TSS. (b,c) Relationship of differential ATAC-seq peaks to gene expression. Based on RNA-seq data, 419 and 493 genes were categorized as potentiated or diminished by IFNβ and IFNγ, respectively. Regions near ATAC-seq peaks are enriched for these genes. (* = $p < 0.01$, ** = $p < 0.001$, *** = $p < 0.0001$) (d) Example of gene potentiated by IFNγ, with more rapid response to TNF and Pam3CSK when primed. (e) ATAC-seq tracks at CXCL10 locus in replicate, showing three peaks that are gained by IFNγ conditioning. Asterisks (*) denote differential peaks, and arrows (^) denote NFκB motifs. (f) Example of gene diminished by IFNβ, with more delayed and decreased response to Pam3CSK and Lipid A after IFNβ conditioning. (g) ATAC-seq tracks at GEM locus show three peaks that are lost in with IFNβ conditioning. Asterisks (*) denote differential peaks, and arrows (^) denote NFκB motifs.

were not randomly distributed in the genome but may correspond to *cis*-acting gene regulatory elements.

Next, we investigated whether there was a correlation between these ATAC-seq peaks and our gene expression data. We utilized the previously described nine categories of gene expression responses (Fig 2.S3a) and focused on four conditions relevant to the ATAC-seq analysis. We inferred that if an enhancer was gained or lost by IFN conditioning, the resultant gene expression response to stimulus would fall into one of four categories: "no change / potentiated," "no change / diminished," "up / potentiated," or "down / diminished." 419 and 493 genes fell into these categories for one or more stimuli for IFNβ and IFNγ, respectively.

We then asked whether the regions around ATAC-seq peaks were enriched for these potentiated or diminished genes. We found that, compared to the whole genome, the regions around ATAC-seq differential peaks were significantly enriched, with a trend towards greater enrichment at the most proximal genes (Fig 2.6b, 6c). Genomic regions within 10kb of a differential ATAC-seq peak were enriched 5.1-fold in IFNβ conditioning and 3.1-fold in IFNγ conditioning. Interestingly, despite the enrichment near ATAC-seq peaks, the majority of potentiated or diminished genes still fell in regions of the genome that are not near an ATAC-seq peak. This may reflect the difficulty in relating enhancer function to a particular gene, or may suggest that other mechanisms not assayable by ATAC-seq are responsible for their gene expression.

To corroborate our genome-wide analyses, we investigated single gene examples where differential ATAC-seq peaks were correlated with gene expression changes. *CXCL10* is an NFκB target gene and is induced by TNF and Pam3CSK in naïve macrophages at late time points (Fig 2.6d). When conditioned with IFNγ, *CXCL10* was more highly expressed at basal

steady-state, and its response to TNF and Pam3CSK was much more rapid, peaking at (or before) 1.5 hours. ATAC-seq analysis revealed three peaks near *CXCL10* that were gained in IFNγ conditions, one at the promoter, one 5.1 kb upstream, and one 11.4 kb downstream of the TSS (Fig 2.6e). Each of these peaks contained at least one NFκB binding motif, strongly suggesting a mechanism where IFNγ renders these latent enhancers more accessible and *CXCL10* primed to respond more rapidly to NFκB-activating stimuli.

Similarly, the expression of *GEM* in response to TNF and Pam3CSK is diminished by conditioning with IFNβ (Fig 2.6f). *GEM* is also an NFκB target gene, and IFNβ conditioning results in the loss of three ATAC-seq peaks, one in the promoter, and two downstream (Fig 2.6g). The ATAC-seq peaks at the promoter and 17.8 kb downstream of the TSS contain NFκB binding motifs, suggesting a mechanism where IFNβ conditioning results in silencing of previously active NFκB enhancers. These examples and our genome-wide analysis both imply that the differential peaks identified by ATAC-seq were biologically relevant and co-localized with genes whose expression is potentiated or diminished by IFN conditioning.

Discussion

Here we have reported the results of an unbiased, genome-wide analysis of the effects of Type I vs Type II IFN conditioning on the stimulus-responsive gene expression patterns of primary human macrophages. An essential feature of this study was the use of a sequential conditioning and stimulation approach. By examining not only the direct consequences of IFN treatment but focusing on subsequent responses to pathogen-associated stimuli, we gained novel insight into the gene-specific and stimulus-specific effects of Type I and II IFN. Our approach enabled us to identify subtle but important differences between Type I and II IFN, including their

opposing effects on TNF-inducible genes, the negative regulation of antiviral Type I IFN-stimulated genes by IFNγ conditioning, and the potentiation of Type III IFN genes by IFNγ. We found that the IFNs modulate macrophage function in a highly nuanced manner that is not uniformly pro- or anti-inflammatory. These immune regulatory functions of IFN could not be gleaned by examining only direct IFN-induced gene expression programs, thus highlighting the importance of the sequential conditioning-stimulation approach.

One of our most notable findings was that IFNγ and IFNβ have opposing effects on macrophage responses to TNF. IFNγ substantially diminished TNF responses, with 120 genes falling into our "no-change / diminished" category. This was a surprising finding given that IFNγ-conditioned macrophages are thought to be more pro-inflammatory, and TNF is a prototypical inflammatory cytokine. The mechanism of this phenomenon is uncertain; our analysis of signaling networks was unrevealing in this respect as a number of factors in the TNF signaling pathway such as *TRAF1*, *TRAF2*, *CIAP2*, and *MADD* were actually increased by IFNγ (Fig 2.4a). One possibility, since TNF is an IFNγ target gene [36] and is upregulated three-fold by IFNγ in our dataset, is that IFNγ conditioning leads to an increase in tonic TNF which tolerizes macrophages to additional TNF[37]. Together with a recent study showing that IFNγ restricts the induction of some inflammatory cytokines in response to TLR4 stimulation[38], our data challenges the generalization that IFNγ makes macrophages more inflammatory.

In contrast to IFNγ, IFNβ conditioning generally potentiated macrophage responses to TNF. This is in agreement with previous observations that TNF and IFNβ synergistically induce gene expression, possibly through a STAT1-independent ISGF3 complex[18,39]. Additionally, a recent study showed that conditioning with both IFNβ and TNF potentiates responses to LPS compared to TNF conditioning alone[40]. Our data thus provides additional support for the model

where TNF and IFNβ can cooperatively regulate macrophage gene expression and extends this notion to describe that prior IFNβ exposure enables TNF to potently activate a new set of target genes. The contrasting effects of Type I and II IFN on TNF gene expression responses are highly relevant for our understanding of immune responses *in vivo*, where all three cytokines could be present simultaneously, and cautions against the simple characterization of Type I IFN as being anti-inflammatory. The regulatory logic controlling the interplay of these key cytokines deserves further attention.

While IFNβ and IFNγ had opposing effects on TNF responses, conversely, we found that they had similar effects on poly(I:C) and IFNβ responses (Figs 3f, 3g, 4b, 4c). Both IFNs diminished these gene expression programs, demonstrating the importance of negative feedback loops in the IFN regulatory system. Indeed, a number of negative regulators, including SOCS1, SOCS3, and USP18[32,33,41], are upregulated by IFN conditioning. Physiologically, it makes sense that prolonged Type I IFN stimulation tolerizes cells to subsequent Type I IFN stimulation. However, the repressive effect of IFNγ conditioning on subsequent response to Type I IFN stimulation is noteworthy. It suggests that when IFNγ is dominant or pre-existent, as in an intracellular bacterial infection, there is a functional advantage to silencing the antiviral portion of the IFNβ transcriptome, which may be superfluous in this context. Together with prior work showing a similar inhibition in the reverse direction where IFNβ inhibits IFNγ gene expression[24], one can begin to conclude that Type I and II IFN gene expression programs are cross-repressive when macrophages are conditioned in one and then exposed to the other.

Another intriguing and novel finding was that IFNγ conditioning dramatically potentiated induction of Type III IFN genes in response to Lipid A. This result was particularly noteworthy for its specificity for TLR4 and not TLR2 or TLR3 stimulation. That TLR4, typically a receptor

for bacterial PAMPs and host-derived DAMPs, results in IFNλ expression under IFNγ conditions suggests that IFNλ might play additional roles beyond its described antiviral function at epithelial barriers[42]. The specificity for TLR4 stimulation also raises questions about the mechanisms controlling IFNλ expression. The *IFNL1* promoter shares many features with *IFNB,* and it is thought that NFκB and IRFs, particularly IRF1, cooperatively induce gene expression of IFNλ genes[34,35,42]. IRF1 is highly upregulated by IFNγ conditioning, suggesting a potential mechanism for IFNγ's potentiation of IFNλ induction. Additionally, a recent study found that in human monocyte-derived dendritic cells, *IFNL1* expression was p38 MAPK-dependent[43]. This may provide an explanation for TLR4-specificity, but further studies into the mechanisms of IFNλ regulation are clearly warranted.

Many prior studies have implicated Type I and II IFNs in regulating expression of cytokines and chemokines, with wide-ranging clinical implications such as viral-bacterial co-infections, host response to leprosy, response to DAMPs, and connections to autoimmunity. The contribution of our study to this field is to show that chemokines and cytokine production is modulated by IFN conditioning in a stimulus-specific manner. It is overly simplistic, for instance, to say IFNγ potentiates inflammatory cytokines when poly(I:C) stimulation actually induces much less *IL1B* and *IL6* when conditioned with IFNγ. Here we have addressed specificity for synthetic TLR stimuli. By extension, our findings imply that *in vivo* there will also be specificity for different pathogens. For example, although IFNβ increases susceptibility to *streptococcus* following influenza infection due to an impairment of neutrophil recruitment[44], this mechanism may not hold true for gram negative bacteria or fungi, which activate the immune system through different receptors.

In this study, we also explored potential mechanisms of context-specific responses. We found that Type I and II IFNs altered both the basal signaling network and the chromatin accessibility of cells and described examples of potentiated and diminished gene expression that may be a consequence of these perturbations. These findings support prior models that posit that signaling networks encode stimulus information into the activity of transcriptional effectors, and epigenetic states decode that information into a context-dependent, stimulus-specific gene-expression program and biological response[45]. We show here that both the encoding and decoding steps are affected by cytokine context. It is likely that stimulus-specificity is driven by alterations in signaling networks while gene-specific differences are a result of epigenetic transcriptional control, and the interdependent relationship between the two is what gives rise to highly tunable, context-specific immune responses.

Indeed, *in vivo,* macrophages are simultaneously exposed to multiple cytokines that may also vary in dose and duration of exposure. The space of possible conditions is in fact too large to systematically probe experimentally, and therefore one goal of studies such as the present, that characterize well-defined points within this space, is to catalyze the development of data-driven and mechanistic computational models (e.g. Cheng et al 2017)[46] to fill in the regulatory landscape. Such models may then also provide analytical frameworks without the use of intuitive thresholds we have employed here to analyze high-complexity data and define categories such as expressed, inducible, potentiated, or diminished genes. However, what constitutes a feasible strategy for developing such models that account for condition- or context-dependent states of signaling systems and epigenomic responsiveness requires further theoretical work before they can be deployed. The present dataset and the scope, range, and granularity of the observations should prove useful in guiding such computational modeling investigations.

Supplemental Figures

a

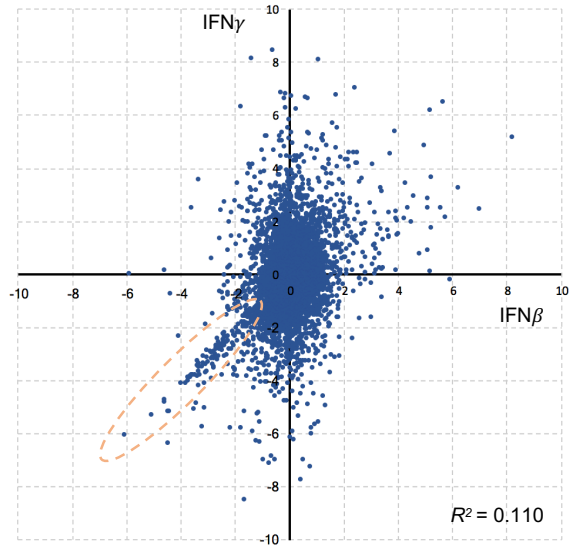

b

GO term	*p*-value
Cell cycle	6.86×10^{-54}
Mitotic cell cycle	4.34×10^{-42}
Chromosome segregation	1.25×10^{-32}
Cell division	3.77×10^{-32}
Chromosome organization	1.67×10^{-25}

Figure 2.S1: IFN effects on basal gene expression (a) Scatter plot of IFNβ vs IFN-γ conditioning effect on basal (pre-stimulation) expression, each point representing one gene. Axes are log(2) fold-change of IFN-conditioned gene expression over naïve gene expression. Concordantly down-regulated genes are highlighted. **(b)** Gene ontology analysis of concordantly down-regulated genes, top five non-redundant results.

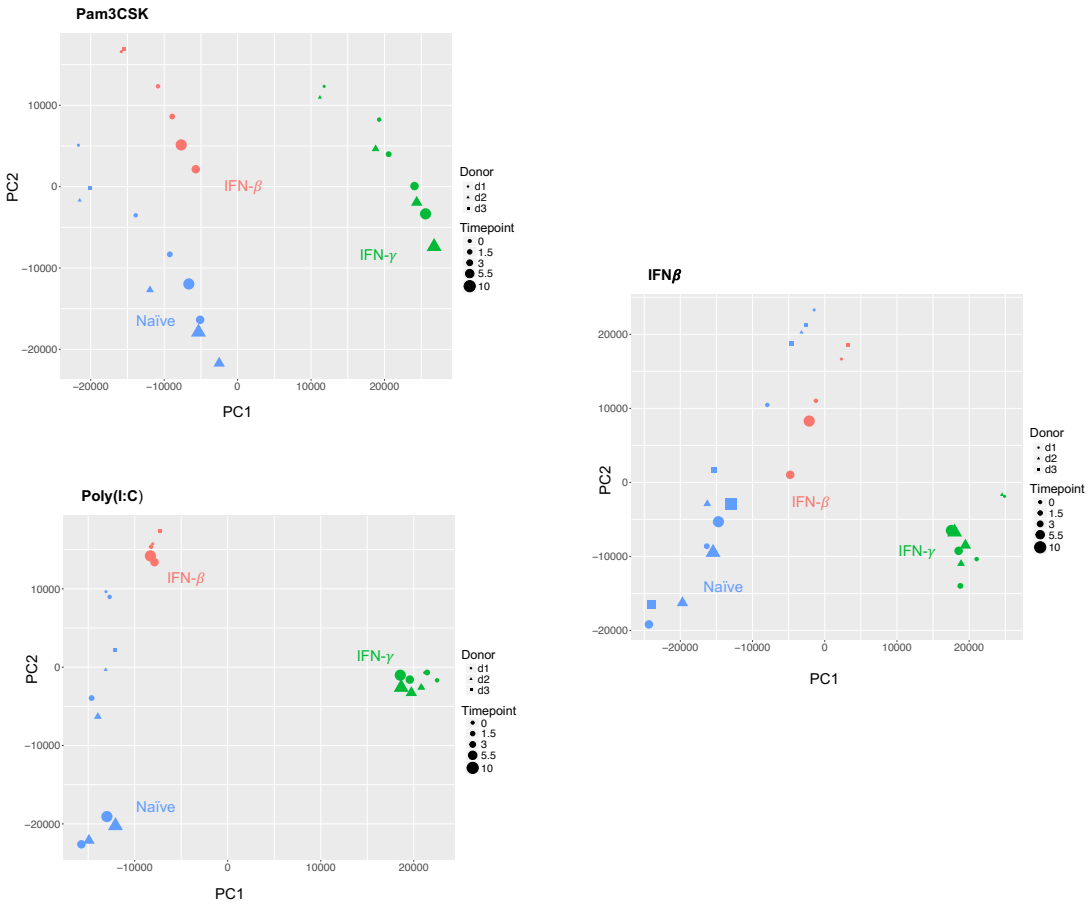

Figure 2.S2: PCA plots for Pam3CSK, poly(I:C), and IFN-β stimulation conditions illustrate the differential effect of IFNβ vs IFNγ conditioning on stimulus-responsive gene expression. Biological replicates are denoted by shape, and time points are denoted by size with the smallest markers showing the effect of IFN conditioning without second stimulation.

a

Basal Change (2-fold)	Change in Inducibility (4-fold)
No Change	Unaffected
	Potentiated
	Diminished
Up	Unaffected
	Potentiated
	Diminished
Down	Unaffected
	Potentiated
	Diminished

b

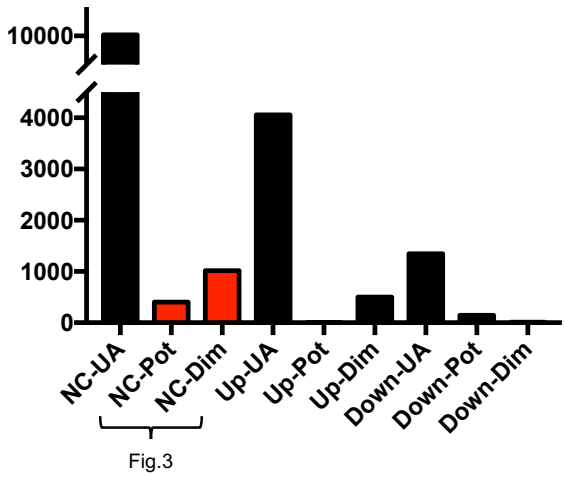

c

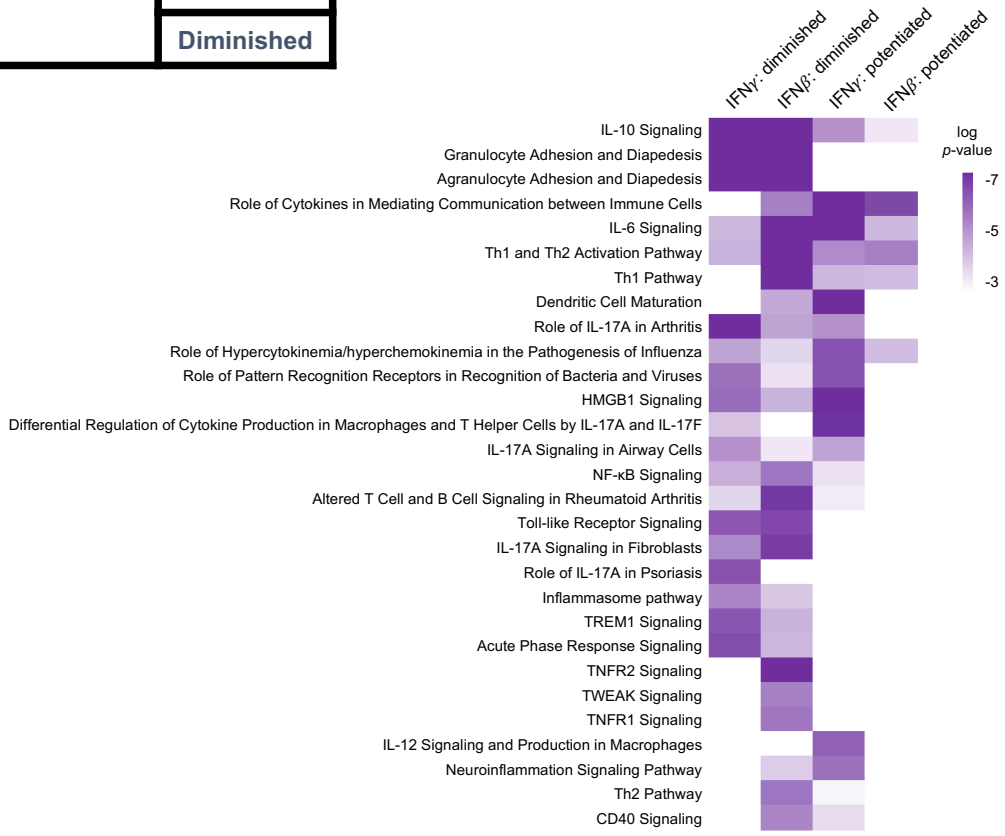

Figure 2.S3: Nine category analysis (a) Gene expression thresholds used to categorize every combination of conditioning regimen, stimulus, and gene into nine categories. **(b)** Distribution of the 17,540 cases across the nine categories. Highlighted categories were further analyzed in Fig.3. **(c)** Ingenuity Pathway Analysis of the genes falling into "no change / diminished" and "down / diminished" or "no change / potentiated" and "up / potentiated" categories, separated by IFN conditioning. The canonical pathways with log(*p*-value) < -5 in at least one category are ordered by hierarchical clustering.

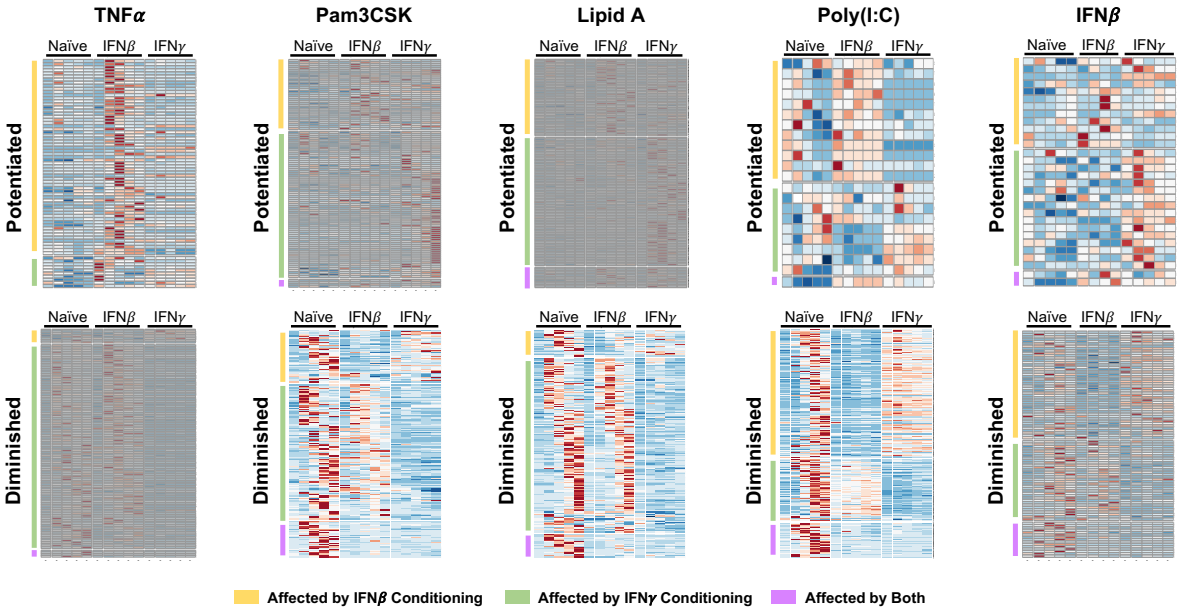

Figure 2.S4: Heatmaps of all genes that are unaffected by IFN alone but have a potentiated (top) or diminished (bottom) response to second stimulation, clustered by whether the criteria are met in IFNβ conditioning, IFNγ conditioning, or both.

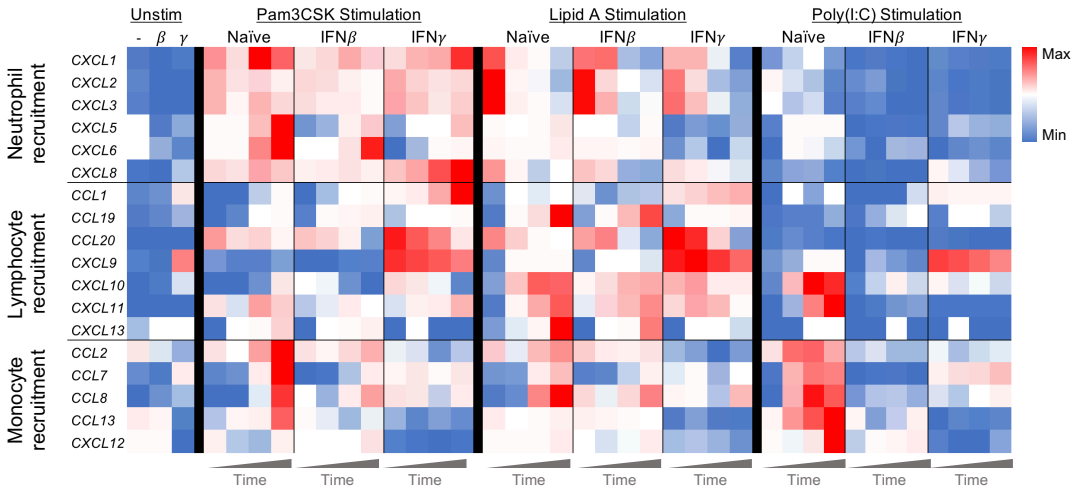

Figure 2.S5: Heat map of stimulus-responsive chemokines, grouped by primary cell type recruited (Mantovani et al., *Nat Rev Immunology* 2006), and the effect of IFN conditioning on their response to TLR ligands Pam3CSK, Lipid A, and poly(I:C).

Materials and Methods

Macrophage cell culture

Whole blood was obtained from healthy donors with written informed consent prior to inclusion in the study according to protocol #11-001274 approved by the UCLA Institutional Review Board. Peripheral blood mononuclear cells (PBMCs) were isolated using Ficoll (GE Healthcare, Piscataway, NJ) gradient centrifugation. Monocytes were purified by positive selection of CD14+ cells using MACS CD14 microbeads (Miltenyi Biotec, Cologne, Germany) from PBMCs according to manufacturer's instructions. Macrophages were derived from CD14+ positively-selected monocytes by differentiation for seven days in RPMI (Thermo Fisher Scientific, Waltham, MA) with 10% fetal bovine serum (Omega Scientific, Tarzana, CA), glutamine, and penicillin-streptomycin supplemented with 50 ng/ml recombinant human M-CSF (CHO-derived, R&D Systems, Minneapolis, MN) at a concentration of 0.5 x 10^6 monocytes/ml in 24-well plates (Corning Inc., Corning, NY). On day four, 64 hours prior to stimulation, a $1/5^{th}$ volume of fresh medium was added containing conditioning cytokines 10 ng/ml IFNγ (BD Biosciences, La Jolla, CA) or 200 U/ml IFNβ (PBL Assay Science, Piscataway, NJ). On Day 4 M-CSF was also refreshed by adding an extra 25 ng/ml (final concentration) on top of any exhausted M-CSF.

Stimulation and RNA preparation

On day 7, a $1/6^{th}$ volume of fresh medium with stimuli were added to the following final concentrations: 100 ng/ml Lipid A (InvivoGen), 5 ng/ml TNFα (BD Biosciences), 100 ng/ml Pam3CSK (InvivoGen, San Diego, CA), 20 µg/ml poly(I:C) (InvivoGen), 200 U/ml IFNβ (PBL Assay Science). Cells were collected at 1.5, 3, 5.5, and 10 hours post stimulation by lysis with

TRIzol reagent (Life Technologies, Carlsbad, CA). Total RNA was purified with DIRECTzol kit (Zymo Research, Irvine, CA) according to manufacturer's instructions.

Next generation sequencing

For RNA-seq, strand-specific libraries were generated from 500 ng total RNA using KAPA Stranded mRNA-seq Library Preparation kit (KAPA Biosystems, Wilmington, MA) according to the manufacturer's instructions. Resulting cDNA libraries were single-end sequenced with a length of 50bp on an Illumina HiSeq 2000 (Illumina, San Diego, CA).

ATAC-seq libraries were prepared as previously described[47]. Briefly, cells were dissociated with Accutase (Thermo Fisher Scientific), and 50,000 cells were used to prepare nuclei. Cell membrane was lysed using cold lysis buffer (10mM Tris-HCl pH7.5, 3mM MgCl2, 10mM NaCl and 0.1% IGEPAL CA-630). Nuclei were pelleted by centrifugation for 10 minutes at 500 x *g*, and suspended in the transposase reaction mixture (25 µl of 2X TD Buffer (Illumina), 2.5 µl of TD Enzyme 1 (Illumina), and 22.5 µl of nuclease-free water). The transposase reaction was performed for 30 minutes at 37 ℃ in a thermomixer shaker. Then, fragmented DNA in the reaction was purified using MinElute PCR purification kit (QIAGEN, Hilden, Germany). The purified DNA fragments were amplified by PCR to obtain ATAC-seq libraries with Illumina Nextera sequencing primers. The libraries were purified using MinElute PCR purification kit (QIAGEN) and quantified using KAPA Library Quantification Kit (KAPA Biosystems). The libraries were single-end sequenced with a length of 50bp on an Illumina HiSeq 2500.

Global RNA-seq analysis

The low quality 3'ends of reads were trimmed (cutoff q=30), and remaining adapters

sequences were removed using cutadapt[48]. Reads were aligned to the hg19 genome build with STAR[49] with the following options: --outFilterMultimapNmax 20, --alignSJoverhangMin 8, --alignSJDBoverhangMin 1, --outFilterMismatchNmax 999, --outFilterMismatchNoverLmax 0.04, --alignIntronMin 20, and --alignIntronMax 1000000 --seedSearchStartLmax 30. Only uniquely mapped reads with a mapping quality ≥ 30 were kept for further analysis, using samtools. Read counts were normalized for library size and transcript length by conversion to CPM and RPKM. Genes below an expression threshold of 4 RPKM in all samples were excluded from downstream analysis. Biological replicates of "unstimulated" samples were averaged and considered to be the zero-hour time point or basal expression. The zero-hour data were then placed in a log2-transformed bimodal distribution using the Mix-Tools Package[50]. The first equivalent overlap of the two distributions was 2.2 CPMs, and this pseudo-count was added to all expressed genes. Induced genes were defined as those with a 4-fold increase over basal by any stimulation with FDR threshold of 0.01 calculated with edgeR[51]. Principle components were calculated with the prcomp package[52] and plotted with ggplots[53]. K-means clustering was performed with the mclust package[54] with spherical clustering and constant shape and orientation, and the choice of number of clusters was based on the plateau of logliklihood scores. The linear z-score transformation of the CPM values across all samples were plotted as heatmaps using heatmap2 and pheatmap packages[55].

Thresholds for Nine-Category analysis

The effect of conditioning on basal gene expression ("up," "down," or "no-change") was determined by calculating fold change of the IFN-conditioned basal over naïve basal, with a threshold of two-fold and FDR of 0.01. Next, the effect of conditioning on inducible gene

expression was determined. For cases of "no-change" at basal the direct fold-change was calculated at each time point as the change of conditioned-stimulated over naïve-stimulated gene expression. For each case, the greatest absolute change across time-points was used to categorize the effect of conditioning on inducible gene expression, using a threshold of four-fold and FDR of 0.01, as "potentiated," "diminished," or "unaffected." For cases of "up" or "down" at basal the change in fold change was calculated at each time point to increase the stringency of the analysis for genes already differentially expressed at the basal state. For each case, the greatest change in fold-change across time-points was then used to categorize the effect of conditioning on inducible gene expression, using a threshold of four-fold and FDR of 0.01, as "potentiated," "diminished," or "unaffected." Altogether this yielded nine categories: three basal categories, each with three inducibility subcategories (Fig 2.S3).

Ingenuity Pathway Analysis

Gene lists falling into "no change / diminished" and "down / diminished" or "no change / potentiated" and "up / potentiated" categories from the Nine Category analysis (above) were uploaded to the Ingenuity Pathway Analysis (IPA) tool (QIAGEN). Default settings were used to obtain enrichment scores for canonical pathways, and *p*-values were calculated by Fisher's exact test. Hierarchical clustering was performed using default IPA settings.

Transcription factor motif and Gene Ontology analysis

Transcription factor motif analysis was performed using HOMER[56] with JASPAR matrices for known NFκB and ISRE motifs to derive *p*-values for overrepresentation of these motifs within a defined promoter region of -600bp to +50bp. Search options included absolute

match length of 8, 10, 12, 14, or 16bp; allowed mismatch of 4bp; and all expressed genes as the background for control. Gene ontology (GO) analysis was performed using the PANTHER database with entire human genome as background[57].

ATAC-seq analysis

ATAC-seq reads were aligned to the hg38 genome build using bowtie2 with default parameters except --very-sensitive and --non-deterministic options and filtered based on mapping score (MAPQ ≥ 30) by Samtools version 1.3.1[58]. Duplicated reads were removed using Picard MarkDuplicates (version picard-tools-2.1.0). MACS2 version 2.1.0 was used to identify peaks for each sample individually with default settings except FDR of 0.01[59]. These peaks were merged to generate a single reference peak file, and the number of reads that fell into each peak was counted using bedtools multicov[60]. DESeq2 was used to normalize and identify differential peaks across treatment conditions with p-value <0.05[61]. ChipPeakAnno[62] was used to assess overlap of differential peaks and relate peaks to annotated transcription start sites using default options except --PeakLocForDistance = “middle”. NFκB motifs within ATAC-seq peaks were defined by the consensus sequence GGRNNN(N)YCC.

Bibliography

1 Ginhoux, F., Schultze, J. L., Murray, P. J., Ochando, J. & Biswas, S. K. New insights into the multidimensional concept of macrophage ontogeny, activation and function. *Nat Immunol* **17**, 34-40, doi:10.1038/ni.3324 (2016).

2 Murray, P. J. & Wynn, T. A. Protective and pathogenic functions of macrophage subsets. *Nat Rev Immunol* **11**, 723-737, doi:10.1038/nri3073 (2011).

3 Murray, P. J. *et al.* Macrophage activation and polarization: nomenclature and experimental guidelines. *Immunity* **41**, 14-20, doi:10.1016/j.immuni.2014.06.008 (2014).

4 Xue, J. *et al.* Transcriptome-Based Network Analysis Reveals a Spectrum Model of Human Macrophage Activation. *Immunity* **40**, 274-288, doi:10.1016/j.immuni.2014.01.006 (2014).

5 Glass, C. K. & Natoli, G. Molecular control of activation and priming in macrophages. *Nature Immunology* **17**, 26-33, doi:10.1038/ni.3306 (2015).

6 Ostuni, R. *et al.* Latent enhancers activated by stimulation in differentiated cells. *Cell* **152**, 157-171, doi:10.1016/j.cell.2012.12.018 (2013).

7 Qiao, Y. *et al.* Synergistic Activation of Inflammatory Cytokine Genes by Interferon-γ-Induced Chromatin Remodeling and Toll-like Receptor Signaling. *Immunity* **39**, 454-469, doi:10.1016/j.immuni.2013.08.009 (2013).

8 Piccolo, V. *et al.* Opposing macrophage polarization programs show extensive epigenomic and transcriptional cross-talk. *Nat Immunol*, doi:10.1038/ni.3710 (2017).

9 Mancino, A. *et al.* A dual cis-regulatory code links IRF8 to constitutive and inducible gene expression in macrophages. *Genes & development* **29**, 394-408, doi:10.1101/gad.257592.114 (2015).

10 Deng, H., Maitra, U., Morris, M. & Li, L. Molecular Mechanism Responsible for the Priming of Macrophage Activation. *J Biol Chem* **288**, 3897-3906, doi:10.1074/jbc.M112.424390 (2013).

11 Pestka, S., Krause, C. D. & Walter, M. R. Interferons, interferon-like cytokines, and their receptors. *Immunological reviews* **202**, 8-32, doi:10.1111/j.0105-2896.2004.00204.x (2004).

12 Buchmeier, N. A. & Schreiber, R. D. Requirement of endogenous interferon-gamma production for resolution of Listeria monocytogenes infection. *Proc Natl Acad Sci U S A* **82**, 7404-7408 (1985).

13 Flynn, J. L. C., John; Triebold, Karla J.; Dalton, Dyana K.; Stewart, Timothy A.; Bloom, Barry R. An essential role for interferon gamma in resistance to Mycobacterium tuberculosis infection. *J Exp Med* **178**, 2249-2254 (1993).

14 Ivashkiv, L. B. & Donlin, L. T. Regulation of type I interferon responses. *Nature Reviews Immunology* **14**, 36-49, doi:10.1038/nri3581 (2013).

15 McNab, F., Mayer-Barber, K., Sher, A., Wack, A. & O'Garra, A. Type I interferons in infectious disease. *Nat Rev Immunol* **15**, 87-103, doi:10.1038/nri3787 (2015).

16 Benveniste, E. N. & Qin, H. Type I interferons as anti-inflammatory mediators. *Science's STKE : signal transduction knowledge environment* **2007**, pe70, doi:10.1126/stke.4162007pe70 (2007).

17 Boscá, L., Bodelón, O. G., Hortelano, S., Casellas, A. & Bosch, F. Anti-inflammatory action of type I interferons deduced from mice expressing interferon β. *Gene Therapy* **7**, 817, doi:10.1038/sj.gt.3301179 (2000).

18 Fink, K. *et al.* IFNbeta/TNFalpha synergism induces a non-canonical STAT2/IRF9-dependent pathway triggering a novel DUOX2 NADPH oxidase-mediated airway antiviral response. *Cell Res* **23**, 673-690, doi:10.1038/cr.2013.47 (2013).

19 Montoya, M. *et al.* Type I interferons produced by dendritic cells promote their phenotypic and functional activation. *Blood* **99**, 3263-3271 (2002).

20 Thyrell, L. *et al.* Mechanisms of Interferon-alpha induced apoptosis in malignant cells. *Oncogene* **21**, 1251-1262, doi:10.1038/sj.onc.1205179 (2002).

21 Trinchieri, G. Type I interferon: friend or foe? *J Exp Med* **207**, 2053-2063, doi:10.1084/jem.20101664 (2010).

22 Teles, R. M. *et al.* Type I interferon suppresses type II interferon-triggered human anti-mycobacterial responses. *Science* **339**, 1448-1453, doi:10.1126/science.1233665 (2013).

23 Novikov, A. *et al.* Mycobacterium tuberculosis triggers host type I IFN signaling to regulate IL-1beta production in human macrophages. *Journal of immunology (Baltimore, Md. : 1950)* **187**, 2540-2547, doi:10.4049/jimmunol.1100926 (2011).

24 Kearney, S. J. *et al.* Type I IFNs downregulate myeloid cell IFN-gamma receptor by inducing recruitment of an early growth response 3/NGFI-A binding protein 1 complex that silences ifngr1 transcription. *Journal of immunology (Baltimore, Md. : 1950)* **191**, 3384-3392, doi:10.4049/jimmunol.1203510 (2013).

25 McNab, F. W. *et al.* Type I IFN induces IL-10 production in an IL-27-independent manner and blocks responsiveness to IFN-gamma for production of IL-12 and bacterial killing in Mycobacterium tuberculosis-infected macrophages. *Journal of immunology (Baltimore, Md. : 1950)* **193**, 3600-3612, doi:10.4049/jimmunol.1401088 (2014).

26 Waddell, S. J. *et al.* Dissecting interferon-induced transcriptional programs in human peripheral blood cells. *PLoS One* **5**, e9753, doi:10.1371/journal.pone.0009753 (2010).

27 Raza, S. *et al.* Analysis of the transcriptional networks underpinning the activation of murine macrophages by inflammatory mediators. *J Leukoc Biol* **96**, 167-183, doi:10.1189/jlb.6HI0313-169R (2014).

28 Lin, S. *et al.* Comparison of the transcriptional landscapes between human and mouse tissues. *Proceedings of the National Academy of Sciences* **111**, 17224-17229, doi:10.1073/pnas.1413624111 (2014).

29 Schroder, K. *et al.* Conservation and divergence in Toll-like receptor 4-regulated gene expression in primary human versus mouse macrophages. *Proc Natl Acad Sci U S A* **109**, E944-953, doi:10.1073/pnas.1110156109 (2012).

30 Fleetwood, A. J., Dinh, H., Cook, A. D., Hertzog, P. J. & Hamilton, J. A. GM-CSF- and M-CSF-dependent macrophage phenotypes display differential dependence on type I interferon signaling. *J Leukoc Biol* **86**, 411-421, doi:10.1189/jlb.1108702 (2009).

31 Mantovani, A., Bonecchi, R. & Locati, M. Tuning inflammation and immunity by chemokine sequestration: decoys and more. *Nat Rev Immunol* **6**, 907-918, doi:10.1038/nri1964 (2006).

32 Malakhova, O. A. *et al.* UBP43 is a novel regulator of interferon signaling independent of its ISG15 isopeptidase activity. *The EMBO journal* **25**, 2358-2367, doi:10.1038/sj.emboj.7601149 (2006).

33 Croker, B. A., Kiu, H. & Nicholson, S. E. SOCS Regulation of the JAK/STAT Signalling Pathway. *Seminars in cell & developmental biology* **19**, 414-422, doi:10.1016/j.semcdb.2008.07.010 (2008).

34 Yang, J., Tian, B., Sun, H., Garofalo, R. P. & Brasier, A. R. Epigenetic silencing of IRF1 dysregulates type III interferon responses to respiratory virus infection in epithelial to mesenchymal transition. *Nature Microbiology* **2**, 17086, doi:10.1038/nmicrobiol.2017.86

https://www.nature.com/articles/nmicrobiol201786 - supplementary-information (2017).

35 Odendall, C. *et al.* Diverse intracellular pathogens activate type III interferon expression from peroxisomes. *Nature Immunology* **15**, 717, doi:10.1038/ni.2915

https://www.nature.com/articles/ni.2915 - supplementary-information (2014).

36 Vila-del Sol, V., Punzon, C. & Fresno, M. IFN-gamma-induced TNF-alpha expression is regulated by interferon regulatory factors 1 and 8 in mouse macrophages. *Journal of immunology (Baltimore, Md. : 1950)* **181**, 4461-4470 (2008).

37 Huber, R. *et al.* TNF Tolerance in Monocytes and Macrophages: Characteristics and Molecular Mechanisms. *Journal of Immunology Research* **2017**, 9, doi:10.1155/2017/9570129 (2017).

38 Hoeksema, M. A. *et al.* IFN-gamma priming of macrophages represses a part of the inflammatory program and attenuates neutrophil recruitment. *Journal of immunology (Baltimore, Md. : 1950)* **194**, 3909-3916, doi:10.4049/jimmunol.1402077 (2015).

39 Bartee, E., Mohamed, M. R., Lopez, M. C., Baker, H. V. & McFadden, G. The addition of tumor necrosis factor plus beta interferon induces a novel synergistic antiviral state against poxviruses in primary human fibroblasts. *J Virol* **83**, 498-511, doi:10.1128/jvi.01376-08 (2009).

40 Park, S. H. *et al.* Type I interferons and the cytokine TNF cooperatively reprogram the macrophage epigenome to promote inflammatory activation. *Nat Immunol* **18**, 1104-1116, doi:10.1038/ni.3818 (2017).

41 Song, M. M. & Shuai, K. The suppressor of cytokine signaling (SOCS) 1 and SOCS3 but not SOCS2 proteins inhibit interferon-mediated antiviral and antiproliferative activities. *J Biol Chem* **273**, 35056-35062 (1998).

42 Lazear, H. M., Nice, T. J. & Diamond, M. S. Interferon-lambda: Immune Functions at Barrier Surfaces and Beyond. *Immunity* **43**, 15-28, doi:10.1016/j.immuni.2015.07.001 (2015).

43 Jiang, M. *et al.* MAP kinase p38α regulates type III interferon (IFN-λ1) gene expression in human monocyte-derived dendritic cells in response to RNA stimulation. *Journal of leukocyte biology* **97**, 307-320, doi:10.1189/jlb.2A0114-059RR (2015).

44 Shahangian, A. *et al.* Type I IFNs mediate development of postinfluenza bacterial pneumonia in mice. *J Clin Invest* **119**, 1910-1920, doi:10.1172/jci35412 (2009).

45 O'Dea, E. & Hoffmann, A. The Regulatory Logic of the NF-κB Signaling System. *Cold Spring Harbor Perspectives in Biology* **2**, doi:10.1101/cshperspect.a000216 (2010).

46 Cheng, C. S. *et al.* Iterative Modeling Reveals Evidence of Sequential Transcriptional Control Mechanisms. *Cell Syst* **4**, 330-343 e335, doi:10.1016/j.cels.2017.01.012 (2017).

47 Buenrostro, J. D., Giresi, P. G., Zaba, L. C., Chang, H. Y. & Greenleaf, W. J. Transposition of native chromatin for fast and sensitive epigenomic profiling of open chromatin, DNA-binding proteins and nucleosome position. *Nat Methods* **10**, 1213-1218, doi:10.1038/nmeth.2688 (2013).

48 Martin, M. Cutadapt removes adapter sequences from high-throughput sequencing reads. *2011* **17**, doi:10.14806/ej.17.1.200 pp. 10-12 (2011).

49 Dobin, A. *et al.* STAR: ultrafast universal RNA-seq aligner. *Bioinformatics* **29**, 15-21, doi:10.1093/bioinformatics/bts635 (2013).

50 Benaglia, T., Chauveau, D., Hunter, D. R. & Young, D. S. mixtools: An R Package for Analyzing Mixture Models. *2009* **32**, 29, doi:10.18637/jss.v032.i06 (2009).

51 Robinson, M. D., McCarthy, D. J. & Smyth, G. K. edgeR: a Bioconductor package for differential expression analysis of digital gene expression data. *Bioinformatics* **26**, 139-140, doi:10.1093/bioinformatics/btp616 (2010).

52 R: A Language and Environment for Statistical Computing (2014).

53 Wickham, H. *ggplot2: Elegant Graphics for Data Analysis*. (Springer-Verlag, 2009).

54 Chris Fraley, A. E. R., T. Brendan Murphy, Luca Scrucca. mclust Version 4 for R: Normal Mixture Modeling for Model-Based Clustering, Classification, and Density Estimation. Report No. 597, (University of Washington, 2012).

55 Pheatmap: pretty heatmaps (2015).

56 Heinz, S. *et al.* Simple combinations of lineage-determining transcription factors prime cis-regulatory elements required for macrophage and B cell identities. *Mol Cell* **38**, 576-589, doi:10.1016/j.molcel.2010.05.004 (2010).

57 Mi, H. *et al.* PANTHER version 11: expanded annotation data from Gene Ontology and Reactome pathways, and data analysis tool enhancements. *Nucleic Acids Research* **45**, D183-D189, doi:10.1093/nar/gkw1138 (2017).

58 Langmead, B. & Salzberg, S. L. Fast gapped-read alignment with Bowtie 2. *Nat Methods* **9**, 357-359, doi:10.1038/nmeth.1923 (2012).

59 Zhang, Y. *et al.* Model-based analysis of ChIP-Seq (MACS). *Genome biology* **9**, R137, doi:10.1186/gb-2008-9-9-r137 (2008).

60 Quinlan, A. R. & Hall, I. M. BEDTools: a flexible suite of utilities for comparing genomic features. *Bioinformatics* **26**, 841-842, doi:10.1093/bioinformatics/btq033 (2010).

61 Love, M. I., Huber, W. & Anders, S. Moderated estimation of fold change and dispersion for RNA-seq data with DESeq2. *Genome biology* **15**, 550, doi:10.1186/s13059-014-0550-8 (2014).

62 Zhu, L. J. *et al.* ChIPpeakAnno: a Bioconductor package to annotate ChIP-seq and ChIP-chip data. *BMC bioinformatics* **11**, 237, doi:10.1186/1471-2105-11-237 (2010).

CHAPTER THREE

NFκB dynamics determine the stimulus-specificity of epigenomic reprogramming in macrophages

Summary

The epigenome defines the cell type, but also possesses plasticity to tune gene expression in the context of extracellular cues. This tuning is evident in immune sentinel cells such as macrophages, which respond to pathogens and cytokines with phenotypic shifts driven by epigenomic reprogramming[1]. Recent studies[2–4] indicate that this reprogramming may be triggered by signal-dependent transcription factors, including nuclear factor kappa-light-chain-enhancer of activated B cells (NFκB). NFκB binds not only to available enhancers[5], but may also produce *de novo* enhancers in previously silent areas of the genome[3]. Here, we show that NFκB reprograms the macrophage epigenome in a stimulus-specific manner, in response only to a subset of pathogen-derived stimuli. The basis for these surprising differences lies in the stimulus-specific temporal dynamics of NFκB activity. In response to different stimuli, NFκB enters the nucleus with distinct speeds, amplitudes, and durations, and may oscillate between the nucleus and cytoplasm. These dynamical features encode information about the identity and dose of a given stimulus[6]. We demonstrate through live cell imaging, mathematical modeling, and genetic perturbations that NFκB promotes open chromatin and formation of *de novo* enhancers most strongly when its dynamics are non-oscillatory. These *de novo* enhancers result in the activation of additional response genes. We propose a mechanistic paradigm in which the temporal dynamics of transcription factors are a key determinant of their capacity to elicit epigenomic reprogramming, thus enabling the formation of stimulus-specific memory in innate immune sentinel cells.

Body Text

The cellular epigenome, a regulatory network involving transcription factors, chromatin architecture and histone modifications, contains stable, heritable information that determines cell type-specific programs of gene expression[7]. Nevertheless, the epigenome of differentiated cells remains highly plastic, particularly in immune cells like macrophages[8,9]. These immune sentinel cells detect and "remember" environmental signals through epigenomic reprogramming to coordinate immune responses that are both context- and stimulus-appropriate[1]. At a molecular level, this reprogramming is initiated by the activity of signal-dependent transcription factors (TFs) such as NFκB[10]. In cooperation with pioneer factors such as Pu.1, signal-dependent TFs increase chromatin accessibility and positive-acting histone marks at previously silent regions of the genome, thus forming *de novo* enhancers[2,3]. NFκB activated by LPS has been a model TF in the study of "poised" *vs.* "latent" or *de novo* enhancers. However, the degree to which NFκB or other TFs can alter the epigenome in response to different stimuli is unknown.

To investigate the stimulus-specificity of *de novo* enhancer formation, we stimulated bone marrow-derived macrophages (BMDMs) with five well-characterized ligands: TNF (signaling through TNFR), Pam3CSK (TLR1/2), CpG (TLR9), LPS (TLR4), and Poly(I:C) (TLR3). We performed H3K4me1 ChIP-seq to identify stimulus-dependent *de novo* enhancers as previously-defined[3,4] and identified 3978 regions of the genome that segregated into two clusters. (Fig. 3.1a). The enhancers in Cluster 1 were most strongly induced by LPS and Poly(I:C) and were enriched for IRF and ISRE motifs (Fig. 3.1a), consistent with the fact that these stimuli activate IRF3 and type I interferon via the signaling adaptor TRIF[11]. In *Irf3*$^{-/-}$*Ifnar*$^{-/-}$ BMDMs these regions no longer acquired H3K4 methylation in response to LPS and Poly(I:C) (Fig. 3.1c).

Weak induction in response to TNF was consistent with the observation that TNF does not induce IRF3 but IRF1[12].

In contrast, the enhancers in Cluster 2 were highly enriched for NFκB motifs. Surprisingly, although all five stimuli activate NFκB[13], these regions acquired H3K4me1 in a stimulus-specific manner. TNF and Poly(I:C) had little effect on these regions, while Pam3CSK, CpG, and LPS produced prominent gains in H3K4me1. These differences were consistent across replicates (Extended Data Fig. 3.1) and were preserved in *Irf3*$^{-/-}$*Ifnar*$^{-/-}$ BMDMs (Fig. 3.1c). Furthermore, 1071 of these regions contained an NFκB-RelA ChIP-seq peak[14] (Fig. 3.1d). We concluded that these 1071 *de novo* enhancers were highly likely to be NFκB-driven. A pairwise comparison between samples quantitatively confirmed the stimulus-specificity of these

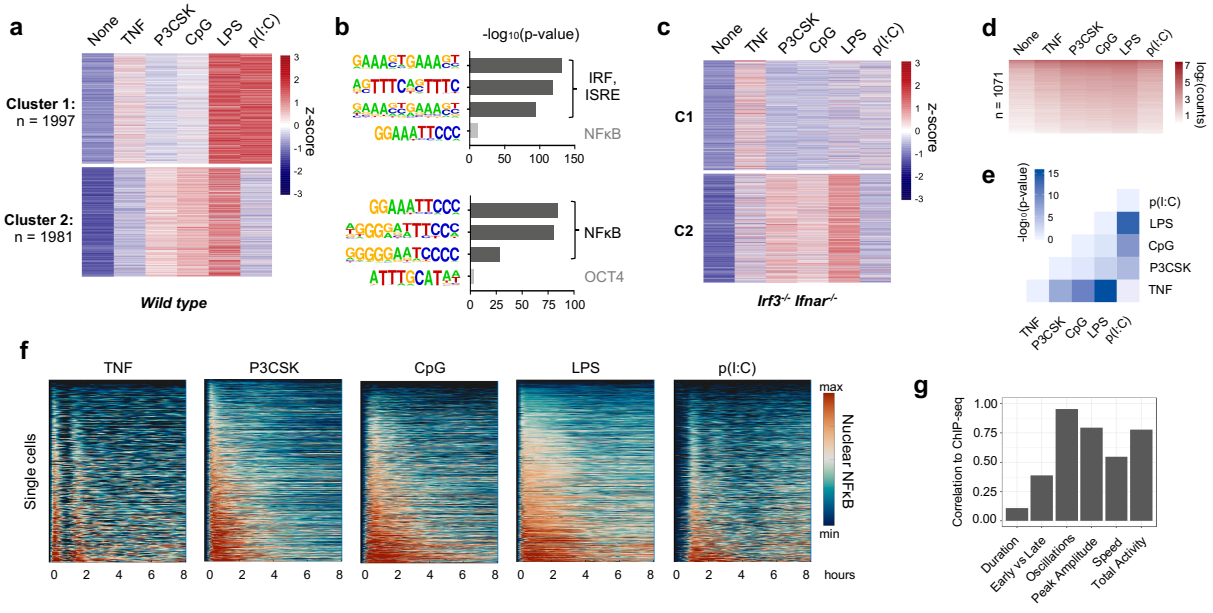

Figure 3.1: NFκB-driven *de novo* enhancers are stimulus-specific and correlate to dynamic features of NFκB activity.
a) Heat map of H3K4me1 ChIP-seq inducible peaks from BMDMs stimulated with five ligands for eight hours, unsupervised K-means clustering. Average of two replicates. **b)** Known transcription factor motifs with greatest enrichment in Cluster 1 and Cluster 2 peaks. **c)** Heat map of H3K4me1 ChIP-seq in *Irf3*$^{-/-}$*Ifnar*$^{-/-}$ BMDMs, using same clusters as panel (a). **d)** Heat map of subset of Cluster 2 peaks that overlap with a RelA binding event by ChIP-seq. **e)** Heat map of matrix of *p*-values between ChIP-seq counts in panel (d), by two-tailed t-test between pairs of conditions. **f)** Heat maps of NFκB activity in single cells by live cell microscopy of *mVenus-RelA* BMDMs, showing nuclear abundance of NFκB in response to five stimuli. **g)** Bar graph of correlations (absolute value) between mean ChIP-seq counts in panel (d) and the six key features of NFκB dynamics[3] (see also Extended Data, Fig. 3.2).

enhancers (Fig. 3.1e), as the H3K4me1 ChIP-seq signals of Pam3CSK, CpG, and LPS were significantly different from TNF or Poly(I:C) ($p < 10^{-5}$) in these regions.

Such differences would be difficult to explain if NFκB were a binary on-off switch, but NFκB is in fact activated with complex, stimulus-specific temporal dynamics[13,15,16]. Using live-cell microscopy of macrophages from mVenus-RelA mice[6], we characterized the single-cell dynamics of NFκB p65 in response to all five ligands (Fig. 3.1f). We have previously identified six essential features of NFκB dynamics that function as "codewords" to encode ligand identity and dose[6]. We correlated mean H3K4me1 counts in the NFκB-driven enhancers with these six features: duration, early vs late activity, oscillatory power, peak amplitude, activation speed, and total activity (Extended Data Fig. 3.2). We found that oscillatory power (r = -0.95), total activity (r = 0.77), and peak amplitude (r = 0.78) were correlated with the capacity of a given stimulus to form *de novo* enhancers (Fig. 3.1g).

We hypothesized that temporal dynamics of NFκB activity might affect its interaction with chromatin. Crystallographic studies imply that stable NFκB-DNA binding requires the DNA to be nucleosome-free because NFκB dimers embrace the DNA double helix circumferentially[17,18] (Fig. 3.2a). However, NFκB is capable of interacting with nucleosomal DNA[19], and can displace nucleosomes in cooperation with pioneer factor Pu.1[3] or remodeling machinery such as SWI/SNF[20]. Furthermore, the DNA-histone interface is composed of low-affinity interactions that promote spontaneous disassociation or "breathing"[21]. Thus, successive disruptions of DNA-histone contacts by NFκB may displace the nucleosome (Fig. 3.2b), and be followed by binding of lineage-determining TFs such as Pu.1 and the deposition of histone modifications on neighboring nucleosomes marking the region as a *de novo* enhancer[3].

This data provided the mechanistic basis for a multi-step model describing how dynamical NFκB activity might affect chromatin. We constructed a series of 14 Hill equations describing the competition between NFκB and histone for interacting with DNA (Fig. 3.2c) based on the number of contact points in the histone-DNA crystal structure[22]. Relative rates of nucleosome wrapping and unwrapping were based on available biophysical data[23]. Using measured single-cell NFκB activities (Fig. 3.1e) as inputs, the model simulations reproduced the differences in experimental ChIP-seq data (Fig. 3.2d-2e and Extended Data Fig. 3.3a) across a range of parameter values (Extended Data Fig. 3.4).

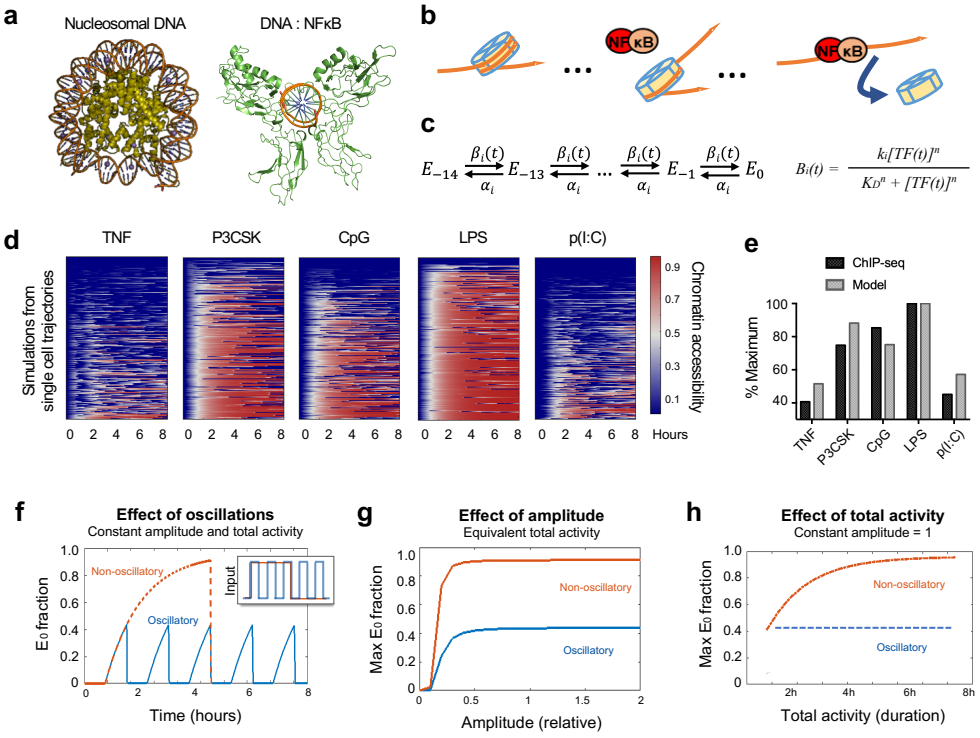

Figure 3.2: Mathematical model predicts epigenetic response to distinct dynamic features of NFκB.
a) Crystal structures of nucleosomal DNA (PDB 1F66) *vs.* NFκB-bound DNA (PDB 1VKX), where p65:p50 NFκB dimer is in green. **b)** Schematic of model illustrating NFκB-driven displacement of nucleosome. **c)** Multi-step model with 14 steps to complete nucleosome unwrapping, each expressed as a Hill function. **d)** Heat maps of simulations of chromatin opening in response to different stimuli, using single cell trajectories from microscopy data as input. **e)** Model simulation *vs.* ChIP-seq data. Mean ChIP-seq counts from Fig. 1a Cluster 2, background-subtracted and scaled to maximum signal (LPS stimulation). Model simulations are mean of maximum E_0 fraction per cell (cf. Extended Data Fig 3.3a), scaled to LPS condition. **f)** Model simulation of predicted chromatin accessibility comparing oscillatory *vs.* non-oscillatory input activities. **g-h)** Model simulation of predicted chromatin opening across a range of amplitudes and durations.

We used the model to investigate which features of NFκB dynamical activity had the greatest impact on chromatin accessibility. We examined the contribution of the three features most highly correlated with the H3K4me1 ChIP-seq data (Fig. 3.1g): oscillations, amplitude, and total activity. When we compared oscillatory *vs.* non-oscillatory activity while holding amplitude and total activity constant, the model predicted that a non-oscillatory dynamic produces a two-fold greater chromatin accessibility than an oscillatory dynamic (Fig. 3.2f) due to the rapid closing of chromatin when oscillatory NFκB leaves the nucleus. The model also indicated that NFκB activity must have a minimal amplitude (Fig. 3.2g) and extend for a minimal duration (Fig. 3.2h) to open chromatin, but above these thresholds non-oscillatory NFκB has greater capacity to open chromatin than oscillatory NFκB for any given amplitude or duration. The striking conclusion from these simulations was that the presence or absence of oscillations, not the maximum amplitude or duration of activity, are the key determinant of whether NFκB preserves or alters the chromatin state.

To test this prediction, we generated a knockout mouse in which NFκB dynamics are perturbed. In response to TNF, NFκB rapidly induces expression of *Nfkbia*, whose gene product is the negative regulator IκBα[24] (Fig. 3.3a) and mediates oscillatory behavior of NFκB. As IκBα knockout mice are embryonic lethal due to chronic hyperinflammation[25], we bred the *Nfkbia*$^{-/-}$ allele into a *Rel*$^{-/-}$*Tnf*$^{-/-}$*Nfkbie*$^{-/-}$ background, enabling the isolation of BMDMs from adult IκB$\alpha^{-/-}$ mice.

We examined the dynamics of NFκB in IκB$\alpha^{-/-}$ BMDMs by crossing these mice with *mVenus-RelA* knock-in mice and performing live cell imaging of BMDMs stimulated with TNF. We observed that knockout of IκBα significantly disrupted NFκB dynamics (Fig. 3.3b). We quantified the differences in the distribution of single cell dynamic features by Kolmogorov–

Smirnov (K-S) test (Fig. 3.3c, Extended Data Fig. 3.5a) and found that the greatest dynamic difference between IκBα$^{-/-}$ and WT was a loss of oscillatory activity, with a K-S test statistic (*D*) of 0.85, corresponding to a *p*-value < 10^{-16}. The other key dynamic features were either unaffected, or in the case of activation speed (D = 0.66) and early-vs-late activity (D = 0.52) would intuitively favor NFκB activity in WT cells. In addition, we calculated the area under the NFκB activity curve at the time points used in subsequent experiments and found no difference (Extended Data Fig. 3.5b). Based on single-cell microscopy measurements, we concluded that the primary impact of IκBα knockout was loss of oscillations.

To profile the chromatin state, we stimulated BMDMs from IκBα$^{-/-}$ and littermate controls with TNF and performed ATAC-seq at two, four, and eight hours. This was followed by

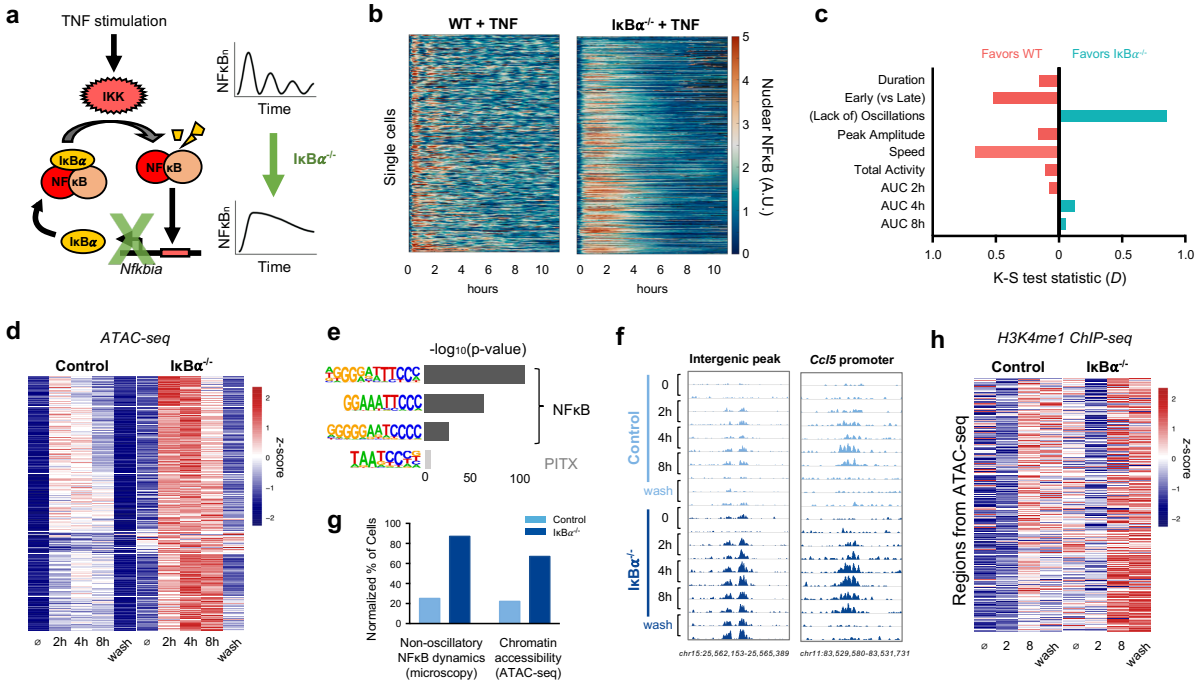

Figure 3.3: IκBα knockout abolishes NFκB oscillations, increasing chromatin accessibility and *de novo* enhancer formation.
a) Schematic of IκBα as key regulator of NFκB oscillations. **b)** Heat map of single cell NFκB activity by microscopy comparing TNF response in WT *vs.* IκBα$^{-/-}$ macrophages. **c)** Bar graph of K-S test statistic for difference in distribution of six key signaling features and areas under NFκB activity curve, comparing IκBα$^{-/-}$ and WT. **d)** Heat map of ATAC-seq signal at 322 genomic regions that are TNF-inducible and differential between IκBα$^{-/-}$ and control. Average of two replicates. "wash" = 16h washout. **e)** Known transcription factor motifs with greatest enrichment in differentially inducible ATAC-seq regions. **f)** Genome browser tracks for representative differentially inducible ATAC-seq regions, two replicates per time point. **g)** Percentage of cells with non-oscillatory NFκB trajectories by microscopy, compared with relative percentage of cells with accessible chromatin at *Chr15* intergenic peak by ATAC-seq. **h)** Heat map of H3K4me1 ChIP-seq signal over the 322 regions defined as differentially inducible by ATAC-seq. Average of two replicates. "wash" = 16h washout.

a 16-hour washout period, and a final time point was collected after washout (Extended Data Fig. 3.6a). We identified 1443 genomic regions that demonstrated TNF-inducible chromatin accessibility in either genotype. Of these, 332 were differentially inducible between control and IκB$\alpha^{-/-}$. Strikingly, 97% of these regions (n=322) had greater chromatin accessibility in the knockout than control (Fig. 3.3d). These differentially inducible regions were strongly enriched for NFκB motifs (Fig. 3.3e), and 311 of 322 overlapped with a RelA ChIP-seq peak (Extended Data Fig. 3.6c). Differentially inducible regions were more likely than constitutively accessible regions to fall in intergenic portions of the genome (Extended Data Fig. 3.6b), suggesting that they tend to function as *cis*-acting enhancer elements near key innate immune genes such as *Ccl5* (Fig. 3.3f), which has previously been shown to require chromatin remodeling for full induction[14].

Our model predicted that chromatin accessibility is primarily determined by whether NFκB is oscillatory or non-oscillatory within a single cell. We therefore considered that the magnitude of ATAC-seq signal can be interpreted as the proportion of cells in a sample in which a particular region of DNA is accessible. By microscopy, 87% of IκB$\alpha^{-/-}$ cells have non-oscillatory NFκB, compared to 25% in WT cells. This was similar to the magnitude of ATAC-seq differences between IκB$\alpha^{-/-}$ and control. For example, at an intergenic peak on chromosome 15, 67% of IκB$\alpha^{-/-}$ cells showed accessible chromatin, compared to 22% of control cells (Fig. 3.3g).

To investigate more definitively that the negative feedback function of IκBα rather than its basal activity is critical for the observed effects, we utilized a recently described IκB$\alpha^{\kappa B/\kappa B}$ mutant in which NFκB-binding sites in the promoter of the *Nfkbia* gene are disrupted[26] (Extended Data Fig. 3.7a). In this model, basal IκBα expression is preserved, and the mice live

into adulthood without requiring compound suppressor mutations. We confirmed that upon TNF stimulation IκB$\alpha^{\kappa B/\kappa B}$ BMDMs activate NFκB in a non-oscillatory manner (Extended Data Fig. 3.7b). ATAC-seq analysis of TNF-stimulated WT vs IκB$\alpha^{\kappa B/\kappa B}$ BMDMs recapitulated our findings in the IκB$\alpha^{-/-}$ system, with 131 genomic regions demonstrating greater gain of chromatin accessibility in the mutant compared to WT (Extended Data Fig. 3.7c). These regions were enriched for NFκB motifs, and 90% overlapped with a RelA ChIP-seq peak (Extended Data Fig. 3.7d-7e). Taken together, the ATAC-seq data from both IκB$\alpha^{-/-}$ and IκB$\alpha^{\kappa B/\kappa B}$ experimental models indicated that loss of inducible negative feedback in the NFκB signaling system, which results in a loss of oscillations, results in greater chromatin accessibility.

Next, we examined whether regions with differentially inducible chromatin accessibility acquire the corresponding histone mark of enhancers. We performed H3K4me1 ChIP-seq in TNF-stimulated control and IκB$\alpha^{-/-}$ BMDMs and found that in the 322 differentially inducible ATAC-seq regions there was also a greater gain of H3K4me1 signal in IκB$\alpha^{-/-}$ than control (Fig. 3.3h). Notably, these histone marks persisted even after a 16-hour washout. This suggests that chromatin opening facilitated by NFκB may be transient but leads to durable H3K4 methylation even after the stimulus is removed, marking the region as a *de novo* enhancer and reprogramming the epigenome.

Because histone methylation is more durable and indicative of enhancer function, we analyzed the H3K4me1 ChIP-seq data independently and identified 2081 regions that acquired more H3K4 methylation in IκB$\alpha^{-/-}$ than control (Fig. 3.4a). These differentially induced, dynamics-dependent *de novo* enhancers persisted after the TNF stimulus was washed out, and they were strongly enriched for NFκB motifs (Fig. 3.4b). We then asked whether these regions, which are dependent on non-oscillatory NFκB in the IκB$\alpha^{-/-}$ system, corresponded to the

stimulus-specific NFκB-driven *de novo* enhancers in WT BMDMs (Fig. 3.1d). We found that there was a highly significant overlap (p = 10 e-45), and the inducible ChIP-seq signal was consistently greater when NFκB dynamics were non-oscillatory rather than oscillatory, whether by genetic perturbation or by stimulus-specific signaling mechanisms (Fig. 3.4c).

Next, we asked whether these NFκB dynamics-dependent enhancers had a functional role in macrophage gene expression. We hypothesized that *de novo* enhancers would alter transcriptional responses to subsequent stimulation. We primed control and IκBα$^{-/-}$ BMDMs with TNF for eight hours followed by 16-hour washout as before, then re-stimulated with secondary

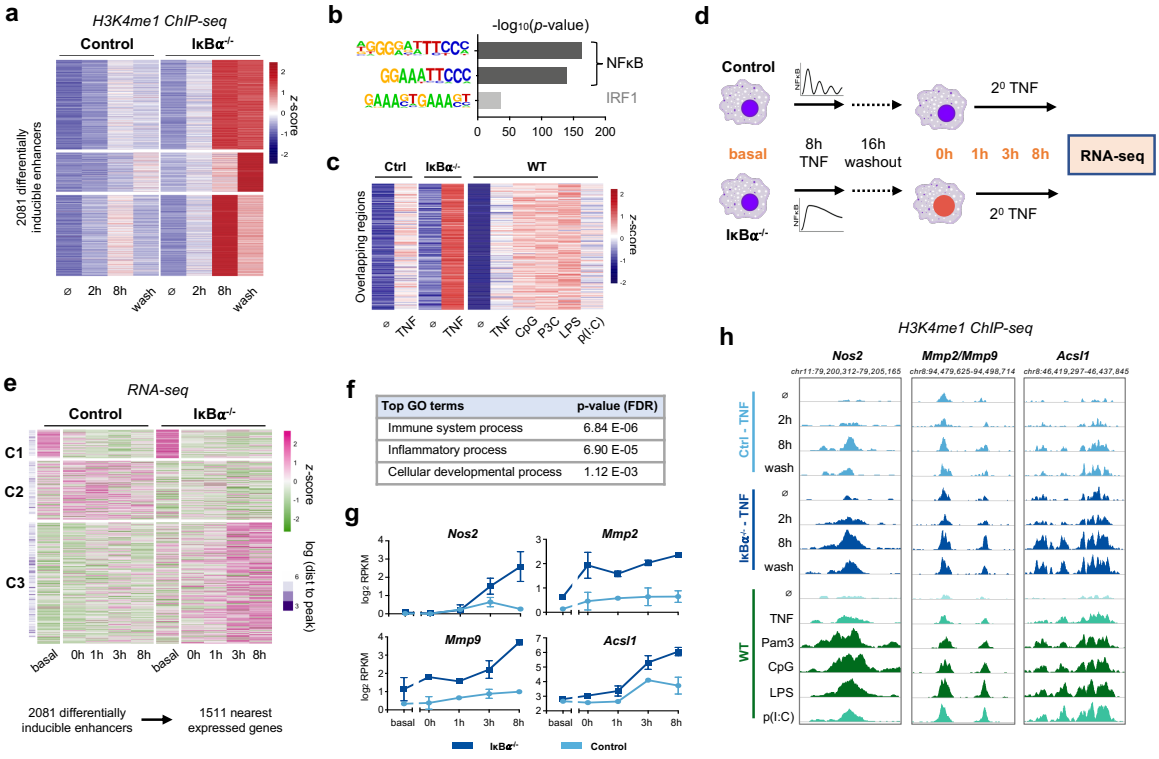

Figure 3.4: NFκB dynamics-dependent enhancers are associated with dynamics-dependent gene expression.
a) Heat map of H3K4me1 ChIP-seq signal at 2081 regions that are TNF-inducible and differential between IκBα$^{-/-}$ and control, i.e. dynamics-dependent enhancers. Average of two replicates. "wash" = 16h washout. **b)** Known transcription factor motifs with greatest enrichment in dynamics-dependent enhancers. **c)** Heat map of H3K4me1 signal after 8h stimulation at regions that overlap between Fig. 4a and Fig. 1d (n=211, p for overlap=10 e-45). **d)** Schematic of RNA-seq experiment. **e)** Heat map showing expression of genes closest to dynamics-dependent enhancers, where Cluster 3 exhibits differential gene expression between IκBα$^{-/-}$ and control. Average of two replicates. **f)** Top biological process ontology terms for genes in Cluster 3 of Fig. 4e. **g)** Examples of genes differentially induced between IκBα$^{-/-}$ and control, average and standard deviation of two replicates. **h)** Genome browser tracks of differentially inducible H3K4me1 peaks near differentially inducible genes, showing TNF-stimulated IκBα$^{-/-}$ *vs.* control and stimulus-specific response in WT BMDMs. More darkly shaded tracks indicate non-oscillatory NFκB conditions. Average of two replicates.

TNF over eight hours (Fig. 3.4d). We performed mRNA-seq in the basal (untreated) condition and at zero, one, three, and eight hours of secondary TNF stimulation. We explored the relationship between differentially inducible enhancers and gene expression using two approaches. First, using a peak-centric approach, we linked the 2081 enhancers to their nearest expressed genes, removed duplicates, and identified three distinct patterns of expression for the remaining 1511 genes. Cluster 1 and 2 genes were not TNF-responsive in either condition, reflecting an intrinsic limitation of this approach when enhancers often do not regulate their nearest genes[27]. Despite this limitation, 58% of nearest genes were both TNF-responsive and more strongly induced in IκB$\alpha^{-/-}$ BMDMs (Fig. 3.4e Cluster 3). Many of these genes were not induced in controls at all. The differentially induced genes were enriched for ontology terms "Immune system process" and "Inflammatory process" (Fig. 3.4f).

To corroborate the results from the peak-centric analysis, we also examined our data using a gene-centric approach. From the RNA-seq dataset we identified 1958 TNF-inducible genes, 482 of which were differentially regulated in IκB$\alpha^{-/-}$ versus control (Extended Data Fig. 3.8a-8b). For each gene, we measured the genomic distance to the nearest differentially inducible H3K4me1 ChIP-seq region. We found that differentially inducible genes were significantly closer to differentially inducible enhancers (p = 1.13 e-9) than genes that were not differentially inducible (Extended Data Fig. 3.8c-8d). Thus, both analytical approaches indicated that NFκB dynamics-dependent *de novo* enhancers play a functional role in differentially regulating gene expression response to secondary TNF.

The dynamics-dependent gene expression program included *Nos2, Mmp2,* and *Mmp9*, which are well-defined markers of classical macrophage activation[28], as well as *Acsl1*, which plays a role in the pathogenesis of atherosclerosis[29] (Fig. 3.4g). Each of these genes had a nearby

enhancer that gained more H3K4me1 signal in the presence of non-oscillatory NFκB, whether in the IκB$\alpha^{-/-}$ system or in WT BMDMs stimulated with different ligands (Fig. 3.4h). These specific examples further suggested that *de novo* enhancers formed by non-oscillatory NFκB regulate genes involved in macrophage activation.

In summary, our results indicate that the dynamics of NFκB activity, particularly whether they are oscillatory or non-oscillatory, determine NFκB's capacity to reprogram the macrophage epigenome. We show with a mathematical model how biophysical principles governing nucleosome dynamics might decode stimulus-specific NFκB dynamical features. The role of temporal dynamics may thus complement the structure-function model in which pioneering TFs access nucleosomal DNA based on their recognition of partially exposed DNA motifs[30]. Notably, to date the function of NFκB oscillations has been unclear, given that there is little difference in the expression of poised inflammatory-response genes induced by oscillatory *vs.* non-oscillatory NFκB[31,32]. We propose that in response to some ligands, the role of oscillations is to maintain the epigenomic state while exploiting existing poised enhancers for inflammatory gene activation. However, in response to other ligands, non-oscillatory NFκB induces a comparable gene expression program while also forming *de novo* enhancers, thus changing the epigenomic state of the cell and its capacity to respond to subsequent stimuli. While further work will be needed to determine the physiological functions of NFκB dynamics-dependent *de novo* enhancers, our study establishes a mechanistic paradigm of TF temporal dynamics being a key determinant of epigenomic reprogramming.

Extended Data Figures

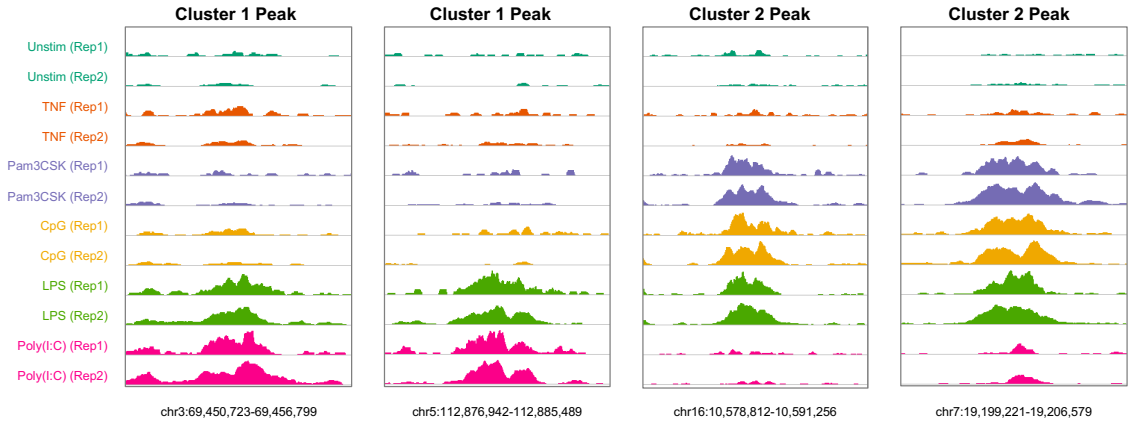

Extended data, Figure 3.1: Genome browser tracks of representative H3K4me1 ChIP-seq peaks showing stimulus-specific *de novo* enhancers from Fig. 3.1a., two replicates per condition.

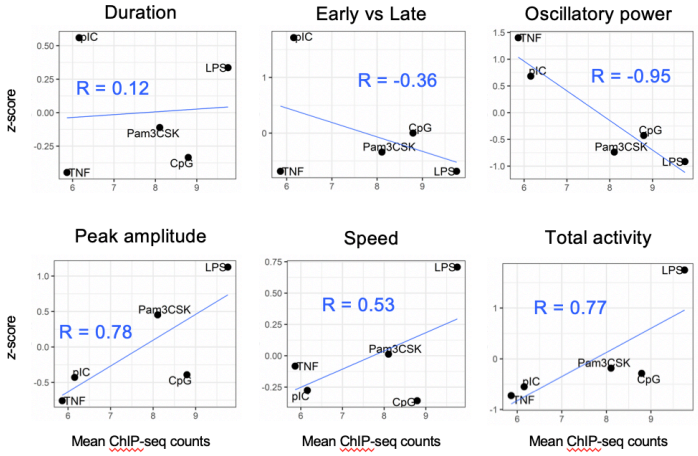

Extended data, Figure 3.2: Correlation of NFκB dynamics to ChIP-seq data. Scatterplots and correlations of mean Cluster 2 ChIP-seq counts *vs.* stimulus-specific z-scores for each of the six key features of NFκB signaling dynamics

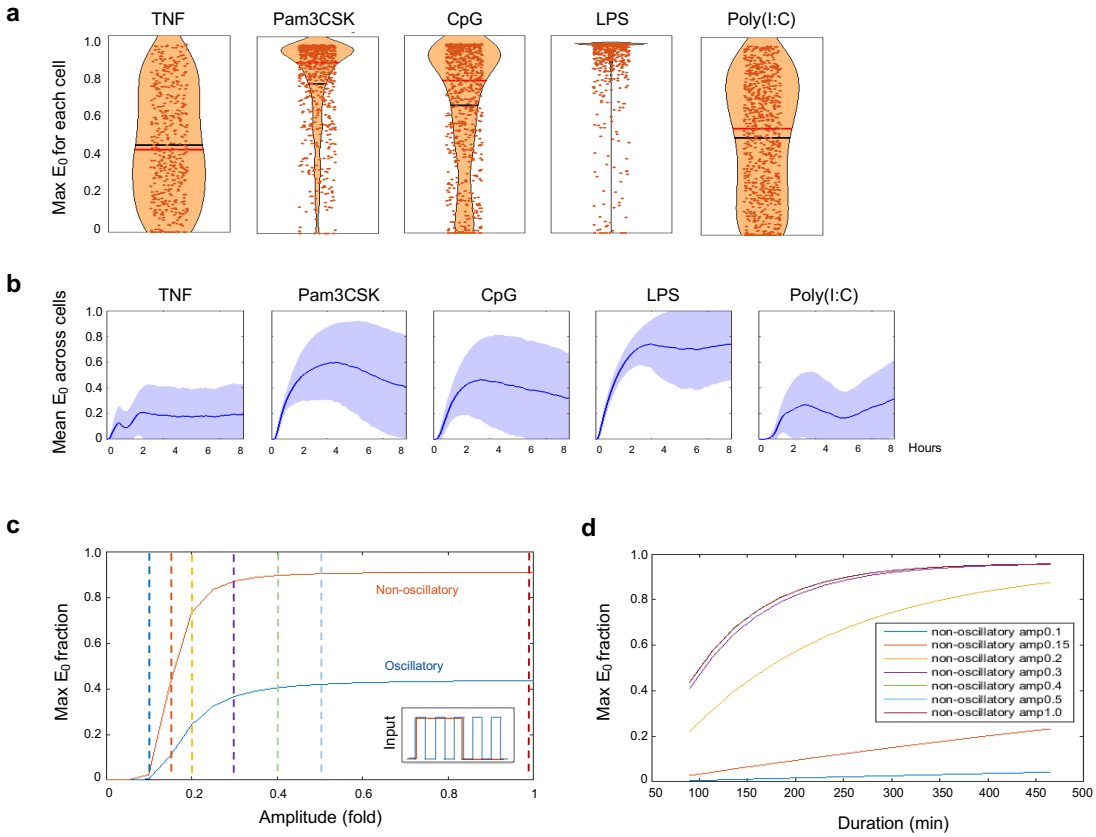

Extended data, Figure 3.3: Supplemental model simulations. a) Violin plots of maximum chromatin opening over eight hours per single-cell stimulation, using NFκB trajectories as input to the model. Black line = mean, Red line = median. **b)** Simulated mean chromatin opening over time across all single cells. **c)** Model simulations across a range of NFκB amplitudes, comparing oscillatory and non-oscillatory trajectories. **d)** Model simulations across a range of NFκB durations, comparing a range of NFκB amplitudes marked by dotted lines in (c).

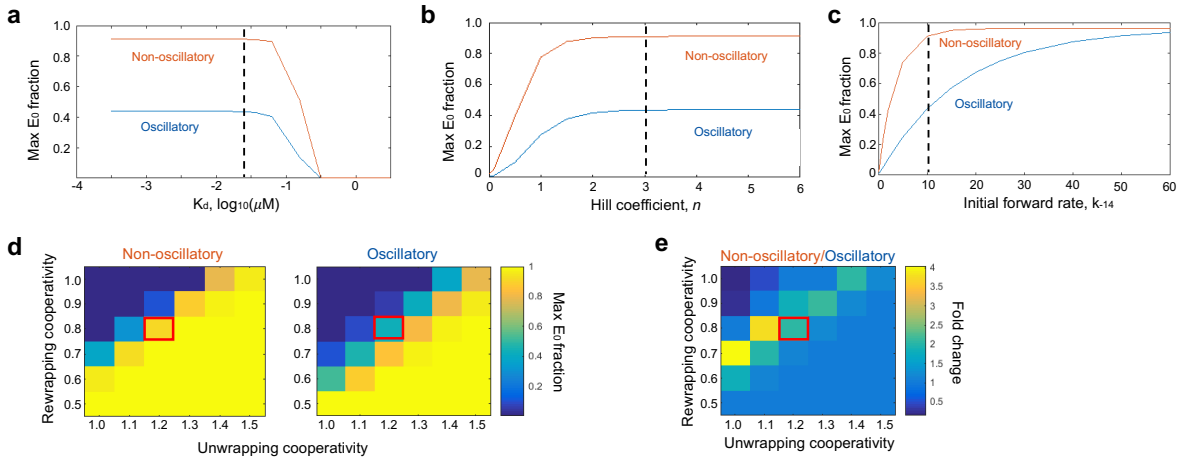

Extended data, Figure 3.4: Parameter sensitivity analysis. (a) Chromatin opening behavior when the model is tested across a range of K_Ds, **(b)** across a range of Hill coefficients, or **(c)** across a range of forward rates for the first unwrapping step, k_{-14}. For model simulations (Fig. 3.2d), $K_D = 0.025$, Hill = 3, and $k_{-14} = 10$ were used, marked by the dotted black line. **(d-e)** Heat map of chromatin opening across a range of unwrapping and rewrapping cooperativity factors, showing maximum E_0 fraction in non-oscillatory and oscillatory conditions (d) and fold change difference between maximum non-oscillatory and oscillatory conditions (e). Red box indicates the parameter values used for model simulations.

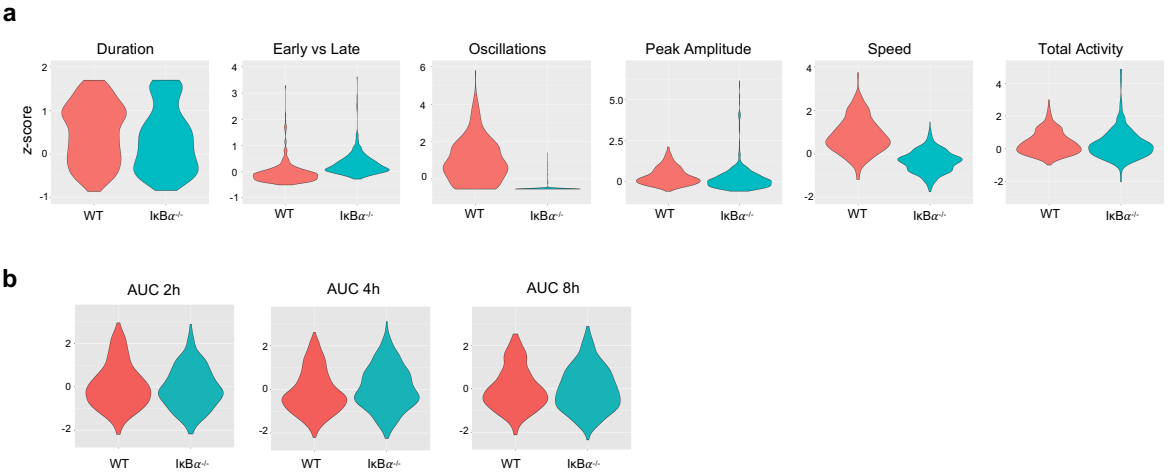

Extended data, Figure 3.5: NFκB dynamics in TNF-stimulated IκB$\alpha^{-/-}$ vs WT BMDMs. (a) Violin plots of single-cell distributions for the six key NFκB signaling features. **(b)** Violin plots of single-cell distributions for areas under the NFκB activity curve at two, four, and eight hours. **(c)** Bar graph of Kolmogorov–Smirnov (K-S) test statistic for difference between distributions of IκB$\alpha^{-/-}$ and WT cells for key signaling features and areas under the curve. Directionality of bars is based on whether observed differences would intuitively favor greater NFκB activity in WT or knockout cells.

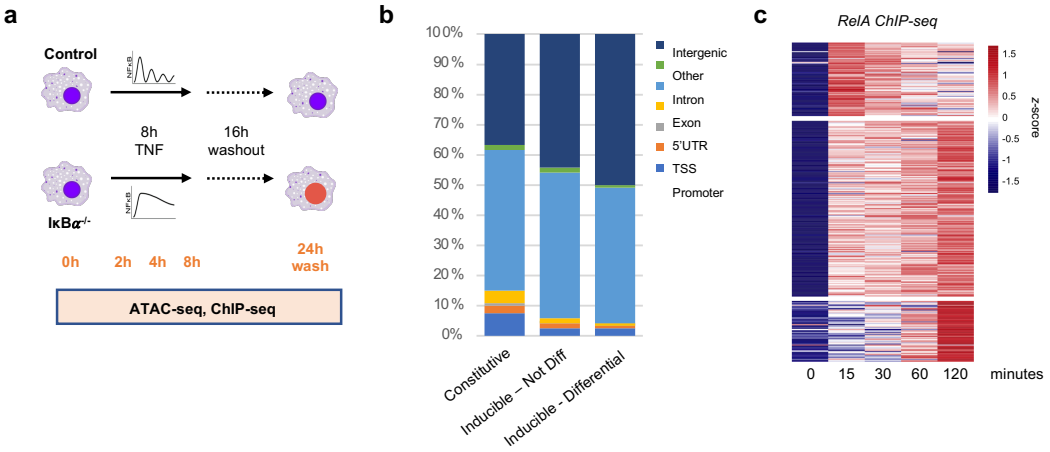

Extended data, Figure 3.6: Supplemental ATAC-seq data. a) Schematic of ATAC and ChIP-seq experiments in IκBα$^{-/-}$ and control BMDMs. **b)** Genomic distribution of three categories of accessible regions identified by ATAC-seq. **c)** Heat map of Lipid A-stimulated NFκB RelA ChIP-seq signal[25] at 322 inducible-differential ATAC-seq regions, 311 of which overlap with a RelA ChIP-seq peak.

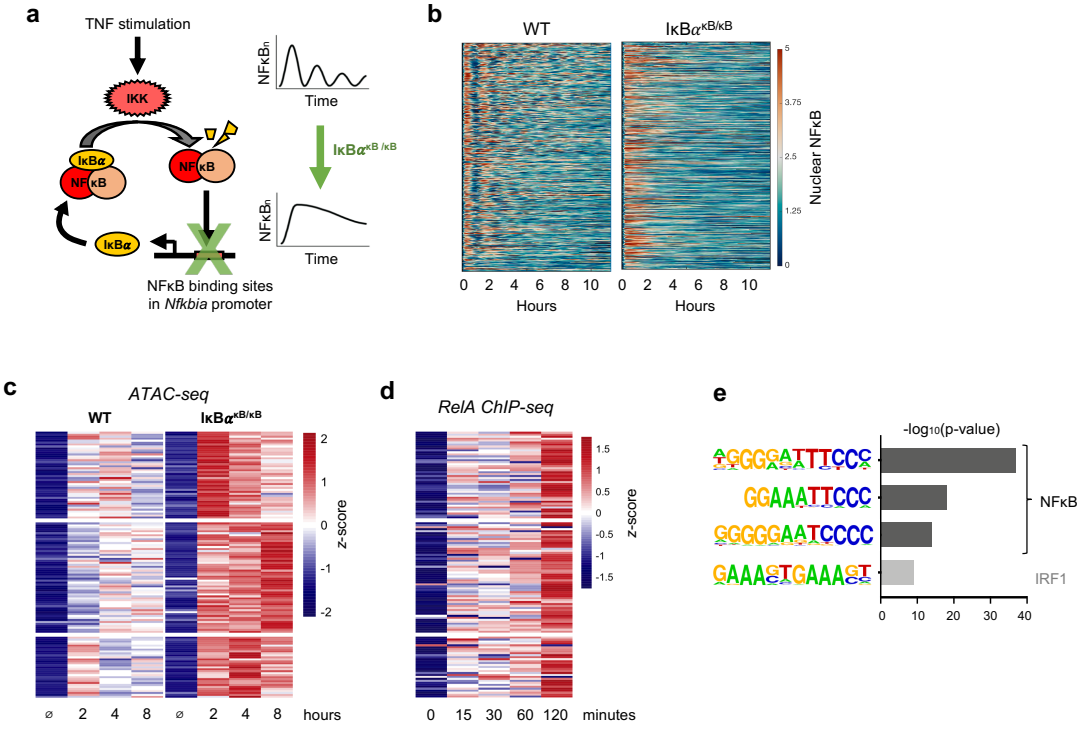

Extended data, Figure 3.7: *Nfkbia*$^{κB/κB}$ mutant as a complementary model of non-oscillatory NFκB. a) Schematic of *Nfkbia*$^{κB/κB}$ mutation, abolishing inducible IκBα by disrupting NFκB binding sites in promoter[26]. **b)** Heat map of single cell NFκB trajectories by microscopy, comparing TNF response in WT *vs.* IκBα$^{κB/κB}$ BMDMs. **c)** Heat map of ATAC-seq signal at 131 genomic regions that are TNF-inducible and differential between IκBα$^{κB/κB}$ and WT. Average of two replicates. **d)** Heat map of Lipid-A stimulated NFκB RelA ChIP-seq signal[25] at 131 inducible-differential ATAC-seq regions, 118 of which overlap with a RelA ChIP-seq peak. **e)** Known transcription factor motifs with greatest enrichment in differentially inducible ATAC-seq regions.

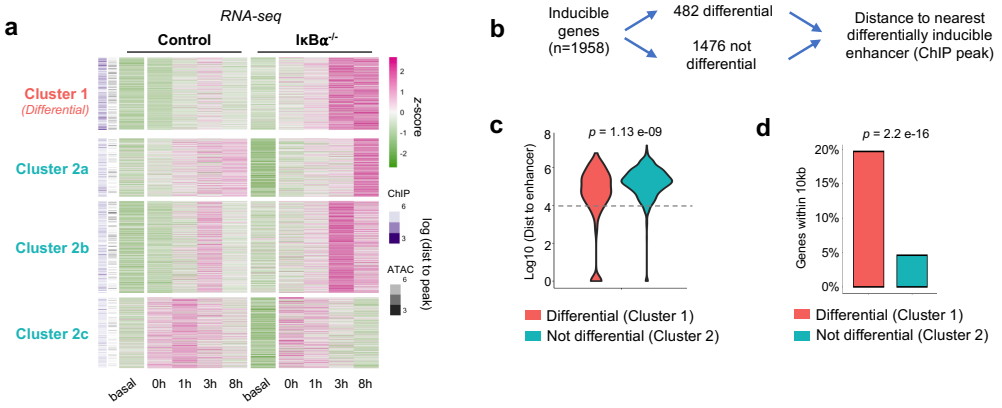

Extended data, Figure 3.8: Gene-centric approach to investigate the function of dynamics-dependent enhancers. a) Heat map of TNF-inducible genes in control or IκBα$^{-/-}$ BMDMs (n=1958), average of two replicates. Cluster 1 genes are differentially induced between IκBα$^{-/-}$ and control. Clusters 2a-2c genes are inducible but not differential. **b)** Gene-centric approach to map inducible genes to nearest dynamics-dependent enhancers. **c)** Violin plots of distance from gene TSS to nearest differentially inducible enhancer, comparing genes in Cluster 1 (differential) and Cluster 2 (not differential) by K-S test. **d)** Percentage of genes in each cluster within 10kb (dashed line, panel c) of a differentially inducible enhancer, evaluated by *chi* square test.

Methods

Mice

All mouse experiments were performed in a C57Bl/6 background. The mVenus-RelA reporter mouse (*Rela*$^{V/V}$), in which an mVenus-RelA fusion is knocked in to the endogenous *Rela* locus, has been previously described[6]. As *Nfkbia*$^{-/-}$ mice are perinatal lethal due to chronic inflammation they were crossed with *Rel*$^{-/-}$*Tnf*$^{-/-}$ alleles to achieve rescue and enable BMDM isolation[33]; they were also crossed with *Nfkbie*$^{-/-}$ alleles to avoid compensation by IκBe[34]. For ATAC, ChIP, and RNA-seq experiments *Rel*$^{-/-}$*Tnf*$^{-/-}$*Nfkbie*$^{-/-}$*Nfkbia*$^{+/-}$ heterozygotes were mated, and *Nfkbia*$^{+/+}$ *and Nfkbia*$^{-/-}$ littermates were used for control and knockout, respectively. The *Nfkbia*$^{\kappa B/\kappa B}$ mice have been previously described[26] and were a gift from Dr. Paul Chiao. For live cell microscopy, *Rel*$^{+/-}$*Tnf*$^{+/-}$*Nfkbie*$^{+/-}$*Nfkbia*$^{-/-}$*Rela*$^{V/V}$ and *Nfkbia*$^{\kappa B/\kappa B}$*Rela*$^{V/V}$ mice were compared to *Rela*$^{V/V}$ controls. Animal work was approved by the UCLA IRB under protocol B-14-110.

Tissue culture

BMDMs were generated by isolating bone marrow from the femurs and tibias of sex-matched mice between the ages of six and 12 weeks. Bone marrow cells were incubated in L929-conditioned media (RPMI + 30% L929 media, 10% FBS, 100 IU/ml penicillin, 100 μg/ml streptomycin, 2 mM L-glutamine) at 37^{0}C for seven days. Cells were stimulated with TNF-α (10 ng/ml, R&D Systems 410-MT), Pam3CSK4 (100 ng/ml, Invivogen tlrl-pms), CpG (1 μM, Invivogen tlrl-1668), LPS (100 ng/ml, Sigma-Aldrich L2880), or Poly(I:C) (50 μg/ml, Invivogen tlrl-picw). Ligand doses were chosen to maximize differences in NFκB signaling dynamics[6].

Live cell microscopy and analysis

Microscopy and analysis have been described in detail previously[6,35]. Briefly, BMDMs derived from mVenus-RelA reporter mice were plated in an 8-well ibidi SlideTek chamber,

stained with 2.5 ng/mL Hoechst 33342 in PBS, then stimulated with the ligands listed. Cells were imaged at 5-minute intervals on a Zeiss Axio Observer platform with live-cell incubation, using epifluorescent excitation from a Sutter Lambda XL light source. Images were recorded on a Hamamatsu Orca Flash 2.0 CCD camera. Time-lapse images were exported for single-cell tracking and measurement in MATLAB R2016a. Cells were identified using DIC images, and nuclear/cytoplasmic compartments were defined by the Hoechst image. Nuclear NFκB levels in the mVenus channel were quantified on a per-cell basis, and normalized to image background levels. Mitotic cells, dead cells, and cells that drifted out of the field of view, were excluded from analysis. Dynamic features of NFκB activity were measured for each single cell trajectory. The complete library of features and identification of six signaling "code words" was described previously[6].

H3K4me1 ChIP-seq libraries

BMDMs were cross-linked with 1% formaldehyde, quenched with 125 mM glycine, frozen and stored at -80^{0}C. Cell pellets were lysed in 50 mM HEPES-KOH pH 7.6, 140 mM NaCl, 1 mM EDTA, 10% glycerol, 0.5% NP-40, 0.25% Triton X-100, and 1x protease inhibitor cocktail (Thermo Scientific 78439) with one 15-second cycle of sonication in a Bioruptor (Diagenode). Nuclei were washed in 10 mM Tris-HCl pH 8.0, 200 mM NaCl, 1 mM EDTA, 0.5 mM EGTA, and 1x protease inhibitor cocktail. Nuclei were then resuspended in 10 mM Tris-HCl pH 8.0, 100 mM NaCl, 1 mM EDTA, 0.5 mM EGTA, 0.1% Na Deoxycholate, 0.5% N-lauroylsarcosine, 0.2% SDS, and 1x protease inhibitor cocktail, and subjected to twelve 30-second cycles of sonication in a Bioruptor. The resulting chromatin fragments were diluted with 5.2 volumes of 10 mM Tris-HCl pH 8.0, 160 mM NaCl, 1 mM EDTA, 0.01% SDS, 1.2% Triton X-100, 1x protease inhibitor cocktail, and incubated for 1.5 hours with Protein-G DynaBeads

(Thermo Fisher 10004D) for pre-clearing. Protein G beads were removed, a 1% aliquot of DNA was taken as input, and remaining chromatin was incubated with rabbit anti-H3K4me1 antibody (Abcam ab8895) overnight at 4^0C at a ratio of 2 μg antibody per 6 million cells of starting material.

For immunoprecipitation, 30 μL of Protein G beads were added to antibody-chromatin complexes and incubated at 4^0C for three hours. Supernatant was removed, and beads were serially washed with Low Salt buffer (50 mM HEPES-KOH pH 7.6, 140 mM NaCl, 1 mM EDTA, 1% Triton X-100, 0.1% Na Deoxycholate, 0.1% SDS), High Salt buffer (50 mM HEPES-KOH pH 7.6, 500 mM NaCl, 1 mM EDTA, 1% Triton X-100, 0.1% Na Deoxycholate, 0.1% SDS), LiCl buffer (20 mM Tris-HCl pH 8.0, 250 mM LiCl, 1 mM EDTA, 0.5% Na Deoxycholate, 0.5% NP-40), and TE buffer (10 mM Tris-HCl pH 8.0, 1 mM EDTA). Immunoprecipitated chromatin complexes were treated with RNAse A (Thermo Fisher 12091021) at 37^0C for one hour, and crosslinks were reversed with 10% SDS and 0.6 mg/ml Proteinase K (New England Biolabs P81075) overnight with shaking at 65^0C. Immunoprecipitated DNA fragments were purified with AMPure XP SPRI beads (Beckman Coulter A63881) at a 0.95 volume ratio according to manufacturer's instructions.

Libraries were prepared for sequencing using NEBNext Ultra II DNA Library Prep Kit (New England Biolabs E7645) with NEBNext Multiplex Oligos (New England Biolabs E7335 and E7500). Each library was prepared from 100 ng of starting DNA. Input samples were pooled from input DNA of the same genotype. Final libraries were checked for quality by agarose gel, quantified with Qubit (Life Technologies Q32851), and multiplexed with a maximum of 24 samples per sequencing reaction.

ATAC-seq libraries

BMDMs were dissociated with Accutase (Thermo Fisher Scientific), and 50,000 cells were used to prepare nuclei. Cell membranes were lysed using cold lysis buffer (10mM Tris-HCl pH7.5, 3mM MgCl2, 10mM NaCl and 0.1% IGEPAL CA-630). Nuclei were pelleted by centrifugation for 10 minutes at 500 x *g* and suspended in transposase reaction mixture (25 µl of 2X TD Buffer (Illumina), 2.5 µl of TD Enzyme 1 (Illumina), and 22.5 µl of nuclease-free water). The transposase reaction was performed for 30 minutes at 37^0C in a thermomixer shaker. Fragmented DNA in the reaction was purified using MinElute PCR purification kit (QIAGEN, Hilden, Germany). Libraries were prepared for sequencing using Nextera DNA Library Preparation Kit (Illumina, FC-121). The libraries were purified using MinElute PCR purification kit (QIAGEN) and quantified using KAPA Library Quantification Kit (KAPA Biosystems). The libraries were multiplexed with a maximum of 24 samples per sequencing reaction.

RNA-seq libraries

BMDMs were lysed with TRIzol reagent (Life Technologies), and total RNA was purified using DIRECTzol RNA miniprep kit (Zymo Research). Strand-specific libraries were generated from 500 ng total RNA using KAPA Stranded mRNA-seq Library Preparation kit (KAPA Biosystems). Final libraries were checked for quality by agarose gel, quantified with Qubit, and multiplexed with a maximum of 24 samples per sequencing reaction.

Sequencing and processing

ChIP, ATAC, and RNA-seq libraries were single-end sequenced with a length of 50bp on an Illumina HiSeq 2500 at the UCLA Broad Stem Cell Research Center. The low quality 3'ends of reads were trimmed (cutoff q=30), and remaining adapter sequences were removed using cutadapt[36]. For ChIP and ATAC-seq, reads were aligned to the mm10 genome build using

bowtie2[37] with default parameters except --very-sensitive and --non-deterministic options. For RNA-seq, reads were aligned to the mm10 genome using STAR[38] with the following options: --outFilterMultimapNmax 20, --alignSJoverhangMin 8, --alignSJDBoverhangMin 1, --outFilterMismatchNmax 999, --outFilterMismatchNoverLmax 0.04, --alignIntronMin 20, and --alignIntronMax 1000000 --seedSearchStartLmax 30. Aligned reads were filtered based on mapping score (MAPQ ≥ 30) by Samtools. For ChIP and ATAC-seq, duplicated reads were removed using Picard MarkDuplicates. Genome browser tracks for ChIP and ATAC-seq were generated using the bamCoverage function in deepTools[39] with the following options: --binSize 10, --smoothLength 30, --normalizeUsing RPGC, and for ChIP-seq only, --extendReads to average fragment length.

ChIP-seq analysis

MACS2 version 2.1.0[40] was used in broad mode to identify peaks for each sample using pooled input samples as control, FDR < 0.01, and extension size of average fragment length. These peaks were merged to generate a single reference peak file, and the number of reads that fell into each peak was counted using deeptools multiBamSummary[41] with extension size of average fragment length. edgeR[42] was used to perform normalization using the trimmed mean of M values (TMM) method and to construct a negative binomial model. For stimulus-specific dataset (Fig. 1), inducible peaks were identified in any stimulation condition compared to unstimulated by FDR < 0.05 and log2FC > 1. For IκBα KO vs control dataset (Fig. 4), inducible peaks were identified in TNF-treated samples compared to unstimulated by FDR < 0.05. Differentially inducible peaks between IκBα and KO were identified by FDR < 0.05 after re-constructing the negative binomial model to include only inducible peaks. Heat maps were generated with the pheatmap R package.

Analysis of transcription factor motif enrichment was performed using findMotifsGenome function in the HOMER suite[5], using the entire width of differential peaks as foreground and all detected peaks as background. Peaks of interest were annotated using HOMER annotatePeaks function with default parameters. ChipPeakAnno[43] was used to assess statistical significance of the overlap of differential peaks in the IκBα KO dataset and the stimulus-specific WT dataset.

RelA ChIP-seq data in Lipid A-stimulated BMDMs was previously published[14]. BAM files were obtained from Gene Expression Omnibus (accession number GSE67343). Peaks were called on each sample against input with FDR threshold < 0.01. A merged peak file was obtained, and overlaps between RelA ChIP-seq peaks and H3K4me1 ChIP-seq or ATAC-seq regions of interest were determined using the intersect function in the Bedtools suite[44].

ATAC-seq analysis

BAM files were analyzed with the R package csaw[45], using windows 200-nt wide, with 100-nt spacing. Windows with zero or background signal were removed. Sex-associated regions on chromosome X were also discarded[46]. Juxtaposed windows were merged in a single peak call up to a maximal chaining distance of 1,200 bp. Libraries were normalized using the TMM method. Batch effects were removed from the normalized count matrix with the RemoveBatchEffect function from the limma R package. Differential peaks were required to pass log2FC and FDR thresholds using csaw's Genewise negative binomial generalized linear models with quasi-likelihood tests, with batch effects controlled by modeling as blocking factors. Thresholds were 1 log2FC and 0.05 FDR for TNF-inducible peaks; and 0.5 log2FC and 0.1 FDR for IκBα KO vs control. For each peak call, the single 200-nt window with the highest abundance was retained as representative of that peak. Clustering was performed using the

partitioning around medoids (PAM) algorithm on peak counts per million z-scaled across samples. Heat maps of peak signals were generated using the pheatmap R package. H3K4me1 signal from windows matching those selected from ATAC-seq analysis was extracted using csaw by extending each 200-nt ATAC-seq window by additional 200 nt from 5' end and 200 nt from 3'end, normalized using TMM offsets computed genome-wide.

To obtain a normalized percentage of cells with open chromatin (Fig. 3g), ATAC counts were normalized as follows: over the 322 regions of interest, the 0.1 percentile of ATAC-seq signal was assigned a value of "0% of cells accessible." The 99.9 percentile of ATAC-seq signal was assigned a value of "100% of cells accessible," and all data points were scaled to these values.

RNA-seq analysis

Transcript read counts were computed by the featureCounts function in the Subread package[47]. TMM normalization was performed using the edgeR package. Genes below an expression threshold of 4.6 CPM in all samples were excluded from downstream analysis. Inducible genes were identified in TNF-treated samples compared to unstimulated by FDR < 0.05. Differentially inducible genes between IκBα and KO were identified by FDR < 0.05 after re-constructing the negative binomial model to include only inducible genes. Heat maps were generated with the pheatmap R package. Gene ontology analysis was performed using the PANTHER database[48] with all expressed genes as background

Model of nucleosome opening

Model formulation: A multistep model of DNA unwrapping from the histone octamer was formulated based on structural studies that identified 14 contacts between the histone octamer and double helical DNA and biophysical studies of single nucleosomes *in vitro* that

revealed multiple, step-wise transitions in DNA unwrapping[23,49,50]. The model describes the population average or probability of many stochastic events, with each species representing the fraction of NFκB-responsive latent enhancers in a cell (*E*) at a given state of accessibility. E_{-14} describes the most closed state in which all 14 contact points are engaged, and E_0 the most open state in which the histone octamer is entirely evicted.

$$E_{-14} \underset{\alpha_{-14}}{\overset{\beta_{-14}(t)}{\rightleftharpoons}} E_{-13} \cdots \underset{\alpha_i}{\overset{\beta_i(t)}{\rightleftharpoons}} E_{i+1} \cdots \underset{\alpha_{-1}}{\overset{\beta_{-1}(t)}{\rightleftharpoons}} E_0$$

A system of ordinary differential equations was formulated to describe this model:

$$\frac{dE_{-14}}{dt} = \alpha_{-14}E_{-13} - \beta_{-14}(t)E_{-14} \tag{1}$$

$$\frac{dE_{-13}}{dt} = \beta_{-14}(t)E_{-14} - \alpha_{-14}E_{-13} - \beta_{-13}(t)E_{-13} + \alpha_{-13}E_{-12} \tag{2}$$

...

$$\frac{dE_i}{dt} = \beta_{i-1}(t)E_{i-1} - \alpha_{i-1}E_i - \beta_i(t)E_i + \alpha_i E_{i+1} \tag{3}$$

...

$$\frac{dE_0}{dt} = \beta_{-1}(t)E_{-1} - \alpha_{-1}E_0 \tag{4}$$

The rate constant α_i describes the closing transition. The term $\beta_i(t)$ represents an NFκB-dependent opening transition that varies with time as nuclear NFκB concentration varies with time. Experimental studies have demonstrated that NFκB can interact with nucleosomal DNA[19] while the lowest energy structure of the NFκB-DNA complex is sterically incompatible with DNA-histone octamer interactions[17,18], suggesting that NFκB can promote nucleosome unwrapping. The opening transition is thus formulated as:

$$\beta_i(t) = \frac{k_i[NF\kappa B(t)]^n}{K_D^n + [NF\kappa B(t)]^n}$$

where K_D is the dissociation constant of the NFκB -DNA interaction, n is the Hill coefficient, k_i is the transition rate constant, and [NFκB*(t)*] represents the time-dependent nuclear NFκB concentration.

Model parameters: K_D and n were surveyed across reasonable ranges, producing qualitatively similar results (Extended Data Fig. 4a,b). For the shown simulations K_D was set to 0.025 μM and the Hill coefficient was set to three. The rate of nucleosome unwrapping was also surveyed across a wide range (Extended Data Fig. 4c), and the ratio of unwrapping to rewrapping rates was selected based on biophysical measurements[23]. Based on this literature, the initial rewrapping rate is approximately 5-10 times faster than the unwrapping rate, so we set the ratio of rewrapping to unwrapping to 7.5 at the first step. As *in vivo* nucleosomes are stabilized by linker histones and cooperative binding within the nucleosome array, we scaled transition rates to be 50-fold slower than *in vitro* measurements, with the unwrapping rate constant of the first opening step k_{-14} set to 10 $\mu M^{-1} min^{-1}$, and the rewrapping rate constant $\square_{-14}$ to 75 min^{-1}. To account for the inherent cooperativity of contact points within a nucleosome[51], stepwise increases in unwrapping rates and decreases in rewrapping rates were included. These cooperativity factors were examined through a parameter sweep (Extended Data Fig. 4d,e), and cooperativity factors of 1.2 for unwrapping and 0.8 for rewrapping were selected.

Model simulations: Simulations were performed in MATLAB R2014b. Experimental and theoretical single cell traces (Supplemental Table 1) were used as input to the ODE system described above. Experimental values of mVenus-RelA fluorescent intensities were

converted to μM concentrations of NFκB based on previously published NFκB models, with the maximum fluorescence of the first peak for the single cell trajectories approximating the maximal nuclear NFκB concentration of 0.25 μM reported in previous studies[52]. For simulations, the initial value of the E_{-14} state was set to 1, and all other states set to 0. The MATLAB function *ode*15*s* was used to solve the ODE system, and the concentration of the most open chromatin state E_0 was plotted.

Bibliography

1. Murray PJ, Wynn TA. Protective and pathogenic functions of macrophage subsets. Nat Rev Immunol. 2011 Oct 14;11(11):723–37. PMCID: PMC3422549

2. Kaikkonen MU, Spann NJ, Heinz S, Romanoski CE, Allison KA, Stender JD, Chun HB, Tough DF, Prinjha RK, Benner C, Glass CK. Remodeling of the enhancer landscape during macrophage activation is coupled to enhancer transcription. Mol Cell. 2013 Aug 8;51(3):310–325. PMCID: PMC3779836

3. Ostuni R, Piccolo V, Barozzi I, Polletti S, Termanini A, Bonifacio S, Curina A, Prosperini E, Ghisletti S, Natoli G. Latent enhancers activated by stimulation in differentiated cells. Cell. 2013 Jan 17;152(1–2):157–71. PMID: 23332752

4. Heinz S, Romanoski CE, Benner C, Glass CK. The selection and function of cell type-specific enhancers. Nat Rev Mol Cell Biol. 2015 Mar;16(3):144–154. PMCID: PMC4517609

5. Heinz S, Benner C, Spann N, Bertolino E, Lin YC, Laslo P, Cheng JX, Murre C, Singh H, Glass CK. Simple combinations of lineage-determining transcription factors prime cis-regulatory elements required for macrophage and B cell identities. Mol Cell. 2010 May 28;38(4):576–589. PMCID: PMC2898526

6. Taylor B, Adelaja A, Liu Y, Luecke S, Hoffmann A. Macrophages classify immune threats using at least six codewords of the temporal NFkB code. BioRxiv. 2020;

7. Allis CD, Jenuwein T. The molecular hallmarks of epigenetic control. Nat Rev Genet. 2016 Aug;17(8):487–500.

8. Glass CK, Natoli G. Molecular control of activation and priming in macrophages. Nature Immunology. 2015;17:26–33.

9. Ivashkiv LB. Epigenetic regulation of macrophage polarization and function. Trends Immunol. 2013 May;34(5):216–223. PMCID: PMC3647003

10. Lawrence T. The Nuclear Factor NF- B Pathway in Inflammation. Cold Spring Harbor Perspectives in Biology. 2009 Dec 1;1(6):a001651–a001651.

11. Honda K, Takaoka A, Taniguchi T. Type I Inteferon Gene Induction by the Interferon Regulatory Factor Family of Transcription Factors. Immunity. 2006 Sep;25(3):349–360.

12. Yarilina A, Park-Min K-H, Antoniv T, Hu X, Ivashkiv LB. TNF activates an IRF1-dependent autocrine loop leading to sustained expression of chemokines and STAT1-dependent type I interferon-response genes. Nat Immunol. 2008 Apr;9(4):378–387. PMID: 18345002

13. Werner SL, Barken D, Hoffmann A. Stimulus specificity of gene expression programs determined by temporal control of IKK activity. Science. 2005 Sep 16;309(5742):1857–1861. PMID: 16166517

14. Tong A-J, Liu X, Thomas BJ, Lissner MM, Baker MR, Senagolage MD, Allred AL, Barish GD, Smale ST. A Stringent Systems Approach Uncovers Gene-Specific Mechanisms Regulating Inflammation. Cell. 2016 Mar 24;165(1):165–179. PMCID: PMC4808443

15. Behar M, Hoffmann A. Understanding the temporal codes of intra-cellular signals. Curr Opin Genet Dev. 2010 Dec;20(6):684–693. PMCID: PMC2982931

16. Covert MW, Leung TH, Gaston JE, Baltimore D. Achieving stability of lipopolysaccharide-induced NF-kappaB activation. Science. 2005 Sep 16;309(5742):1854–1857. PMID: 16166516

17. Chen FE, Huang DB, Chen YQ, Ghosh G. Crystal structure of p50/p65 heterodimer of transcription factor NF-kappaB bound to DNA. Nature. 1998 Jan 22;391(6665):410–413. PMID: 9450761

18. Suto RK, Clarkson MJ, Tremethick DJ, Luger K. Crystal structure of a nucleosome core particle containing the variant histone H2A.Z. Nat Struct Biol. 2000 Dec;7(12):1121–1124. PMID: 11101893

19. Lone IN, Shukla MS, Charles Richard JL, Peshev ZY, Dimitrov S, Angelov D. Binding of NF-κB to Nucleosomes: Effect of Translational Positioning, Nucleosome Remodeling and Linker Histone H1. Schübeler D, editor. PLoS Genet. 2013 Sep 26;9(9):e1003830.

20. Kobayashi K, Hiramatsu H, Nakamura S, Kobayashi K, Haraguchi T, Iba H. Tumor suppression via inhibition of SWI/SNF complex-dependent NF-κB activation. Sci Rep. 2017 Dec;7(1):11772.

21. Li G, Levitus M, Bustamante C, Widom J. Rapid spontaneous accessibility of nucleosomal DNA. Nat Struct Mol Biol. 2005 Jan;12(1):46–53.

22. Davey CA, Sargent DF, Luger K, Maeder AW, Richmond TJ. Solvent mediated interactions in the structure of the nucleosome core particle at 1.9 a resolution. J Mol Biol. 2002 Jun 21;319(5):1097–1113. PMID: 12079350

23. Tims HS, Gurunathan K, Levitus M, Widom J. Dynamics of Nucleosome Invasion by DNA Binding Proteins. Journal of Molecular Biology. 2011 Aug;411(2):430–448.

24. Hoffmann A, Levchenko A, Scott ML, Baltimore D. The IkappaB-NF-kappaB signaling module: temporal control and selective gene activation. Science. 2002 Nov 8;298(5596):1241–1245. PMID: 12424381

25. Beg AA, Sha WC, Bronson RT, Baltimore D. Constitutive NF-kappa B activation, enhanced granulopoiesis, and neonatal lethality in I kappa B alpha-deficient mice. Genes Dev. 1995 Nov 15;9(22):2736–2746. PMID: 7590249

26. Peng B, Ling J, Lee AJ, Wang Z, Chang Z, Jin W, Kang Y, Zhang R, Shim D, Wang H, Fleming JB, Zheng H, Sun S-C, Chiao PJ. Defective feedback regulation of NF-kappaB underlies Sjogren's syndrome in mice with mutated kappaB enhancers of the IkappaBalpha promoter. Proc Natl Acad Sci USA. 2010 Aug 24;107(34):15193–15198. PMCID: PMC2930541

27. Corces MR, Granja JM, Shams S, Louie BH, Seoane JA, Zhou W, Silva TC, Groeneveld C, Wong CK, Cho SW, Satpathy AT, Mumbach MR, Hoadley KA, Robertson AG, Sheffield NC, Felau I, Castro MAA, Berman BP, Staudt LM, Zenklusen JC, Laird PW, Curtis C, The Cancer Genome Atlas Analysis Network†, Greenleaf WJ, Chang HY. The chromatin accessibility landscape of primary human cancers. Science. 2018 Oct 26;362(6413):eaav1898.

28. Murray PJ, Allen JE, Biswas SK, Fisher EA, Gilroy DW, Goerdt S, Gordon S, Hamilton JA, Ivashkiv LB, Lawrence T, Locati M, Mantovani A, Martinez FO, Mege JL, Mosser DM, Natoli G, Saeij JP, Schultze JL, Shirey KA, Sica A, Suttles J, Udalova I, van Ginderachter JA, Vogel SN, Wynn TA. Macrophage activation and polarization: nomenclature and experimental guidelines. Immunity. 2014 Jul 17;41(1):14–20. PMCID: PMC4123412

29. Kanter JE, Kramer F, Barnhart S, Averill MM, Vivekanandan-Giri A, Vickery T, Li LO, Becker L, Yuan W, Chait A, Braun KR, Potter-Perigo S, Sanda S, Wight TN, Pennathur S, Serhan CN, Heinecke JW, Coleman RA, Bornfeldt KE. Diabetes promotes an inflammatory macrophage phenotype and atherosclerosis through acyl-CoA synthetase 1. Proc Natl Acad Sci USA. 2012 Mar 20;109(12):E715-724. PMCID: PMC3311324

30. Soufi A, Garcia MF, Jaroszewicz A, Osman N, Pellegrini M, Zaret KS. Pioneer transcription factors target partial DNA motifs on nucleosomes to initiate reprogramming. Cell. 2015 Apr 23;161(3):555–568. PMCID: PMC4409934

31. Barken D, Wang CJ, Kearns J, Cheong R, Hoffmann A, Levchenko A. Comment on "Oscillations in NF-kappaB signaling control the dynamics of gene expression." Science. 2005 Apr 1;308(5718):52; author reply 52. PMCID: PMC2821939

32. Cheng CS, Behar MS, Suryawanshi GW, Feldman KE, Spreafico R, Hoffmann A. Iterative Modeling Reveals Evidence of Sequential Transcriptional Control Mechanisms. Cell Syst. 2017 Mar 22;4(3):330-343 e5. PMCID: PMC5434763

33. Shih VF-S, Kearns JD, Basak S, Savinova OV, Ghosh G, Hoffmann A. Kinetic control of negative feedback regulators of NF- B/RelA determines their pathogen- and cytokine-receptor signaling specificity. Proceedings of the National Academy of Sciences. 2009 Jun 16;106(24):9619–9624.

34. Kearns JD, Basak S, Werner SL, Huang CS, Hoffmann A. IkappaBepsilon provides negative feedback to control NF-kappaB oscillations, signaling dynamics, and inflammatory gene expression. J Cell Biol. 2006 Jun 5;173(5):659–664. PMCID: PMC2063883

35. Selimkhanov J, Taylor B, Yao J, Pilko A, Albeck J, Hoffmann A, Tsimring L, Wollman R. Accurate information transmission through dynamic biochemical signaling networks. Science. 2014 Dec 12;346(6215):1370–1373.

36. Martin M. Cutadapt removes adapter sequences from high-throughput sequencing reads. EMBnet j. 2011 May 2;17(1):10.

37. Langmead B, Salzberg SL. Fast gapped-read alignment with Bowtie 2. Nature Methods. 2012 Mar 4;9(4):357–9. PMCID: PMC3322381

38. Dobin A, Davis CA, Schlesinger F, Drenkow J, Zaleski C, Jha S, Batut P, Chaisson M, Gingeras TR. STAR: ultrafast universal RNA-seq aligner. Bioinformatics. 2013;29(1):15–21.

39. Ramírez F, Ryan DP, Grüning B, Bhardwaj V, Kilpert F, Richter AS, Heyne S, Dündar F, Manke T. deepTools2: a next generation web server for deep-sequencing data analysis. Nucleic Acids Res. 2016 Jul 8;44(W1):W160–W165.

40. Zhang Y, Liu T, Meyer CA, Eeckhoute J, Johnson DS, Bernstein BE, Nusbaum C, Myers RM, Brown M, Li W, Liu XS. Model-based analysis of ChIP-Seq (MACS). Genome biology. 2008;9(9):R137. PMCID: PMC2592715

41. Ramírez F, Ryan DP, Grüning B, Bhardwaj V, Kilpert F, Richter AS, Heyne S, Dündar F, Manke T. deepTools2: a next generation web server for deep-sequencing data analysis. Nucleic Acids Res. 2016 Jul 8;44(W1):W160–W165.

42. Robinson MD, McCarthy DJ, Smyth GK. edgeR: a Bioconductor package for differential expression analysis of digital gene expression data. Bioinformatics. 2010 Jan 1;26(1):139–40. PMCID: PMC2796818

43. Zhu LJ, Gazin C, Lawson ND, Pagès H, Lin SM, Lapointe DS, Green MR. ChIPpeakAnno: a Bioconductor package to annotate ChIP-seq and ChIP-chip data. BMC Bioinformatics. 2010 Dec;11(1):237.

44. Quinlan AR, Hall IM. BEDTools: a flexible suite of utilities for comparing genomic features. Bioinformatics. 2010 Mar 15;26(6):841–2. PMCID: PMC2832824

45. Lun ATL, Smyth GK. csaw: a Bioconductor package for differential binding analysis of ChIP-seq data using sliding windows. Nucleic Acids Res. 2016 Mar 18;44(5):e45. PMCID: PMC4797262

46. Mognol GP, Spreafico R, Wong V, Scott-Browne JP, Togher S, Hoffmann A, Hogan PG, Rao A, Trifari S. Exhaustion-associated regulatory regions in CD8 $^{+}$ tumor-infiltrating T cells. Proc Natl Acad Sci USA. 2017 Mar 28;114(13):E2776–E2785.

47. Liao Y, Smyth GK, Shi W. featureCounts: an efficient general purpose program for assigning sequence reads to genomic features. Bioinformatics. 2014 Apr 1;30(7):923–930. PMID: 24227677

48. Mi H, Muruganujan A, Ebert D, Huang X, Thomas PD. PANTHER version 14: more genomes, a new PANTHER GO-slim and improvements in enrichment analysis tools. Nucleic Acids Res. 2019 Jan 8;47(D1):D419–D426. PMCID: PMC6323939

49. Möbius W, Neher RA, Gerland U. Kinetic Accessibility of Buried DNA Sites in Nucleosomes. Phys Rev Lett. 2006 Nov 14;97(20):208102.

50. Luger K, Mäder AW, Richmond RK, Sargent DF, Richmond TJ. Crystal structure of the nucleosome core particle at 2.8 A resolution. Nature. 1997 Sep 18;389(6648):251–260. PMID: 9305837

51. Miller JA, Widom J. Collaborative competition mechanism for gene activation in vivo. Mol Cell Biol. 2003 Mar;23(5):1623–1632. PMCID: PMC151720

52. Shih VF-S, Davis-Turak J, Macal M, Huang JQ, Ponomarenko J, Kearns JD, Yu T, Fagerlund R, Asagiri M, Zuniga EI, Hoffmann A. Control of RelB during dendritic cell activation integrates canonical and noncanonical NF-κB pathways. Nat Immunol. 2012 Dec;13(12):1162–1170.

CHAPTER FOUR:

Conclusion

The studies presented in this dissertation contribute to a growing literature on macrophages reprogramming. The results in Chapter Two demonstrated the specificity with which cytokines reprogram macrophages, revealing that differences between Type I and II IFNs are more nuanced than previously thought. These insights were enabled by the sequential conditioning-stimulation experimental strategy and systems-level analytical approach. Our study therefore not only advanced the biological understanding of IFNs but also highlighted the value of measuring not just direct gene expression effects of cytokines but also their effects on response to secondary stimulation. Indeed, the field of macrophage activation is shifting towards a paradigm of thinking in terms of conditioning and secondary response, as similar experimental approaches have provided insight into other cytokines. For instance, IL-4 treated "M2" macrophages, which have frequently been considered an "anti-inflammatory" phenotype due to the fact that they produce less TNF and IL6 than "M0" macrophages[1], are in fact very much capable of producing inflammation when secondarily stimulated with LPS[2]. Our study further validates the utility of this approach, demonstrating that Type I and II IFNs have differential gene- and stimulus-specific effects when probed with secondary stimuli.

The results in Chapter Three provide a novel paradigm for stimulus-specificity in the molecular reprogramming of macrophages. While the notion that SDTFs can trigger formation of *de novo* enhancers is gaining acceptance, precisely how SDTF activity results in *de novo* enhancer formation and what features of SDTFs confer this ability have not been clearly shown. One hypothesis has extrapolated from studies of LDTFs[3] that some SDTFs may contain structural motifs that confer the functional ability to interact with nucleosome-bound DNA. Our study provides an alternative mechanistic framework: that temporal dynamics of SDTFs determine their ability to interact with nucleosome-bound DNA and produce *de novo* enhancers.

This hypothesis is a better explanation for the observation that *de novo* enhancer formation is stimulus-specific. If structural features of NFκB are solely responsible for its capacity to alter the epigenome, then the same enhancers should be formed whenever NFκB is activated. But in the temporal dynamics framework, NFκB dynamics are stimulus-specific, and thus whether they are oscillatory or non-oscillatory determines the ability of a given stimulus to produce *de novo* enhancers.

The results presented in this dissertation provide motivation for further investigation in at least two important lines of inquiry. The conclusions from Chapter Three, which have broad implications for stimulus-specificity in macrophage biology, need to be assessed functionally *in vivo*. Do the mechanisms that result in stimulus-specific, NFκB dynamics-dependent epigenomic changes have an effect on innate immune memory? Innate immune memory, which has substantial implications on human health and disease[4], is thought to arise from epigenomic reprogramming of myeloid cells[5]. However, thus far, the relationship between the molecular and physiologic phenotypes has been largely correlative, and it is assumed that epigenomic differences seen *in vitro* are responsible for the physiologic responses seen *in vivo*. This knowledge gap can be addressed by studying the role of NFκB dynamics-dependent enhancers in host defense using a mouse model of infection. One limitation is that *in vivo* models of innate immune memory, such as infections in mice, do not lend themselves well to mechanistic studies. Genetic perturbations in mice affect not only memory formation but also the host response to secondary infection, making results difficult to interpret. To overcome this challenge, it will be necessary to de-couple the memory formation and secondary infection steps. For instance, one could condition monocytes *in vitro* with stimuli that induce oscillatory *vs.* non-oscillatory NFκB,

adoptively transfer these cells into mice depleted of their native monocytes, and subsequently infect the mice to assess the effects of the transferred, reprogrammed monocytes.

A second direction for further investigation is to translate results from murine experiments to human clinical scenarios. Epigenomic studies of human monocytes and macrophages stimulated with a spectrum of ligands has not been reported, and the extent of stimulus-specificity in human macrophage reprogramming is not known. These types of *in vitro* experiments are simple to perform and could then be extended to study the effect of other types of disease-relevant context on human myeloid cells. For instance, how do high glucose levels alter myeloid cell epigenomes and subsequent response to PAMPs? How do common immunomodulatory drugs like corticosteroids alter innate immune epigenomes and function? These questions could be addressed by isolating monocytes or tissue-resident macrophages from humans with diseases like diabetes and performing epigenomic and transcriptional-response assays. These studies would provide tremendous insight into the way disease contexts shape immune sentinel cells and alter gene expression responses in infectious diseases. Additionally, one could explore the impact of recent infection on human myeloid cell epigenome and function. This could be done by infecting human volunteers in a controlled setting[6], or by prospectively following patients with infection into the resolution phase of disease. These experiments could identify the enhancers and genes that alter subsequent immune function and contribute to the pathogenesis of post-infectious complications.

Ultimately, the goal of these lines of inquiry would be to translate the mechanistic insight gained from the studies in this dissertation into tangible and clinically useful tools. The long-term application of these studies could include the identification of epigenetic and gene expression markers of disease risk. One can imagine, for instance, being able to measure the

epigenetic and gene expression response patterns of a patient recovering from influenza and predict their risk for a secondary bacterial pneumonia, heart attack, or stroke. If they are high risk, simple interventions such as prophylactic antibiotics or anti-platelet therapy could be employed during the risk period. More targeted therapy could also be prescribed, where drivers of detrimental epigenetic reprogramming could be inhibited by epigenome-modifying drugs such as bromodomain inhibitors of BET enzymes[7]. With the rapid advance of CRISPR-based technologies, one could even imagine someday bringing targeted epigenetic modifying therapies to specific sites in the genome, modifying the state of a single enhancer that confers risk for disease in reprogrammed macrophages. While these diagnostic and therapeutic tools may be many years away, this dissertation contributes to the fundamental understanding of how macrophages are reprogrammed.

Bibliography

1. McBride WH, Economou JS, Nayersina R, Comora S, Essner R. Influences of interleukins 2 and 4 on tumor necrosis factor production by murine mononuclear phagocytes. Cancer Res. 1990 May 15;50(10):2949–2952. PMID: 2334896

2. El Chartouni C, Rehli M. Comprehensive analysis of TLR4-induced transcriptional responses in interleukin 4-primed mouse macrophages. Immunobiology. 2010 Oct;215(9–10):780–787. PMID: 20692533

3. Soufi A, Garcia MF, Jaroszewicz A, Osman N, Pellegrini M, Zaret KS. Pioneer transcription factors target partial DNA motifs on nucleosomes to initiate reprogramming. Cell. 2015 Apr 23;161(3):555–568. PMCID: PMC4409934

4. Netea MG, Domínguez-Andrés J, Barreiro LB, Chavakis T, Divangahi M, Fuchs E, Joosten LAB, van der Meer JWM, Mhlanga MM, Mulder WJM, Riksen NP, Schlitzer A, Schultze JL, Stabell Benn C, Sun JC, Xavier RJ, Latz E. Defining trained immunity and its role in health and disease. Nat Rev Immunol [Internet]. 2020 Mar 4 [cited 2020 Mar 9]; Available from: http://www.nature.com/articles/s41577-020-0285-6

5. Saeed S, Quintin J, Kerstens HHD, Rao NA, Aghajanirefah A, Matarese F, Cheng S-C, Ratter J, Berentsen K, van der Ent MA, Sharifi N, Janssen-Megens EM, Ter Huurne M, Mandoli A, van Schaik T, Ng A, Burden F, Downes K, Frontini M, Kumar V, Giamarellos-Bourboulis EJ, Ouwehand WH, van der Meer JWM, Joosten LAB, Wijmenga C, Martens JHA, Xavier RJ, Logie C, Netea MG, Stunnenberg HG. Epigenetic programming of monocyte-to-macrophage differentiation and trained innate immunity. Science. 2014 Sep 26;345(6204):1251086. PMCID: PMC4242194

6. Darton TC, Blohmke CJ, Moorthy VS, Altmann DM, Hayden FG, Clutterbuck EA, Levine MM, Hill AVS, Pollard AJ. Design, recruitment, and microbiological considerations in human challenge studies. The Lancet Infectious Diseases. 2015 Jul;15(7):840–851.

7. Pérez-Salvia M, Esteller M. Bromodomain inhibitors and cancer therapy: From structures to applications. Epigenetics. 2017 04;12(5):323–339. PMCID: PMC5453193